ANGIOTENSIN II-INDUCED HEART FAILURE DIFFERS BETWEEN THE SEXES AND EXACERBATES FRAILTY IN A SEX SPECIFIC FASHION IN OLDER C57BL/6 MICE

by

Ninh Khuong

Submitted in partial fulfillment of the requirements

for the degree of Master of Science

at

Dalhousie University

Halifax, Nova Scotia

June 2021

"Continuous improvement is better than delayed perfection."

- Mark Twain

Table of Contents

List of Tables

List of Figures

Abstract

This study investigated sex differences in cardiac remodeling in an angiotensin II (Ang II) infused mouse model of heart failure (HF) in older C57BL/6 mice and whether HF exacerbates frailty in a sex-specific fashion. Male and female mice were infused with either Ang II to increase blood pressure or saline (6 weeks). Echocardiography showed concentric hypertrophy with slight left ventricular (LV) chamber dilation in treated females and eccentric hypertrophy with marked LV chamber dilation in males. Treated males had more pronounced diastolic and systolic dysfunction than females. Contractile function was reduced in Langendorff-perfused hearts from treated males but not females. Ang II-treated females exhibited worse cardiac hypertrophy and pulmonary edema. Treated mice had high frailty, increased biological age and lower life expectancies, but this was more pronounced in males. These findings suggest that Ang II-induced hypertension promoted HF in a sex-specific fashion, and these effects were especially severe in males.

List of Abbreviations and Symbols Used

ACE	Angiotensin converting enzyme
ACE2	Angiotensin converting enzyme 2
AFRAID	Analysis of Frail and Death
Ang I	Angiotensin I
Ang II	Angiotensin II
AT_1	Angiotensin subtype 1
AT_2	Angiotensin subtype 2
ANOVA	Analysis of Variance
bpm	Beats per minute
BSC	Biosafety cabinet
$CaCl_2$	Calcium chloride
CO_2	Carbon dioxide
^oC	Degree Celsius
E	Early filling velocity
EF	Ejection fraction
ECM	Extracellular matrix
FS	Fractional shortening
FI	Frailty Index
FRIGHT	Frailty Inferred Geriatric Health Timeline
g	Gram
HEP	Humane endpoint
HF	Heart failure
HFrEF	Heart failure with reduced ejection fraction
HFpEF	Heart failure with preserved ejection fraction
HR	Heart rate
H_2O_2	Hydrogen peroxide
IL	Interleukin
IFN	Interferon

IVRT	Isovolumetric relaxation time
IVCT	Isovolumetric contraction time
kg	Kilogram
A	Late filling velocity
KCl	Potassium chloride
KH_2PO_4	Potassium dihydrogen phosphate
L	Litre
LV	Left ventricle
LVDP	Left ventricular developed pressure
LVAW	Left ventricular anterior wall
LVPW	Left ventricular posterior wall
$MgSO_4$	Magnesium sulfate
NADPH	Nicotinamide adenine dinucleotide phosphate
VO_2	Maximal oxygen consumption
MAP	Mean arterial pressure
MMP	Metalloproteinase
µg	Microgram
µL	Microliter
ml	Milliliter
mg	Milligram
min	Minute
mM	Millimolar
mos	Months
ms	Millisecond
ng	Nanogram
NLRP3	Nod-like receptor protein 3
O_2	Oxygen
% RWC	Percent recent weight change
% TWC	Percent total weight change

+dP/dt	Rate of contraction
-dP/dt	Rate of relaxation
RPP	Rate of product pressure
ROS	Reactive oxygen species
RAAS	Renin angiotensin aldosterone system
RWC	Recent weight change
SR	Sarcoplasmic reticulum
STAT3	Signal transducer and activator of transcription 3
NaCl	Sodium chloride
$NaHCO_3$	Sodium bicarbonate
SD	Standard deviation
SEM	Standard error mean
O_2^-	Superoxide
TIMP	Tissue inhibitor of metalloproteinase
TWC	Total weight change
TNF	Tumor necrosis factor

Acknowledgements

First and foremost, I would like to express my special appreciation and warmest thanks to my supervisor Dr. Susan Howlett. Your tremendous mentorship and expert advice have been invaluable throughout all stages of this project. Thank you for going above and beyond for your students.

I would especially like to thank Peter Nicholl and Dr. Jie-quan Zhu for all their help and expertise. Without you, this work would not have been possible. I would also like to express my sincere gratitude towards my colleagues Stefan Heinze-Milne, Elise Bisset, Shubham Banga, Meghan Breckon, David Sapp, Rita Ribeiro, and Manish Mishra. You provided a cooperative lab environment and useful feedback on my work. I am grateful for your assistance and will always treasure our friendship.

I would like to extend my thanks to my high school biology teacher Mr. David Young. You encouraged my scientific curiosity and provided insightful advice even long after I have graduated. I would also like to thank my family and friends for their encouragement and support.

Finally, I would like to thank my advisory committee members Professor Matthew Herder, Dr. Scott Grandy, Dr. Kishore Pasumarthi, and Dr. Ketul Chaudhary as well as all the staff members of the Department of Pharmacology and the Carleton Animal Care Facility. Thank you for all your help and guidance.

Chapter 1: Introduction

1.1 Broad Overview

Aging modifies ventricular structure and function in both humans and animals (Fares and Howlett, 2010; Feridooni et al., 2015). For example, aging is associated with impaired contractile function, impaired diastolic function, and left ventricular (LV) hypertrophy (Keller and Howlett, 2016). These maladaptive cardiac changes are believed to predispose the heart towards cardiac diseases such as heart failure (HF) (Keller and Howlett, 2016). However, the impact of age on the heart is variable, and these changes associated with cardiac aging may not be present or may be present to varying degrees in individuals of the same age (Howlett and Rockwood, 2013). For instance, ventricular function declines on average with advancing age, but hearts in some individuals of the same age may perform better than others (Nadruz et al., 2017). Thus, effects of aging are variable and some individuals age more rapidly than others.

The term frailty is used to describe the unmeasured heterogeneity in the risk for adverse outcomes associated with aging (Rockwood et al., 2007). Both men and women who are frail are at greater risk of cardiovascular diseases such as HF and are more likely to be hospitalized and die from this condition (Boxer et al., 2014; Uchmanowicz et al., 2014). Why frailty increases susceptibility to heart diseases is not well understood, in part because very little is known about the impact of frailty on the heart. Preclinical work can be used to investigate this, but few studies in animals have looked at the influence of frailty on age-associated cardiac changes. Previous studies from the Howlett lab found that frail male mice exhibit cardiac hypertrophy with contractile dysfunction at both the cellular and organ levels (Parks et al., 2012; Feridooni et al., 2017; Kane et al., 2020; Kane et al., 2021).

Frailty is also associated with lower heart rates and sinoatrial node dysfunction in aging male mice (Moghtadaei et al., 2016). Sinus bradycardia, a form of sinoatrial node dysfunction, may play a role in the development of HF in older people (Baidurin et al., 2020). Thus, there is evidence that frailty is associated with adverse cardiac remodeling but whether this sets the stage for the development of HF is not yet clear. Also, little is known about the relationship between frailty and the heart in female animals since most previous studies have used only male animals.

A key challenge to understanding the relationship between frailty and HF is that this may differ between the sexes. For example, women are frailer than men (Yang et al., 2010; Gordon et al., 2017; Puts et al., 2005). Women are also more likely than men to develop HF with preserved ejection fraction (HFpEF), characterized by problems with relaxation known as diastolic dysfunction (Afilalo et al., 2014). However, links between frailty and HF in both sexes have not been established as preclinical studies typically use male animals (Howlett and Rockwood, 2013; Beery, 2018). Thus, it is important to understand how frailty affects cardiac changes that may lead to HF in both sexes.

Frailty can be quantified clinically with various instruments (Buta et al., 2016; Dent et al., 2016; De Vries et al., 2011). A frailty index (FI) can be created by adding age-related health deficits such as signs, symptoms, diseases, and laboratory data (Mitnitski et al., 2001; Rockwood et al., 2015) and dividing by the total number of deficits considered to yield a score between 0 (low frailty) and 1 (severe frailty). A higher FI score represents a greater chance of adverse health outcomes (Rockwood and Mitnitski., 2011). Our lab has previously developed a murine FI (Whitehead et al., 2014) based on the approach developed in humans (Minitski et al., 2001). Our lab and collaborators have previously

shown that mice and humans have similar rates of deficit accumulation (Whitehead et al., 2014), that the FI increases with age (Rockwood et al., 2015), and that high FI scores predict mortality and cardiac contractile dysfunction (Rockwood et al., 2017; Feridooni et al., 2017). This powerful tool can be used to investigate mechanistic links between frailty and HF in males and females.

The renin-angiotensin-aldosterone system (RAAS) plays a key role in the pathogenesis of both HF and frailty (Abadir, 2011; Khan et al., 2017). Angiotensin II (Ang II) contributes to myocyte hypertrophy, collagen deposition and fibrosis in HF (Khan et al., 2017). The RAAS may also contribute to the development of frailty, as aging is characterized by elevated Ang II levels and enhanced Ang II signaling (Chugh et al., 2013). For example, levels of the Ang II precursor angiotensinogen are higher in frail than non-frail individuals (Lin et al., 2017). Since increased circulating Ang II contributes to cardiac changes that lead to HF, it can be infused into animals via osmotic mini pumps to model HF and is an established model of this condition (Regan et al., 2015). The overall goals of this thesis are: 1) to determine the effects of Ang II infusion on the cardiovascular system in older C57BL/6 mice; 2) to explore sex differences in Ang II-induced cardiac remodeling and 3) to determine if Ang II-induced HF exacerbates frailty in a sex-specific fashion.

1.2 Heart failure

1.2.1 Overview

HF affects about 20 million people in the world and this prevalence is projected to increase by 25% by 2030 (Heidenreich et al., 2013). HF is a condition in which the heart is unable to pump out enough blood to meet the body's metabolic requirements (Bertero

and Maack, 2018). It arises from structural and functional abnormalities in the myocardium resulting in impaired ventricular filling or ejection (Dassanayaka et al., 2015). Reduced LV myocardial function is the most common cause of HF and this can occur along with dysfunction of the pericardium, endocardium, heart valves and/or great vessels (Dassanayaka et al., 2015). Many pathogenic mechanisms lead to HF including volume or pressure overload, ischemia-related cardiac dysfunction, ventricular remodelling, increased neuro-humoral stimulation, abnormal calcium cycling, increased deposition of the extracellular matrix, and myocardial apoptosis (Dassanayaka et al., 2015). Numerous factors such as old age, coronary artery disease, hypertension, diabetes mellitus, obesity, and smoking contribute to the risks of developing HF (Liu et al., 2018). Among these factors, age contributes significantly to the risks of morbidity, mortality, and healthcare expenditures, particularly in people over 40 years of age (Statistics Canada). About 3.6% Canadian adults over 40 years of age have diagnosed HF (Statistics Canada). As the aging population continues to rise, it is projected that health expenditures for HF will more than double by 2030 (Heidenreich et al., 2013). Given the burden HF imposes on not only patients but also on healthcare systems, a better understanding of the etiologies associated with HF in the older population is critically needed.

1.2.2 Types of HF

HF is classified clinically into two main types depending on the functional status of the heart. These types are HFpEF and HF with reduced ejection fraction (HFrEF), where ejection fraction (EF) is defined as the volume fraction of blood ejected from the LV chamber with each contraction. In Figure 1.1, the image at the top is of the normal heart, and the image on the bottom left shows HFrEF where the LV cavity is enlarged and the

LV walls are dilated (Dassanayaka et al., 2015). The image at the bottom right represents HFpEF where the LV wall is thickened and the volume of the LV cavity is reduced (Dassanayaka et al., 2015).

HFrEF is characterised by having an EF of less than 40% and normal or reduced ratio of LV mass/end-diastolic volume (Dassanayaka et al., 2015). In terms of morphology, the shape of the LV becomes more spherical as HFrEF progresses (Triposkiadis et al., 2018). This remodelling to a globular shape leads to the misalignment of the papillary muscles, chordate, and mitral valve which can lead to mitral regurgitation (Triposkiadis et al., 2018). As a result of mitral regurgitation, further adverse remodelling and LV volume enlargement both progress, which worsens HFrEF (Triposkiadis et al., 2018). The LV wall thickness in HFrEF stays the same or decreases (Triposkiadis et al., 2018). The normal or reduced LV wall thickness combined with increased LV chamber size leads to increased wall stress, which is inversely related to EF (Triposkiadis et al., 2018). Thus, increased wall stress in patients with HFrEF contributes to a further decline in EF (Triposkiadis et al., 2018).

The major pathological mechanisms for reduced EF, however, are reduced contractility due to cardiomyocyte dysfunction and/or cardiomyocyte loss (Simmonds et al., 2020). Cardiomyocyte damage and loss causes eccentric remodelling and an imbalance in cardiac wall structure (Gonzalez et al., 2011). Cardiomyocyte damage in HFrEF also leads to a decline in the number of functioning cardiomyocytes and increased accumulation of fibrotic tissue (Paulus et al., 2013; Xu et al., 2013). Apoptosis, necrosis, necroptosis, and autophagy are implicated in cardiomyocyte loss during HFrEF (Simmonds et al., 2020). It has been observed in animal models that even low levels of cardiomyocyte

apoptosis can induce HFrEF (Hartupee et al., 2017). In addition, mitochondrial regulatory proteins are upregulated during HFrEF in a type 1 diabetes mellitus-induced model of cardiac myopathy, which suggests that mitochondrial dysfunction could play a role in cardiomyocyte apoptosis (Hamblin et al., 2007).

There is also evidence that cells other than cardiomyocytes contribute to the pathogenesis of HFrEF. In the healthy heart, the extracellular matrix (ECM) contains thick collagen type I fibers, which maintain tensile strength, and thin collagen type III fibers, which contribute to elasticity (Frangogiannis, 2019). The production and degradation of collagen regulate the amount and composition of the ECM (Cowling et al., 2020). Cardiac fibrosis occurs when the deposition of collagen in the heart exceeds its degradation (Cowling et al., 2020). A multitude of pathological stresses such as aging, hypertension, diabetes, pressure overload, and/or myocardial injury are known to contribute to the development of cardiac fibrosis (Simmonds et al., 2020). In HFrEF, cardiac fibrosis arises from cardiomocyte loss and may result in systolic dysfunction via multiple pathways (Simmonds et al., 2020). Collagen damage or loss may lead to the uncoordinated contraction of cardiomyocytes by disrupting the transduction of cardiomyocyte contraction into myocardial force (Simmonds et al., 2020). In addition, cardiac fibrosis causes impairment of endomysial structures such as laminin, which link together cardiomyocytes and adjacent components, leading to cardiomyocyte impairment (Kong et al., 2014). Thus, there are many factors that contribute to the pathogenesis of HFrEF, with cardiomyocyte damage and loss being the main drivers of this process.

Among HF patients, HFpEF has a higher prevalence than HFrEF (Savares and Lund, 2017). HFpEF has only recently been recognized and is an emerging healthcare

challenge. HFpEF patients generally have a normal EF of equal to or higher than 50%, with thickened and stiff LV walls despite normal LV cavity volume (Ma et al., 2020). There is also a higher ratio of LV mass to end-diastolic volume in HFpEF, unlike HFrEF where this is reduced (Ma et al., 2020). In HFpEF, the diastolic function of the heart is impaired, which means that the LV cannot relax properly and is thus unable to adequately fill with blood (Ponikowski et al., 2016). The thickening of the LV walls also reduces the cavity space to hold blood (Ponikowski et al., 2016). Despite the heart's ability to contract effectively, the reduced volume of blood in the LV results in insufficient blood pumped out to meet the body's metabolic demands (Ponikowski et al., 2016). In HFrEF, reduced LV function leads to decreased cardiac output (King et al., 2012). In HFpEF, cardiac output is impaired by reduced ventricular compliance and abnormal relaxation (King et al., 2012).

At the cellular level, cardiomyocyte diameter and myofibril volume are much larger in HFpEF when compared to HFrEF (Dassanayaka et al., 2015). While excessive collagen deposition as a result of cardiomyocyte loss causes systolic dysfunction in HFrEF, this event contributes to diastolic dysfunction in HFpEF by increasing cardiac wall stiffness without cardiomyocyte loss (Echegaray et al., 2017). In HFpEF patients, circulating troponin-T, which is an indicator of cardiomyocyte apoptosis, is not detectable (Brouwers et al., 2013). However, when apoptotic and autophagic genes are inhibited in a rat model of HFpEF, diastolic dysfunction improves, but apoptosis and/or autophagy do decline (Chaanine et al., 2016). Given the importance of HF prevention in the general population, further investigation into the mechanisms underlying the pathogenesis of HF is critical.

The major risk factors for HFpEF are hypertension, age, female sex, and diabetes (Yancy et al., 2013). Still, compared to HFrEF, the factors contributing to HFpEF are poorly understood (Parikh et al., 2018). Studies suggested that risk factors for HFpEF contribute to the advancement of normal age-related changes in the heart, making it a systemic disease rather than purely a cardiac disease (Van der Velden et al., 2016). In addition, most HFpEF patients have more than two comorbidities such as hypertension, coronary artery disease, atrial fibrillation, obesity, and/or chronic kidney disease (Ergatoudes et al., 2019). A greater understanding of how different factors contribute to HFrEF and HFpEF is needed to better direct further treatment, especially for older patients. Given the importance of aging in promoting HF, the relationship between aging and HF will be further discussed in the next section.

1.2.3 Pathophysiology of HF in aging

Aging increases the risk of developing HF. For example, about 5.2 per 1000 Canadian adults 40 years of aged and older are newly diagnosed with HF (Statistics Canada). There are many physiological and biological factors that link aging to HF (Triposkiadis et al., 2019). A combination of some or all these factors can reduce cardiac reserve over time, which makes the heart more prone to failure (Triposkiadis et al., 2019).

There are a number of cardiac structural and functional changes associated with aging that are implicated in the development of HF. For instance, aging leads to increased deposition of collagen in the myocardial ECM, a reduction in elastin, and increased fibronectin (Meschiari et al., 2017). Together, these age-associated changes lead to increased fibrosis associated with aging increased LV stiffness, which impacts diastolic function (Cowling et al., 2020). Furthermore, cardiomyocyte size increases with age, and

this increases myocardial wall thickness (Akashiva et al., 2015). The shape of the heart also changes from elliptical to spheroid, along with an asymmetric increase in the thickness of the interventricular septum more than the LV free wall (Triposkiadis et al., 2018). These changes in thickness and shape increase cardiac wall stress and reduce contractile capacity (Triposkiadis et al., 2018). With aging, the heart also undergoes functional changes such as decreased contractility, prolonged systolic contraction, and increased EDV, which impairs systolic function (Jakovljevic, 2018). Aging affects the cellular reactions controlling cardiomyocyte contraction including prolonged cytosolic calcium transients and a reduced calcium sequestration into stores in the sarcoplasmic reticulum (SR) (Hamilton and Terentyev, 2019). These factors are thought to contribute to reduced systolic function (Hamilton and Terentyev, 2019). The effects of aging on systolic function are evidenced by lower exercise tolerance in older people (Kim et al., 2016). The maximum consumption of oxygen or VO_2 max declines progressively with advancing age by about of 15% between the age of 50 and 75 (Kim et al., 2016). Thus, aging is associated with marked structural and functional changes in the heart at both the cellular and organ levels. These changes may reduce heart function and increase its susceptibility to HF.

1.2.4 Sex differences in HF

Aging increases the prevalence of HF in both sexes, but women are more likely to develop HF at a later age when compared to men (Bozkurt and Khalaf, 2017). Other risk factors that contribute to HF in both sexes include hypertension, diabetes mellitus, obesity, and ischemic heart diseases (Ahmad et al., 2016). Although males have a higher HF incidence compared to females at all ages, the risk of developing HF is similar in both sexes due to the longer life span in females (Meyer et al., 2015).

The symptoms of HF, including dyspnea, edema, and fatigue, are similar in men and women. However, symptoms are also more severe and more frequent in women when compared to men (Brouwers et al., 2013). In both HFrEF and HFpEF, women have more physical limitations, longer hospital stays, poorer quality of life, and higher depression rates when compared to men (Bozkurt. and Khalaf, 2017). Despite common risk factors, females are more likely to develop HFpEF, whereas males are predisposed towards HFrEF (Ho et al., 2016). Within HFpEF, women have an increased burden of comorbidities over time (Lam et al., 2019). Furthermore, female patients with HFpEF tend to have concentric LV hypertrophy along with severe diastolic dysfunction (Harada et al., 2018; Lundorff et al., 2018). By contrast, men with HFpEF are more likely to develop eccentric LV hypertrophy (Harada et al., 2018). Arterial stiffness and LV end-systolic stiffness are also higher in women with HFpEF than in men with this condition (Lundorff et al., 2018). In patients with HFrEF, women live longer than men do but have worse health outcomes and poorer quality of life (Dewan et al., 2019). Women with HFrEF also have a higher prevalence of nonischemic cardiomyopathy than men (Fairweather et al., 2013). It is clear that there are major male-female differences in HF, although little is known about the underlying mechanisms. Further research is needed to better understand sex differences in HF and the associated pathophysiological factors that underlie this disease.

1.2.5 The role of angiotensin II in promoting HF

The mechanisms underlying age-related cardiac remodeling and HF are not fully understood, although a number of ideas have been suggested. The RAAS is thought to play an important role in the physiopathology of HF (Rossi et al., 2017). In patients with HF, the activity of the RAAS is increased (Rossi et al., 2017). The RAAS is fundamentally

involved in regulating blood pressure, maintaining fluid balance, and vascular tone (Dudoignon et al., 2019). Figure 1.2 shows the RAAS pathway as well as the short-term and long-term effects of Ang II on the cardiovascular system. In response to systemic hypotension and/or reduced sodium levels, the juxtaglomerular cells of the kidneys release renin (Sequeira-Lopez and Gomez, 2021). Renin converts angiotensinogen, which is constitutively secreted by the liver, to angiotensin I (Ang I). The vascular endothelium in the lungs releases angiotensin converting enzyme (ACE) that subsequently cleaves Ang I to Ang II. Ang II increases the reabsorption of water directly, by stimulating sodium retention by the kidneys, and indirectly by triggering the release of aldosterone (Sequeira-Lopez and Gomez, 2021). Both mechanisms cause the body to retain sodium and this subsequently promotes water reabsorption (Sequeira-Lopez and Gomez, 2021). Ang II also causes vasoconstriction and increases blood volume, which increases blood pressure and cardiac output (Sequeira-Lopez and Gomez, 2021). In myocardial injury, cardiac contractility declines and hemodynamic load increases, which activates the RAAS and releases Ang II to maintain cardiovascular homeostasis (Rossi et al., 2017). These adaptive mechanisms induced by Ang II are effective at combatting the sudden decline in cardiac function in the short term, but chronically this leads to adverse cardiac remodelling that progresses to HF (Rastini et al., 2017). Studies in rats between 3 and 24 months old show that cardiac Ang II levels increase with age (Monteonofrio et al., 2021). Over time, chronic release of Ang II results in hypertension, cardiac hypertrophy, and adverse cardiac remodeling that promotes HF (Rastini et al., 2017). Therefore, Ang II plays a role not only in the early stages of HF to maintain cardiac homeostasis, but also in the longer term negative remodeling that progresses to HF.

In animal models of cardiac hypertrophy induced by pressure and volume overload, elevated Ang II levels contribute to cardiac hypertrophy and contractile dysfunction (Zhou et al., 2016). Chronic overproduction of Ang II induces systolic dysfunction and the early onset of diastolic dysfunction that eventually leads to HF and further remodeling (Rastini et al., 2017). Blood flow to vital organs declines as HF progresses and Ang II levels continue to rise (Kemp and Conte, 2012). In an attempt to redirect blood flow to compromised organs, vasoconstriction mechanisms are activated (Kemp and Conte, 2012). However, this only increases the hemodynamic stress on the failing heart and eventually leads to death in animals as it does in humans (Kemp and Conte, 2012). Thus, modulation of Ang II via RAAS activation plays a key role in the pathophysiology of HF in both humans and animals.

1.2.6 Animal models of HF

In order to gain a better understanding of the pathogenesis of HF and develop new treatments for HF, preclinical studies require appropriate HF models that allow for in-depth examination of factors contributing to the condition. Aging spontaneously hypertensive rats (Boluyt et al., 1995), Dahl salt-sensitive rats (Doi et al., 2000; Koltz et al., 2006), aortic banding (Helies-Toussaint et al., 2005), and Ang II infusion via osmotic minipumps (Regan et al., 2015) have commonly been employed to induce HF in rodent models.

The aging spontaneously hypertensive rat is a model of genetic hypertension that was first developed by Okamota and Aoki (1963). This model is thought to have similar characteristics as hypertension in humans (Bing et al., 1995). In aging spontaneously hypertensive rats, the progression from compensative hypertrophy to HF with increasing age is similar to HF development in hypertensive patients (Bing et al., 2002). Thus, this

animal model has been commonly used in preclinical studies to model HF (Bing et al,, 2002; Conrad et al., 1991; Pagan et al., 2015). The Dalh salt-sensitive rat is another genetic model of hypertensive HF. These rats develop hypertension when fed a high-salt diet after 4 weeks (Ogihara et al., 2002). Initiation of high-salt diet at different ages induces different types of HF (Doi et al., 2000). While these models are very useful, they both require the use of rats, which are very expensive to use in studies of aging.

The aortic banding method in rodent models induces chronic pressure overload, which leads to cardiac hypertrophy and interstitial fibrosis that result in HF over time (Patel and Patel, 2021). While this is a useful model of HF, aortic banding requires highly invasive surgical procedures and specific technical skills (Tsukamoto et al., 2013). Furthermore, this method does not entirely mimic HF and the time courses in developing HF is extremely variable (Tsukamoto et al., 2013). For these reasons, other models of HF in mice were considered in this thesis.

Ang II infusion via subcutaneously implantation of osmotic minipumps is often a preferred method of inducing HF, as it overcomes many of the challenges associated with other methods including high cost, technical surgeries, and inconsistency. The administration of drugs using osmotic minipumps minimize the stress experienced by the mice, as they reduce the need to handle the animals. In addition, the pumps allow for delivery of drugs at a constant rate and for a long period, which better mimics clinical conditions associated with chronic hypertension. The dosage can also be adjusted to mimic different physiological conditions. However, one drawback of the pumps is that the surgical implantation procedure is invasive. Still, multiple studies have demonstrated that chronic Ang II infusion effectively induces cardiac hypertrophy and hypertensive HF in

rodents (Huentelman et al., 2005; Mousa et al., 2008; Westermann et al., 2012). Thus, Ang II-infusion via osmotic minipumps provides a reliable, low-cost, and low-stress method of inducing hypertensive HF in rodent models. This animal model will be deployed in this thesis to investigate the physiological mechanisms of HF, and how these may differ between the sexes.

1.2.7 Summary

It is well established that aging modifies cardiac structure and function. This may increase the risk of developing diseases like HF in later life. As mentioned in the previous sections, aging increases the risks of HF in both sexes, but women are more likely to develop HF than men. Sex differences are also present in HF phenotypes and HF-related comorbidities. Within each sex, there is considerable heterogeneity in the manifestations of HF. This is not often considered in pre-clinical and clinical studies. Not all individuals of the same age (and sex) are at similar risk for developing HF and they may not have similar manifestations of this condition. Furthermore, the use of exclusion criteria in studies may mask the heterogeneity in HF phenotypes and responses to HF in patients of the same age (and sex). The concept of frailty is used to account for this heterogeneity and may contribute to variations in HF expression in different groups. This will be further explored in the next section.

1.3 Frailty

1.3.1 Introduction to frailty

It is well established that not everyone ages at the same rate, so their chronological age may not reflect their biological age (Clegg et al., 2013; Mitnitski, Howlett, and

Rockwood, 2017). The term "frailty" is used to describe unmeasured heterogeneity in the risk for adverse outcomes associated with aging (Rockwood et al., 2007). Frailty can be described as a state of increased negative health outcomes in people of the same age (Rockwood et al., 1994; Bergman et al., 2007; Singh et al., 2014). Frailty can be quantified by the accumulation of health deficits wherein the health status of an individual declines as they accumulate more deficits (Rockwood et al., 1994; Howlett and Rockwood, 2013). As these deficits accumulate, the body's ability to repair itself starts to decline leading to failure at the cellular, organ, and eventually the system level (Rockwood et al., 1994; Howlett and Rockwood, 2013). Thus, frailty can be used to quantify overall health status and assess vulnerability to multiple stressors in an individual (Hubbard et al., 2017).

1.3.2 Quantifying frailty in humans

Given the important role of frailty in advancing age-associated diseases, it is important to investigate frailty using a quantitative approach to better understand the underlying mechanisms and develop therapeutic interventions. There are a number of different methods to quantify frailty in clinical and preclinical studies (Dent et al., 2016). It can be challenging to quantify frailty in humans, since some frailty tools have low sensitivity and predictive properties (Hubbard et al., 2017; De Vries et al., 2011). There is also a lack of reliability agreement, responsiveness, and interpretability with many frailty tools (De Vries et al., 2011). Despite the abundance of frailty tools, there is still no standard frailty assessment tool for clinical populations (Howlett and Rockwood, 2013). The two most commonly used methods of frailty assessment in clinical studies are the Frailty Phenotype and the FI tools (De Vries et al., 2011; Howlett and Rockwood, 2013). Fried and colleagues defined frailty as a geriatric physical syndrome with five identifiable

phenotypic criteria including weight loss, exhaustion, weakness, slowness, and lack of physical activity (Fried et al., 2001). This so-called Frailty Phenotype considers an individual as robust or non-frail if none of the above criteria is present, pre-frail if one or two criteria are present, and frail if three or more criteria are present (Fried et al., 2001).

Frailty in an individual can also be quantified with an FI created by counting the proportion of accumulated deficits including symptoms, signs, functional impairments, and laboratory abnormalities (Minitski et al., 2001; Rockwood et al., 2005). The FI concept was developed based on the idea that the number of accumulated deficits increases as people age (Rockwood et al., 2011). This index includes deficits that are age-related, associated with adverse outcomes, and present in multiple organ systems (Searle et al., 2008). An FI score is obtained by counting the number of health deficits in an individual and dividing this by the total number of deficits measured to yield a ratio between 0 and 1 (Searle et al., 2008). A higher FI score indicates that an individual has accumulated many deficits and therefore has a high degree of frailty. When at least 30 different deficits are measured, the resulting FI is not strongly influenced by the nature of the individual deficits considered (Rockwood and Mitnitski, 2011). The FI is strongly correlated with declining health status, hospitalization, and mortality across a wide range of systems (Rockwood and Mitnitski, 2007). A systematic review and meta-analysis on frailty and clinical outcomes in HF by Zhang et al. (2018) reported that frailty significantly predicted mortality and hospitalization in HF patients. It is a useful clinical tool allowing frailty to be quantified based on the number of accumulated deficits rather than simply identifying an individual as frail or non-frail (Rockwood and Mitnitski, 2007).

1.3.3 Quantifying frailty in mice

Although the FI has been used in many clinical studies of frailty, only recently has it been adapted for use in pre-clinical models (Parks et al., 2012; Whitehead et al., 2014; Rockwood et al., 2017). Parks and colleagues were the first to develop an FI measuring deficit accumulation in naturally aging C57BL/6 mice (Parks et al., 2012). This mouse FI measures 31 health-related deficits such as changes in activity levels, hemodynamic parameters, body composition and metabolism. Each deficit is graded with a score of 0, 0.5, 1 for no deficit, mild deficit, and severe deficit respectively. The scores for all the deficits are added and divided by the total number measured to yield a score between 0 and 1 with higher numbers denoting a higher level of frailty (Parks et al., 2012). Since this approach is invasive, time consuming, and requires specialized equipment, Whitehead and colleagues developed a non-invasive mouse FI (Whitehead et al., 2014) based on approaches used in humans (Minitski et al., 2001). This mouse FI consists of 31 observable signs of deficits in multiple systems including digestive, integument, musculoskeletal, vestibulocochlear, ocular, and respiratory systems as well as signs of discomfort (Whitehead et al., 2014). The mouse FI score was found to increase with increasing age (Whitehead et al., 2014) and a higher score is associated with an increased risk of mortality as previously seen in humans (Rockwood et al., 2017). Other similarities to humans are that mice have similar rates of deficit accumulation and the FI distribution broadens with age in both mice and humans (Whitehead et al., 2014; Rockwood et al., 2017). This approach is adaptable for use in different experiments and laboratories as it has been shown to have high inter-rater reliability (Feridooni et al., 2015), and it can also be adapted for use in different animals such as in aging rats (Yorke et al., 2017). The mouse clinical FI is

a useful, inexpensive, and non-invasive method that will facilitate understanding of the pathological mechanisms involved in frailty and help identify new interventions that aim to reduce frailty.

1.3.4 Sex differences in frailty

It has recently been established that frailty is not solely age-dependent, but also sex-dependent (Kane et al., 2020). There are sex differences in biochemical, physiological, and behavioral factors that change with age, which underpins the notion that sex may be an important contributor to frailty status (Pomatto et al., 2018; Le Couteur et al., 2018; Roberts et al., 2018). Both men and women who are frailer are at greater risks for HF, hospitalization, and mortality (Boxer et al., 2014; Uchmanowicz et al., 2014). However, women aged over 65 years tend to be frailer and have poorer health status compared to men of the same age (Collard et al., 2012; Gordon et al., 2017). On the other hand, women appear to be more robust and have a longer lifespan than men at any given biological age or frailty level (Gordon et al., 2017). This phenomenon is termed the sex-frailty paradox or the male-female health-survival paradox (Oksuzyan et al., 2008; Hubbard and Rockwood, 2011).

Using the FI tool, meta-analysis studies demonstrated that the mean FI in women is greater than men for any age (Minitski et al., 2005; Shi et al., 2014; Gordon et al., 2017). This finding suggests that the prevalence of deficits inherently differs between sexes (Gordon et al., 2017). In a study including people over 50 years of age, males and females both accumulated more co-morbidities with age but females accumulated a higher number of deficits overall (Avedano and Mackenbach, 2008). Many studies have demonstrated that the high prevalence of co-morbidities in females negatively impacts their quality of

life and contributes to the increased rates of self-reported disabilities (Crimmins et al., 2010; Shi et al., 2014; Avedano and Mackenbach, 2008). In addition, studies examining sex differences in mortality found that males have a higher mortality rate until 90 years of age, at which point it is surpassed by the female mortality rate (Garcia-Gonzalez et al., 2009; Romero-Ortuno and Kenny, 2012). Other studies also found that the male mortality rate is higher than females for all age groups (Gu et al., 2009; Shi et al., 2014). Minitski et al. (2005) and Romero-Ortuno and Kenny (2012) demonstrated that mortality rates were higher for males than females at each level of FI, despite men having lower FI values. When controlling for age and frailty, the risk of death for females is 33% lower compared with men (Garcia-Gonzalez et al., 2009). These studies show that sex differences in the FI reflect the male-female health-survival paradox.

Sex differences in frailty in mice are generally similar to humans. Kane et al. (2018) found that the prevalence of frailty was higher in female C57BL/6 mice and this increased with age. In addition, Baumann et al. (2019) reported that the level of frailty in female mice at 26 months of age was 66% higher compared to male mice of the same age. This study also demonstrated that frailer mice had a higher mortality rate, regardless of sex (Baumann et al., 2019). Other studies have also reported similar findings in that female C57BL/6 mice have greater FI scores compared to age-matched males (Whitehead et al., 2014; Kane et al., 2018). Furthermore, non-frail female mice were found to be more physically active than non-frail males (Rosenfeld, 2017; Baumann et al., 2019). For example, non-frail females ran about 65% further on voluntary wheels than males (Baumann et al., 2019). These findings show that FI tool provides an avenue to explore sex differences in frailty in animal models.

Whether there are sex differences in mortality for C57BL/6 mice is controversial as studies have reported conflicting findings. Several studies have shown that male C57BL/6 mice live longer than female mice (Baumann et al., 2019; Miller et al., 2002; Ali et al. 2006). A review by Austad and Fischer (2016) examined 29 studies on lifespan of C57BL/6 mice and found that males survived longer in 18 studies, and females survived longer in 11 studies. From these studies, it is still unclear whether the sex-frailty paradox observed in humans also exists in C57BL/6 mice. Nonetheless, these findings suggest that sex differences are present in aging C57BL/6 mice and should be considered when assessing frailty.

1.4 Frailty and HF

1.4.1 Overview

Frailty is common in patients with HF, affecting almost half of people with HF (Denfeld et al., 2017). People over 65 years of age make up over 80% patients with HF, and approximately 25% of this population exhibit frailty (Go et al., 2013; Dodson and Chaudhry, 2012). The prevalence of frailty in HF increases with age, from about 3% in those 65-70 years to 23% in those over 90 years of age (Fried et al., 2001; Newman et al., 2001; Jha et al., 2015). HF prognosis is worse in frail patients when compared to non frail patients, and frailty is an independent risk factor for HF in older patients (Shinmura, 2016). Older HF patients are also at higher risks of adverse health events including falls, hospitalizations, and mortality (Uchmanowicz et al., 2019; Cacciatore et al., 2005). There is evidence that HF patients have a higher susceptibility to falls and cognitive impairment due to reduced cerebral perfusion, which advances frailty and disability (Singh et al., 2014).

Younger HF patients are also susceptible to developing frailty (Chung et al., 2014; Jha et al., 2015). The presence of frailty in younger HF patients suggest that frailty in HF should be considered for patients of all ages rather than only in older adults (Denfeld et al., 2017).

The prevalence of frailty in HF is about 45% across a wide age range, which is higher than the prevalence of frailty among older patients (Denfeld et al., 2017). This suggests that the pathogenesis underlying frailty in HF includes factors other than chronological age. Studies have suggested that factors including neurohormonal dysregulation, inflammation, and skeletal muscle dysfunction contribute to the pathogenesis of frailty; these factors also contribute to the pathogenesis of HF (Boxer et al., 2014). The specific mechanisms of frailty in HF are not well understood but are being investigated for the potential of targeting frailty through HF therapies (Maurer et al., 2017). Since the majority of studies examining HF in frailty are in older HF patients, more research is needed to assess frailty in a wide range of age and HF subpopulations to better understand how frailty plays a role in HF. The next section will further examine the underlying biological factors that contribute to frailty in HF.

1.4.2 Pathogenesis of frailty in HF

Frailty and HF share some common pathological pathways including circulating pro-inflammatory cytokines and sarcopenia (Bellumkonda et al., 2017). It has been suggested that long-term HF induces chronic changes in underlying skeletal muscle leading to loss of lean muscle mass or sarcopenia, which is also present in frailty (Puthucheary et al., 2013; Kitzman et al., 2014). In HF patients, cellular and molecular changes in skeletal muscle are different from those in normal aging and inflammatory processes (Joseph and Rich, 2017). Mechanisms such as dysregulation of neurohormonal, metabolic,

immunologic, and musculoskeletal systems are thought to contribute to this enhanced catabolic state of frailty in HF (Joyce et al., 2016). It is likely that the mechanisms underlying both frailty and HF disrupt homeostasis and contribute to chronic inflammation (Bellumkonda et al., 2017).

Circulating proinflammatory cytokines such as TNF-α, IL-6, and IFN-γ, are associated with frailty and are present at high levels in HF patients (Kalogeropoulos et al., 2010; Mann, 2015). This suggests that both HF and frailty could share common inflammatory pathways (Bellumkonda et al., 2017). The upregulation of inflammatory cytokines contributes to neurohormonal dysregulation, which has been found to advance adverse cardiac remodeling and myocardial damage in chronic HF (Joseph and Rich, 2017). Inflammation affects the regulation of hormones such as cortisol, insulin, and growth hormone, which leads to the enhanced catabolic state observed in frailty in HF (Uchmanowicz et al., 2014; Joyce et al., 2016). The upregulation of inflammatory cytokines can also promote atherosclerosis and vascular senescence which advances aging, negatively affects body composition, and thus exacerbates frailty (Afilalo et al., 2014; Uchmanowicz et al., 2014; Goldwater and Pinney, 2015). Furthermore, increased intravascular hydrostatic pressure due to fluid retention in HF may lead to intestinal congestion, abdominal discomfort, and appetite loss, which may exacerbate cachexia and inflammation (Valentova et al., 2016). Thus, frailty in HF is related to imbalanced anabolic-catabolic systems that involve dysregulation of neurohormonal, inflammatory, and musculoskeletal mechanisms.

Other biological mechanisms that may occur in both frailty and HF including DNA damage, impaired autophagy, and mitochondrial dysfunction (Uchmanowicz et al., 2019).

These factors can also contribute to metabolic dysfunction, cellular senescence and cellular necrosis which activate the production of circulating proinflammatory cytokines (Uchmanowicz et al., 2019). For example, the IL-6 family cytokines and the gp130 receptor have been implicated in the pathogenesis of HF (Jacoby et al., 2003). Signal transducer and activator of transcription 3 (STAT3) is a signaling protein that is activated via the gp130 receptor (Jacoby et al., 2003). The protein STAT3 plays a role in reducing redox stress and enhancing mitochondrial function (Bellumkonda et al., 2017). Aged mice without STAT3 have higher levels of proinflammatory cytokines and cardiac fibrosis (Jacoby et al., 2003; Bellumkonda et al., 2017). STAT-3 deficient mice also develop cardiac dysfunction with age (Jacoby et al., 2003). The Nod-like receptor protein 3 (NLRP3) inflammasome is another mediator of inflammation that is thought to play a role in both HF and frailty. Specifically, NLRP3 inflammasome activation is involved in age-related inflammation (Cutler et al., 2004). Overall functional decline occurs as a result of age-related inflammation in multiple organs even in the absence of diseases (Jacoby et al., 2003). Furthermore, Youm et al. (2013) found that aged mice without the NLRP3 inflammasome walked longer distances and ran for longer durations than wild-type controls, suggesting that NLRP3 may contribute to inflammation that leads to frailty. NLRP3 has also been found to be activated in HF patients (Butts et al., 2015; Bellumkonda et al., 2017). These findings suggest that NLRP3 may be a shared pathophysiological connection between frailty and HF (Bellumkonda et al., 2017). As aging plays a role in both frailty and HF, it is likely that age-related inflammatory processes share common pathways linking frailty and HF.

1.4.3 The influence of frailty on cardiac structure in mice

It has been previously discussed in the HF section that that aging is associated with cardiovascular changes in the cardiac system and that there are differences between the sexes. Still, there is considerable heterogeneity in cardiac remodelling at a given age. Rather than simply measuring chronological age, using frailty as an outcome measurement can lend greater insight into the impact of age on the heart. Preclinical studies looking at the impact of age and frailty on the heart demonstrated that many changes in cardiac structure are influenced by both frailty and chronological age. The findings from these studies are summarized in Table 1.1. Feridooni et al. (2017) showed that cardiac hypertrophy (increased heart weight to body weight or tibia length ratios) in older male mice were strongly correlated with both age and frailty, but this change was significantly graded by frailty only. This suggests that cardiac hypertrophy increases with age and that this change is largely attributable to frailty (Feridooni et al., 2017). Jansen et al. (2017) found that increased interstitial fibrosis and total collagen content in the left and right atria from both young and old male mice was strongly correlated with FI scores (Jansen et al., 2017). Furthermore, Kane et al. (2021) showed that ventricle collagen levels increased with age and were graded by frailty in male but not female mice. Measures of hypertrophy such as septal wall thickness were correlated with frailty in both sexes, whereas LV mass increased with frailty in females only (Kane et al., 2021). Together, these results demonstrate that frailty rather than chronological age is an effective outcome measurement for age and sex-dependent cardiac remodelling.

Studies in mice have shown that frailty also affects the heart at the cellular level. Ventricular myocyte hypertrophy (increased length, width, and cross-sectional area) occurs

in myocytes isolated from aged and frail hearts in mice of both sexes (Parks et al., 2012, Feridooni et al., 2017). Previous studies have reported that ventricular myocyte hypertrophy is linked to age in older animals including mice, rats, and monkeys (Fraticelli et al., 1989; Zhang et al., 2007; Feridooni et al., 2015). By contrast, others have reported no age-related difference in myocyte size (Guo and Ren, 2006; Ren et al., 2007; Mellor et al., 2014). Interestingly, when taking frailty into consideration, cell dimensions (length, width, and cross-sectional area) are positively correlated with and graded by FI scores but not age in male mice (Parks et al., 2012, Feridooni et al., 2017). Thus, ventricular myocyte hypertrophy, which has been traditionally linked to aging, might be more closely related to frailty.

The mechanisms by which frailty influences cellular cardiac hypertrophy are not well understood. Myocyte hypertrophy is accompanied by loss of myocytes which could be due to necrosis, apoptosis, and/or phagocytosis (Miller and Zachary, 2017). The loss of myocytes in the ventricle causes surviving myocytes to bear a larger workload and subsequently undergo hypertrophy as a compensatory mechanism (Miller and Zachary, 2017). The larger workload due to cardiomyocyte loss is also associated with increased proliferation of fibroblasts which produces ECM to compensate for the increased stress (Horn and Trafford, 2016; Piek et al., 2016). Excessive deposition of ECM leads to fibrosis in the atria, sinoatrial node, and ventricles characteristic of HF (Mirza et al., 2012; Dzeshka et al., 2015). Increased interstitial fibrosis in the SA node as well as the right and left atria are seen in hearts isolated from aged and frail male mice (Moghtadaei et al., 2016; Jansen et al., 2017).

Matrix metalloproteases (MMPs) and the interaction of these proteins with tissue inhibitors of metalloproteases (TIMPS) mediate the increase in fibrosis in male mice (Moghtadaei et al., 2016; Jansen et al., 2017). The role of MMPs is to degrade collagens and other ECM proteins, while TIMPs function to inhibit MMPs (Kassiri and Khokha, 2005; Nagase et al., 2006). The potential mechanisms for atrial fibrosis in aged and frail hearts can be explained by the downregulation in the expression of MMP2 (known to degrade collagen type III; Kassiri and Khokha, 2005) and changes in the levels of interactions between MMP2 and various TIMPs (TIMPs 1-4) (Jansen et al., 2017). These alterations in the expression patterns of MMP2 and TIMPs result in less collagen being broken down which contributes to enhanced fibrosis. Furthermore, the cellular events involved in the increased atrial fibrosis (including collagen content, MMP2 expression, MMP2-TIMPs interactions) are all strongly correlated with FI scores but not age, suggesting that frailty strongly predicts age-associated structural remodelling in the atria in male mice (Moghtadaei et al., 2016; Jansen et al., 2017).

1.4.4 Effects of frailty on cardiac contractile function in mice

Frailty has also been shown to affect myocardial contractility by causing dysregulation of calcium homeostasis. During depolarization, L-type calcium channels open to allow calcium into the heart cells (Bers, 2014). This small influx of calcium initiates the release of a large of amount of calcium from the SR into the cytosol, resulting in a rise in the calcium concentration in the cell known as the calcium transient (Bers, 2014). A small decrease in SR calcium being released would result in a significant decrease in the amplitudes of calcium transients (Bers, 2014). Consequently, contractile dysfunction occurs when the process linking cardiomyocyte contraction to intracellular calcium

handling is disrupted. In aged and frail mice of both sexes, ventricular myocytes exhibit smaller and slower contractions (Parks et al., 2012; Feridooni et al., 2017). This decline in myocyte contractions is accompanied by smaller peak calcium transients in aged and frail male mouse hearts. Furthermore, reduced calcium influx and SR calcium release contributes to smaller calcium transients (Feridooni et al., 2017). Aged and frail hearts of male mice also have a lower expression of the Cav 1.2 protein (the pore-forming subunit of the L-type voltage-dependent calcium channel), causing less calcium influx which ultimately contributes to the decline in myocyte contractions (Feridooni et al., 2017). Overall, these components of myocyte contractions (including smaller myocyte contractions; less calcium influx, reduced SR calcium release, and less Cav 1.2 expression) in male mice are highly correlated with and graded by FI scores (Feridooni et al., 2017). This suggests that frailty is a strong predictor of contractile dysfunction during the aging process (Feridooni et al., 2017), at least in male animals.

Recent studies have shown that there are sex differences in the effects of frailty on age-associated cardiomyocyte contractile function. Aging impacts the phosphorylation levels of major myofilament proteins including myosin light chain-1, desmin, and tropomyosin (Kane et al., 2020). Kane et al. (2020) found that age was associated with increased phosphorylation of myosin light chain-1 as well as enhanced phosphorylation of desmin and tropomyosin in males but not females. Interestingly, these adverse changes were also graded by FI scores in males only. Since tropomyosin activity directly or indirectly affects the cooperativity of the actomyosin Mg-ATPase-calcium relationship represented by Hill coefficients (Loong et al., 2012), the study also assessed the effects of age and frailty on this cooperativity. Results showed that Hill coefficients declined with

age and were graded by frailty in males but not females (Kane et al., 2020). A higher Hill coefficient indicates positive cooperativity of the actomyosin Mg-ATPase-calcium relationship (Loong et al., 2012). Research has shown that phosphorylation of tropomyosin in reconstituted cardiac muscle fibers is associated with reduced cooperativity (Lu et al., 2010). Thus, increased phosphorylation of tropomyosin may decrease cooperativity, which negatively affects contractile function in the aging male heart (Kane et al., 2020). These changes were not correlated with frailty in the aging female heart, which suggests that the female heart may be less affected by poor health status (eg. frailty) compared to the male heart (Kane et al., 2020).

Frailty also affects age-related cardiac contractile function at the organ level in a sex-specific fashion. Kane et al. (2021) reported that E/A ratios declined with age and were graded by frailty in male mice only. Furthermore, measures of systolic function, including EF and fractional shortening (FS) increased with age and correlated with FI scores in males but not females (Kane et al., 2021). Research suggests that EF increases in order to compensate for smaller LV-end diastolic volumes that can occur with aging (Gebhard et al., 2013). Elevated LV EF (≥70%) has been shown to be associated with increased mortality in patients with and without HF (Wehner et al., 2020). Changes in phosphorylation levels of myofilament proteins in aging mouse hearts may also at least partially compensate for smaller intracellular calcium transients and cause increased EF (Kane et al., 2020; Kane et al., 2021). Overall, these results suggests that frailty is a better predictor of contractile dysfunction in hearts from male mice when compared to female mice.

1.5 Rationale

Previous studies using the FI tool have shown that frailty facilitates maladaptive changes associated with cardiac aging in mice of both sexes (Feridooni et al., 2017; Kane et al., 2020; Kane et al., 2021). However, this age-associated remodeling differs between sexes (Kane et al., 2021) and may facilitate the development of HF in a sex-specific fashion. As mentioned in previous sections, HF manifestations may differ according to age and sex. Despite this, most preclinical studies of heart diseases have used young adult male animals. The overall goal of this thesis is to use Ang II infusion to determine if hypertension-induced HF differs between the sexes and exacerbates frailty in aging male and female mice in a sex-specific fashion.

1.6 Objectives

The specific objectives of this work were to:

1. Determine the effects of Ang II infusion on the cardiovascular system in older C57BL/6 mice.
2. Explore sex differences in Ang II-induced cardiac remodeling.
3. Determine if Ang II-induced HF exacerbates frailty in a sex-specific fashion.
4. Determine if baseline frailty increased adverse cardiac outcomes in Ang II-infused mice.

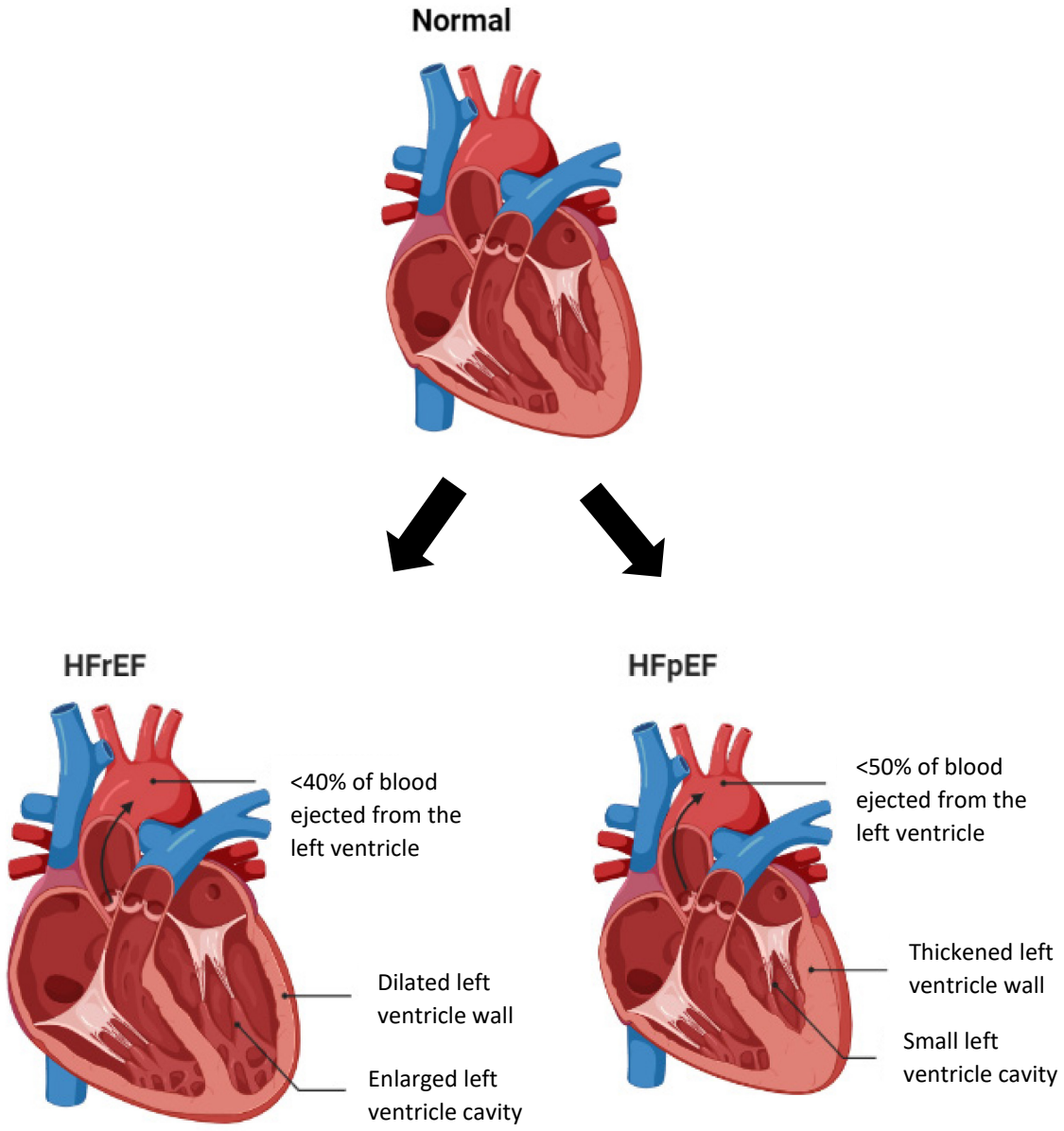

Figure 1.1. Types of heart failure. Top image shows a normal heart, bottom left image shows heart failure with reduced ejection fraction, and bottom right image shows heart failure with preserved ejection fraction. Images were created with Biorender.com.

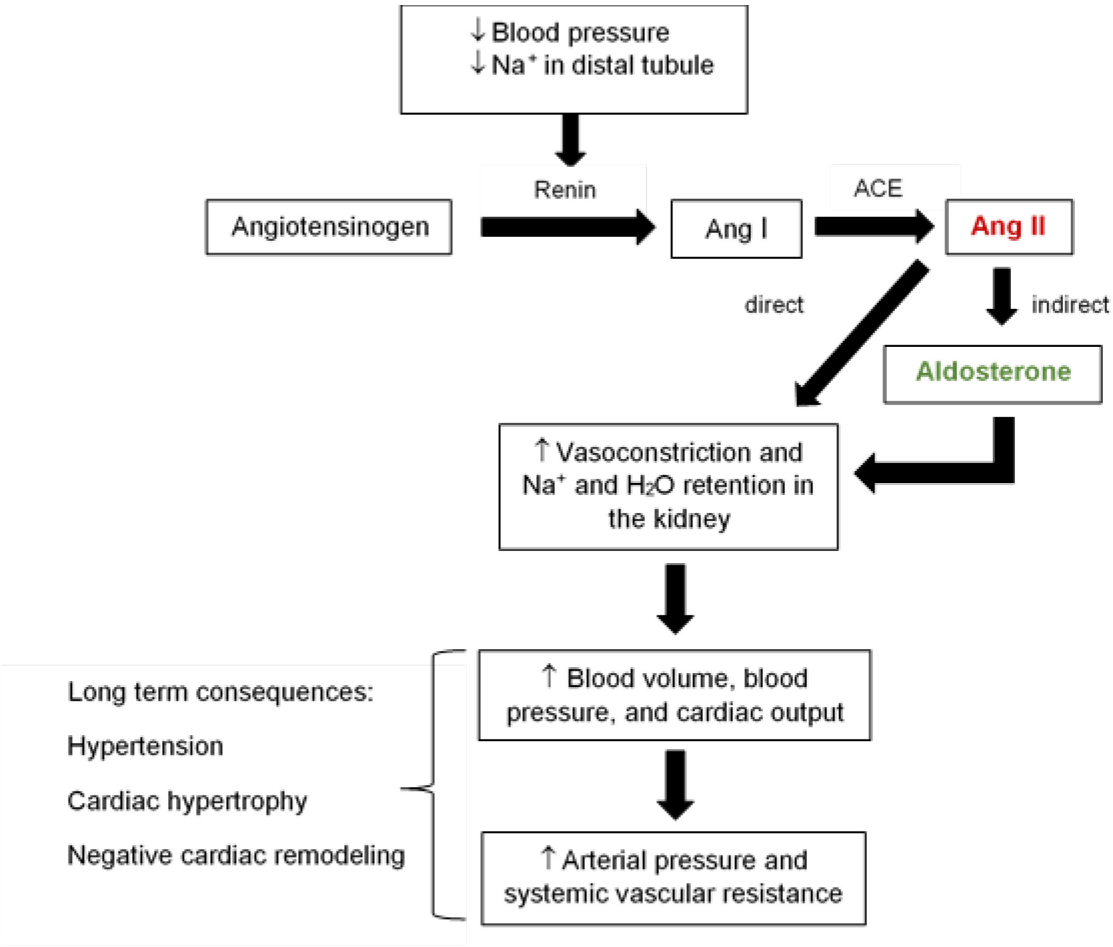

Figure 1.2. Angiotensin II has acute effects on the vasculature and chronic effects on the myocardium. Abbreviations: angiotensin (Ang), angiotensin converting enzyme (ACE).

Table 1.1. The influence of frailty on cardiac structure and function in C57BL/6 mice assessed by the mouse frailty index

References	Age	Sex	Study aims	Results
Parks et al., 2012	30 mos	Both	Influence of frailty on ventricular myocyte structure and function	Ventricular myocyte hypertrophy and reduced myocyte contractility correlated with high frailty scores.
Moghtadaei et al., 2016	25 mos	Male	Influence of frailty on heart rate and sinoatrial node function	Decreased heart rate and sinoatrial node function as well as increased fibrosis are highly correlated with frailty scores in males.
Kane et al., 2017	24 mos	Male	Evaluate cardiac function in the context of frailty	Decreased heart rate and heart rate variability are correlated with frailty scores.
Jansen et al., 2017	27 mos	Male	Influence of frailty on atrial structure, function, and arrhythmogenesis	Impaired cardiac electrical conduction and increased fibrosis are graded by frailty scores.
Feridooni et al., 2017	27 mos	Male	Influence of frailty on cardiac structure and function	Increased cardiac hypertrophy and impaired calcium handling (smaller calcium current, lower gain and decreased expression of Cav1.2 protein) are highly correlated with and graded by frailty scores.
Kane et al., 2020	16 mos and 23 mos	Both	Influence of frailty and inflammation on cardiac structure and function	Changes in EF, E/A ratios, septal wall thickness, and fibrosis were graded by frailty scores in males. Increases in septal wall thickness and LV mass were graded by frailty scores in females.
Kane et al., 2021	12 mos and 24 mos	Both	Influence of sex and frailty on cardiac contractile function	Adverse changes in post-translational modifications in myofilaments in the aging male heart were graded by frailty scores but not in the aging female heart.

Chapter 2: Materials and Methods

2.1 Animals

All experiments were approved by the Dalhousie University Committee on Laboratory Animals and followed Animal Research: Reporting of In Vivo Experiments (ARRIVE) guidelines (Kilkenny, Browne, Cuthill, Emerson & Altman, 2010). This study used C57BL/6 male and female mice obtained from Charles Rivers Laboratories (St. Constant, QC, Canada). All mice were purchased as retired breeders and were between 13 to 16 months when the experiments started. Animals were housed in micro-isolator cages in the Carlton Animal Care Facility at Dalhousie University and maintained on a 12-h light-dark cycle. Mice were allowed *ad libitum* access to Standard Grain-Based Control Rodent Diet (F4059; Bio-Serv, Frenchtown, NJ) and water.

2.2 Quantification of frailty using the clinical frailty index

Frailty was assessed as deficit accumulation with the non-invasive clinical FI created by Whitehead et al. (2014). This FI consists of scoring 31 different health-related deficits. Each deficit was given a score of 0 if absent; 0.5 if mild; or 1 if severe. A clicker used in dog training was used to measure hearing loss. The animal was weighed, and the body temperature was measured at the abdomen using an infrared temperature probe (La Crosse Technology, La Crosse, WI). Weight and temperature were scored based on the number of standard deviations the tested mouse was from the average values measured at baseline. Values that differed from the reference by >1, 2, 3 or 4 SD were scored as 0.25, 0.5, 0.75, and 1 respectively. Once the scores for all parameters were obtained, they were added and divided by 31 to yield an FI score of between 0 and 1. Table 2.1 shows an

example of the frailty assessment form developed by Whitehead et al. (2014). Table 2.2 describes in detail the scoring system for the FI assessment and the criteria for each deficit (Whitehead et al., 2014). FI scores for all mice were measured at baseline to create two age- and sex-matched groups of mice with high or low FI scores. FI scores were measured weekly thereafter for 6 weeks following osmotic minipump implantation. The experimental timeline is illustrated in Figure 2.1.

2.3. Analysis of FRIGHT and AFRAID CLOCKS

The Frailty Inferred Geriatric Health Timeline (FRIGHT) and Analysis of Frail and Death (AFRAID) clocks were calculated based on methods described previously (Schultz et al., 2020). Both clocks are based on FI data as well as weight change data as described below. The FRIGHT clock is a strong predictor of chronological age whereas the AFRAID clock is a predictor of life expectancy. Briefly, data from previously determined FI scores for each mouse at each time-point were input and analyzed by the frailtyclocks.sinclairlab.org website. In addition to the deficits that make up the FI score, prediction variables for body weight change were included for the FRAIL and AFRAID analysis. These include recent percent weight change (% RWC), from 4 weeks before the assessment; percent total weight change (% TWC), from more than 4 weeks before the assessment; and threshold recent weight change in which mice received a score of 1 if they gained more than 8% or lost more than 10% of their body weight in recent weight change.

In the present study, % RWC and % TWC change were entered as 0 for all mice from baseline to week 3. For week 4, % RWC was calculated as the difference between body weight at week 4 and baseline, and % TWC was equal to % RWC. The % RWC at

week 5 was determined from the difference between body weight at week 5 and week 1; % TWC was assessed as the difference between week 5 and baseline. The difference between week 6 and week 2 made up % RWC at week 6; the difference between week 6 and baseline was used as % TWC.

2.4. Measuring blood pressure

Blood pressure was measured at baseline, then at midpoint, and endpoint following pump implantation (refer to the timeline in Figure 2.1) using a tail cuff plethysmography machine (IITC Life Science, Inc., Woodland Hills, CA). The blood pressure monitoring software (IITC Life Science, Inc., Woodland Hills, CA) was used to record systolic and diastolic blood pressure. The machine was calibrated prior to each recording. To do this, a pressure gauge with a manual bulb inflator was connected to the cuff airports on the machine via a tubing adapter. The "calibrate" setting was selected and the pressure was manually adjusted to 0 mmHg, 50 mmHg, and 300 mmHg for subsequent rounds of calibration using the manual bulb inflator. Then the animal was placed in a clear restrainer with a dark cone at the animal's face to limit their vision and movement. A tail cuff attached to the sensor was placed at the base of the tail and secured to the restrainer. The animal was then placed in a warmed chamber and allowed to acclimatize for 10 minutes. As measurements were initiated, the tail cuff was inflated to occlude blood flow to the tail. As the cuff was deflated, the falling pressure allowed the blood to return to the tail. A light sensor within the tail cuff detected this movement of blood, which was transduced into an electrical signal. Four consecutive rounds were performed with each round producing five

recordings. The mouse was acclimatized to the procedure but no data was collected for two days in a row, and measurements were made on the third day.

2.5. Measuring *in vivo* heart structure and function

Animals were placed in an empty cage and an empty cone connected to the anesthetic machine was placed on top of the animal. The animal was then anesthetized with 3% isoflurane in oxygen (1 L/min) delivered via the cone. When the animal lost consciousness, it was placed on a heating pad in a supine position. Isoflurane was the delivered via a nose cone and was maintained between 1-1.5% throughout the procedure. Lubricating eye gel was placed on the animal's eyes to maintain eye moisture. Electro-conductive gel was placed on all four paws to facilitate electrocardiogram and heart rate recordings via the conducting pads. A temperature probe was inserted rectally to record temperature. A heat lamp was used to maintain body temperature at 37ºC. The hair on the animal's chest was removed with depilatory cream to prevent interference with the recordings. Ultrasound transmission gel was applied to the animal's chest and a high-resolution linear transducer was placed on the gel. The heart was imaged with the Vevo 2100 echocardiography imaging system (FUJIFILM VisualSonics Inc., Toronto, Ontario, Canada). Two-dimensional M-Mode echocardiography displayed images of the short-axis section of the heart from which physical measurements of the LV were recorded. The left ventricular anterior wall (LVAW) and left ventricular posterior wall (LVPW) dimensions at systole and diastole indicate LV wall thickness. The LV diameters at systole and diastole indicate the degree of inner chamber dilation. These values were used by the software to calculate EF (the amount of blood pumped out of the heart during a heartbeat), FS (the

degree of shortening of the LV between diastole and systole), diastolic LV volume, LV mass, and corrected LV mass (LV mass x 0.8). The corrected LV mass/diastolic volume ratio was calculated to determine the extent of concentric remodeling and hypertrophy in the heart (Lembo et al., 2019). The LV wall distensibility, an indicator of cardiac wall stiffness, is calculated from the difference between systolic LVPW and diastolic LVPW divided by systolic LVPW (Takeda et al., 2009).

Pulse wave Doppler in the apical, 4 chamber view was used to measure the velocity of the blood flowing to the LV through the mitral valve. The E wave represents the passive filling velocity as the ventricle relaxes, and the A wave represents the active filling velocity as the atria contract. The E/A ratio calculated from these values is indicative of LV diastolic function. The isovolumic relaxation time (IVRT) as well as the isovolumic contraction time (IVCT) were also measured. IVRT is defined as the time between the aortic valve closing and the mitral valve opening. IVCT is defined as the time between the mitral valve closing and the aortic valve opening. The mice were placed on a heating pad for at least 1 hour to recover at the end of the experiment.

2.6. Osmotic minipump implantation

ALZET osmotic pumps model 2006 (Durect Corp., Cupertino, CA, USA) were incubated in saline at 37°C 24 hours before implantation (refer to Figure 2.2, a schematic of the procedure). The Ang II stock solution (0.1 M) was prepared by mixing Ang II in 0.9% saline. The amount of Ang II (µg) needed per pump was calculated using the formula: (body weight x 3 mg/kg/day x pump filling volume)/(24 x pump rate); the pump filling volume and the pump rate were 223.6 µL and 0.13 µL/hr respectively. The volume

of Ang II stock solution needed in each pump was calculated as: (the amount Ang II needed/the molecular weight of Ang II or 1046.19 g/mol)/0.1 M. The volume of saline needed was determine by subtracting the volume of Ang II stock solution needed from the pump filling volume. The Ang II solution required for each pump was made up by mixing the required volumes of saline and Ang II stock solution in an Eppendorf tube before being added to the pump. To prevent the pump from being under filled, the combined volumes were doubled. The pumps were filled with either Ang II solution or 0.9% NaCl (control) in a biosafety cabinet (BSC). This dosage was chosen as infusion of Ang II between 2.1 mg/kg/day (Chinnakkannu et al., 2018) to 3.2 mg/kg/day (Izumiya et al., 2012) has been shown to induce hypertension and pressure-overload induced HF in male C57BL/6 mice.

Mice were weighed then placed in a clean empty cage and taken to the surgical area for pump implantation (Figure 2.3). The mouse was placed under a plastic cone through which 3% isoflurane with a continuous flow of 95%/5% O_2/CO_2 was delivered. Once the mouse lost consciousness, it was placed on a sterile drape on top of a heating pad and a nose cone delivering anesthesia was attached. Eye lubricating gel was used to maintain the mouse's eye moisture during the procedure. A subcutaneous injection of saline and meloxicam (0.5 mg/kg IV) at a 1:1 ratio were delivered to maintain fluids during surgery and provide post-operative pain relief respectively. The area of over the shoulder where the pump was to be implanted was shaved with an electric razor. The shaved area was wiped three times with betadine and three times with alternate 70% ethanol and iodine. A toe pinch test was used to confirm the depth of anesthesia before the implantation began. A surgical blade was used to make a 1 cm horizontal incision behind the ear over the shoulder blade of the front leg on the right side. A pocket for the pump was created by

inserting a hemostat subcutaneously through the incision. The pump was inserted into the pocket with the regulator head towards the tail. Once the pump was inserted, the incision was stapled with wound clips. The mouse was weighed then placed in a clean cage on a heating pad to recover for at least two hours. A post operation card was attached to the cage containing information about the surgical procedure. The mouse was given mashed regular food in water and moved to the recovery room where it was monitored for 24 hours. Then the mice were returned to their home cages. Wound clips were removed 10 to 14 days following the surgery. Mice were monitored for humane endpoint (HEP) weight after the implantation procedure. They were euthanized when the HEP weight (80% of the initial weight plus minipump weight) was reached.

2.7. Langendorff-perfused isolated hearts

FI scores were determined immediately prior to euthanasia for each animal. Mice were anesthetized with an intraperitoneal injection of sodium pentobarbital (200 mg/kg) plus heparin (3,000 U/kg) which was used to prevent blood coagulation. The toe pinch test was used to evaluate the depth of anesthesia. A thoracotomy was performed as soon as there was no pedal withdrawal reflex in both hindlimbs. The aorta was incised and cannulated with a blunt 21-gauge needle. The heart was cannulated and perfused with a Krebs–Henseleit perfusion buffer containing (mM): NaCl, 91.3; glucose, 11; $NaHCO_3$, 25; KCl, 4.7; $MgSO_4.7H_2O$, 1.2; KH_2PO_4, 1.2; $CaCl_2$, 1.8; and pyruvate, 0.79. The buffer was bubbled with 95% O_2 and 5% CO_2 for at 37°C to achieve a pH of 7.4. $CaCl_2$ was added after the solution had been bubbled for 20 minutes and the solution was filtered through a

0.45 μm Vacucap PV filter (PALL, NY, USA) before being added to the perfusate reservoir.

The cannulated heart was then excised and mounted on the Langendorff apparatus (Figure 2.4) for perfusion at a constant pressure of 80 mmHg. The temperature of the perfusate was maintained at 37°C via water jacketed tubing connected to a temperature-controlled water bath. The temperature of the heart was maintained using a glass chamber which was placed over the heart, along with a heat lamp. The left atrium was removed to allow a fluid-filled balloon constructed from GLAD® Cling Wrap (The Clorox Company of Canada LTD., Brampton, ON, Canada) to be inserted into the left ventricle. The balloon was inflated to a minimum pressure of 5-10 mm Hg. The balloon was connected via fluid-filled tubing to a pressure transducer (ADInstruments, Colorado Springs, CO, USA) that converted changes in balloon pressure into digital signals. The PowerLab 8/35 data acquisition system (ADInstruments, Colorado Springs, CO, USA) received and recorded these signals. Heart rate, electrocardiography, pressure and temperature were monitored with Labchart software (ADInstruments, Colorado Springs, CO, USA).

The heart was allowed to stabilize for the 20 minutes and then baseline signals were recorded for 30 minutes. Recordings of LV pressure were used to determine left ventricular developed pressure (LVDP), heart rate, rate of pressure development and decay (+dP/dt and −dP/dt, respectively), and rate pressure product (RPP). The effluent was collected from the heart during the experiment to produce the coronary flow rate expressed as the amount of effluent (mL) collected per minute. At the end of the experiment, the heart was weighed then flash frozen in liquid nitrogen before being stored at -80°C freezer. The lungs were collected, weighed, and stored in a plastic container containing desiccant beads.

The dry lung weigh were later recorded to determine the amount of pulmonary fluid as the difference between wet lung weight and dry lung weight. The tibia was isolated, and its length was measured using calipers (Lee Valley, Halifax, NS). This was done to allow heart weight to be normalized by tibia length, rather than body weight.

2.8. Fibrosis assay

Fibrosis was determined by quantifying the collagen contents in hearts isolated at the end of the experiment. The hydroxyproline assay kit (Sigma-Aldrich, Okaville, ON; Catalog number: MAK008) was used to quantify the concentration of hydroxyproline, a major component of collagen. The kit contained a set of standards with known concentrations of hydroxyproline. Frozen heart samples (10-30 mg of ventricle tissue) were homogenized in water (100 µL) and subsequently hydrolyzed in 12 M HCl at 120ºC for 3 hours. The samples were then centrifuged at 10 000 x g for 3 minutes. The supernatant (20 µL) from each sample and standard was pipetted into a 96 well plate then placed in an oven to dry at 60º for 3 hours. The 96 well plate was removed from the oven after 3 hours. Then chloramine T (6 µL), oxidation buffer (94 µL), perchloric acid/isopropanol solution (50 µL), and 4-(dimethylamino)benzaldehyde (50 µL) were added to the sample wells. The plate was placed back in the oven for incubation at 60ºC for 90 minutes. The plate was subsequently removed and the absorbance was immediately read at 560 mm. The absorbance values of the standards and samples were used to determine the concentration of hydroxyproline in each sample. The concentration of hydroxyproline (µg) in each sample was normalized to the heart weight (mg) used in the assay.

2.9. Chemicals

Ang II acetate salt was purchased from Bachem (Cat# 1705, Torrance, CA, USA). Ang II was stored at -20ºC upon arrival and at 4ºC 24 hours before preparing the stock solution. Stock preparations were made by dissolving 100 mg of Ang II in 1 ml of 0.9% saline. The stock was aliquoted into Eppendorf tubes containing 50 µl each and stored at -20ºC until needed. All chemicals used to make buffer solutions were purchased from Sigma Aldrich (Oakville, ON).

2.10. Statistics

GraphPad Prism V9.0 (GraphPad Software, San Diego, CA) and Sigma Plot 14.0 (Systat Software, Inc., Point Richmond, CA) were used to create all graphs and perform statistical analysis. Systolic and diastolic blood pressure were analyzed using the blood pressure monitor software (IITC Life Science, Inc., Woodland Hills, CA). Echocardiography data were analyzed with the Vivid 7 imaging system (GE Medical Systems, Horten, Norway). Langendorff data were analyzed using Labchart 8.0 (Molecular Devices, Sunnyvale, CA). Two-Way ANOVA with Tukey post-hoc's was used to analyze Langendorff data and isolated tissue morphology data. Mixed effects analysis with Fisher's LSD post-hoc were performed on blood pressure, echocardiography, FI scores, and FRIGHT and AFRAID clocks.

A Kaplan-Meier survival curve was constructed to illustrate the probability of survival over the timeframe of the experiment. Survival data were recorded for mice of

both sexes for the duration of the experiment to generate these survival curves. Mortality was recorded as sudden death or when mice were euthanized as they reached their HEP weight due to weight loss caused by Ang II infusion. Mice that survived to the endpoint were censored and included in the analysis as censored data. Survival data were analyzed with a log-rank test.

FI data for control and treated mice were normalized to percent of baseline FI for control mice for each sex group. The proportion with each deficit was analyzed using a Chi-square test. The effects of frailty on *in vivo* cardiac structure and function were analyzed with linear regression analysis. Data were presented as mean ± SEM and differences were reported as significant if $P < 0.05$.

Table 2.1. Mouse frailty assessment form.

Mouse ID: _____ Date: _____ Date of birth: _____
Sex: F M Body weight (g): _____ Surface body temperature (°C): _____

Mouse Frailty Assessment Form

Rating: 0 = absent, 0.5 = mild, 1 = severe

				Notes:
Integument:				
• Alopecia (hair loss)	0	0.5	1	
• Loss of fur colour	0	0.5	1	
• Dermatitis	0	0.5	1	
• Loss of whiskers	0	0.5	1	
• Coat condition	0	0.5	1	
Musculoskeletal system:				
• Tumours	0	0.5	1	
• Distended abdomen	0	0.5	1	
• Kyphosis/hunched posture	0	0.5	1	
• Tail stiffening	0	0.5	1	
• Gait	0	0.5	1	
• Tremor	0	0.5	1	
• Forelimb grip strength	0	0.5	1	
• Body condition score	0	0.5	1	
Vestibulocochlear/Auditory:				
• Head tilt	0	0.5	1	
• Hearing loss	0	0.5	1	
Ocular/Nasal:				
• Cataracts	0	0.5	1	
• Discharge/swollen/squinting	0	0.5	1	
• Microphthalmia	0	0.5	1	
• Corneal opacity	0	0.5	1	
• Vision loss	0	0.5	1	
• Menace reflex	0	0.5	1	
• Nasal discharge	0	0.5	1	
Digestive/Urogenital system:				
• Malocclusions	0	0.5	1	
• Rectal prolapse	0	0.5	1	
• Penile/Uterine prolapse	0	0.5	1	
• Diarrhoea	0	0.5	1	
Respiratory:				
• Breathing rate/depth	0	0.5	1	
Discomfort:				
• Mouse grimace scale	0	0.5	1	
• Piloerection	0	0.5	1	

Total Score/ Max Score:

Table 2.2. Clinical assessment of deficits in aging mice to create a frailty index.

System/Parameter	Clinical assessment of deficit	Scoring
Integument		
Alopecia	Gently restrain the animal and inspect it for signs of fur loss	0 = normal fur density 0.5 = < 25% fur loss 1 = > 25% fur loss
Loss of fur color	Note any chance in fur color from black to grey or brown	0 = normal color 0.5 = focal grey/brown changes 1 = grey/brown throughout body
Dermatitis	Document skin lesions	0 = absent 0.5 = focal lesions (e.g. neck, flanks, under chine) 1 = widespread/multifocal lesions
Loss of whiskers	Inspect the animal for signs of a reduction in the number of whiskers	Inspect the animal for signs of a reduction in the number of whiskers 0 = no loss 0.5 = reduced number of whiskers 1 = absence of whiskers
Coat condition	Inspect the animal for signs of poor grooming	0 = smooth, sleek, shiny coat 0.5 = coat is slightly ruffled 1 = unkempt and un-groomed, matted appearance
Physical/ Musculoskeletal		
Tumours	Observe the mice to look for symmetry. Hold the base of the tail and manually examine mice for visible or palpable tumors	0 = absent 0.5 = < 1.0 cm 1 = > 1.0 cm or multiple smaller tumors
Distended abdomen	Hold the mouse vertically by the base of the tail and tip backwards over your hand. Excess fluid visible as a bulge below the rib cage	0 = absent 0.5 = slight bulge 1 = abdomen clearly distended
Kyphosis	Inspect the mouse for curvature of the spine or hunched posture. Run your fingers down both sides of the spine to detect abnormalities	0 = absent 0.5 = mild curvature 1 = clear evidence of hunched posture
Tail stiffening	Grasp the base of the tail with one hand, and stroke the tail with a finger of the other hand. The tail should wrap freely around the finger when mouse is relaxed	0 = no stiffening 0.5 = tail responsive but does not curl 1 = tail completely unresponsive
Gait disorders	Observe the freely moving animal to detect abnormalities such as hopping, wobbling, circling, wide stance and weakness	0 = no abnormality 0.5 = abnormal gait but animal can still walk 1 = marked abnormality, impairs ability to move
Tremor	Observe the freely moving animal to detect tremor, both at rest and when the animal is trying to climb up an incline	0 = no tremor 0.5 = slight tremor1 = marked tremor; animal cannot climb

Forelimb grip strength	Hold the mouse. Allow it grip the bars on the cage lid. Lift animal by the base of the tail and assess grip strength	0 = sustained grip 0.5 = reduction in grip strength 1 = no strength, no resistance
Body condition score	Place mouse on flat surface, hold tail base and manually assess the flesh/fat that covers the sacroiliac region (back and pubic bones)	0 = bones palpable, not prominent 0.5 = bones prominent or barely felt 1 = bones very prominent or not felt due to obesity
Vestibulocochlear/ Auditory		
Vestibular disturbance	Hold the base of the tail and lower mouse towards a flat surface. Inspect for head tilt, spinning, circling, head tuck or trunk curling	0 = absent 0.5 = mild head tilt and/or slight spin when lowered 1 = severe disequilibrium
Hearing loss	Test startle reflex. Hold a clicker ~ 10 cm from mouse, sound it 3 times and record responses	0 = always reacts (3/3 times) 0.5 = reacts 1/3 or 2/3 times 1 = unresponsive (0/3 times)
Ocular/ Nasal		
Cataracts	Visual inspection of the mouse to detect opacity in the center of the eye	0 = no cataracts 0.5 = small opaque spot 1 = clear evidence of opaque lens
Eye discharge/ swelling	Visual inspection of the mouse to detect ocular discharge and swelling of the eyes	0 = normal 0.5 = slight swelling and/or secretions 1 = obvious bulging and/or secretions
Microphthalmia	Inspect eyes	0 = normal 0.5 = minimal changes in cornea 1 = marked clouding and/or spotting of cornea
Corneal opacity	Visual inspection of the mouse for superficial white spots and/or clouding of the cornea	0 = normal 0.5 = minimal changes in cornea 1 = marked clouding and/or spotting of cornea
Vision loss	Lower mouse towards a flat surface. Evaluate the height at which the mouse reaches towards the surface	0 = reaches >5 cm above surface 0.5 = reaches 2-5 cm above surface 1 = reaches <2 cm above surface
Menace reflex	Move an object towards the mouse's face 3 times. Record whether the mouse blinks in response	0 = always responds 0.5 = no response to 1 or 2 approaches 1 = no response to 3 approaches
Nasal discharge	Visual inspection of the mouse to detect nasal discharge	0 = no discharge 0.5 = small amount of discharge 1 = obvious discharge, both nares
Digestive/Urogenital		
Malocclusions	Grasp the mouse by the neck scruff, invert and expose teeth. Look for uneven, overgrown teeth	0 = mandibular longer than maxillary incisors 0.5 = teeth slightly uneven 1 = teeth very uneven and overgrown
Rectal prolapse	Grasp the mouse by the base of the tail to detect signs of rectal prolapse	0 = no prolapse 0.5 = small amount of rectum visible below tail 1 = rectum clearly visible below tail

Vaginal/ uterine/ penile prolapse	Grasp the mouse by the base of the tail to detect signs of vaginal/ uterine or penile prolapse	0 = no prolapse 0.5 = small amount of prolapsed tissue visible 1 = prolapsed tissue clearly visible
Diarrhea	Grasp the mouse and invert it to check for signs of diarrhea. Also look for fecal smearing in home cage	0 = none 0.5 = some feces or bedding near rectum 1 = feces + blood and bedding near rectum, home cage smearing
Respiratory		
Breathing rate/ depth	Observe the animal. Not the rate and depth of breathing as well as any gasping behavior	0 = normal 0.5 = modest change in breathing rate and/or depth 1 = marked changes in rate/depth, gasping
Discomfort		
Mouse grimace scale	Note facial signs of discomfort: 1) orbital tightening, 2) nose bulge, 3) check bulge, 4) ear position (drawn back) or 5) whisker change (either backward or forward)	0 = no signs present 0.5 = 1 or 2 signs present 1 = 3 or more signs present
Piloerection	Observe the animal and look for signs of piloerection, in particular on the back of the neck	0 = no piloerection 0.5 = involves fur at base of neck only 1 = widespread piloerection
Other		
Temperature	Measure surface body temperature with an infrared thermometer directed at the abdomen (average of 3 measures). Compare with reference values from sex-matched adult animals	0 = differs by <1 SD from reference value 0.25 = differs by 1 SD 0.5 = differs by 2 SD 0.75 = differs by 3 SD 1 = differs by >3 SD
Weight	Weight the mouse. Compare with reference values from sex-matched adult animals	0 = differs by <1 SD from reference value 0.25 = differs by 1 SD 0.5 = differs by 2 SD 0.75 = differs by 3 SD 1 = differs by >3 SD

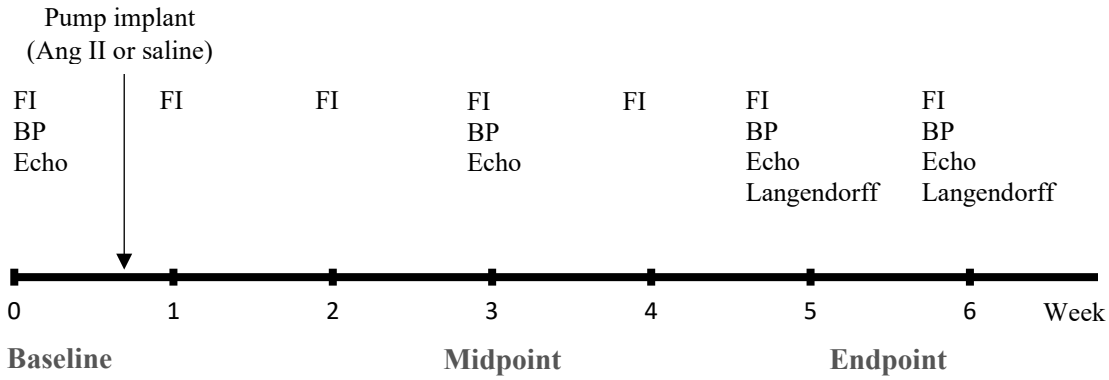

Figure 2.1. General timeline of the experimental interventions. Mice of each sex were FI-matched at baseline to form treatment and control groups. They were then implanted with osmotic minipumps containing Ang II (3 mg/kg/day) or saline respectively. Abbreviations: Ang II, angiotensin II; FI, frailty index; BP, blood pressure; echo, echocardiography.

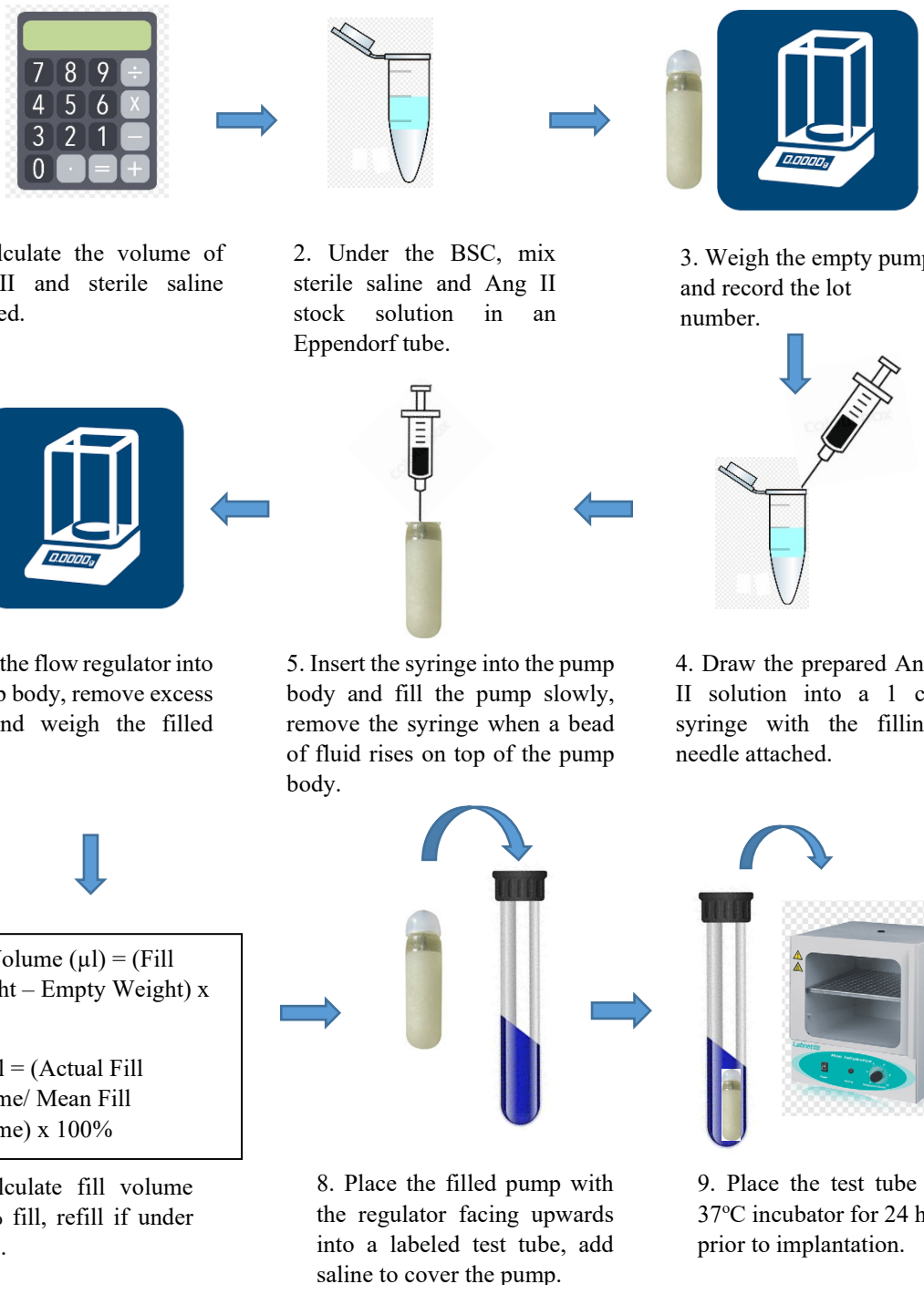

Figure 2.2. A step-by-step flow chart that illustrates the osmotic mini-pump filling procedure. Each step is described in detail in the methods section.

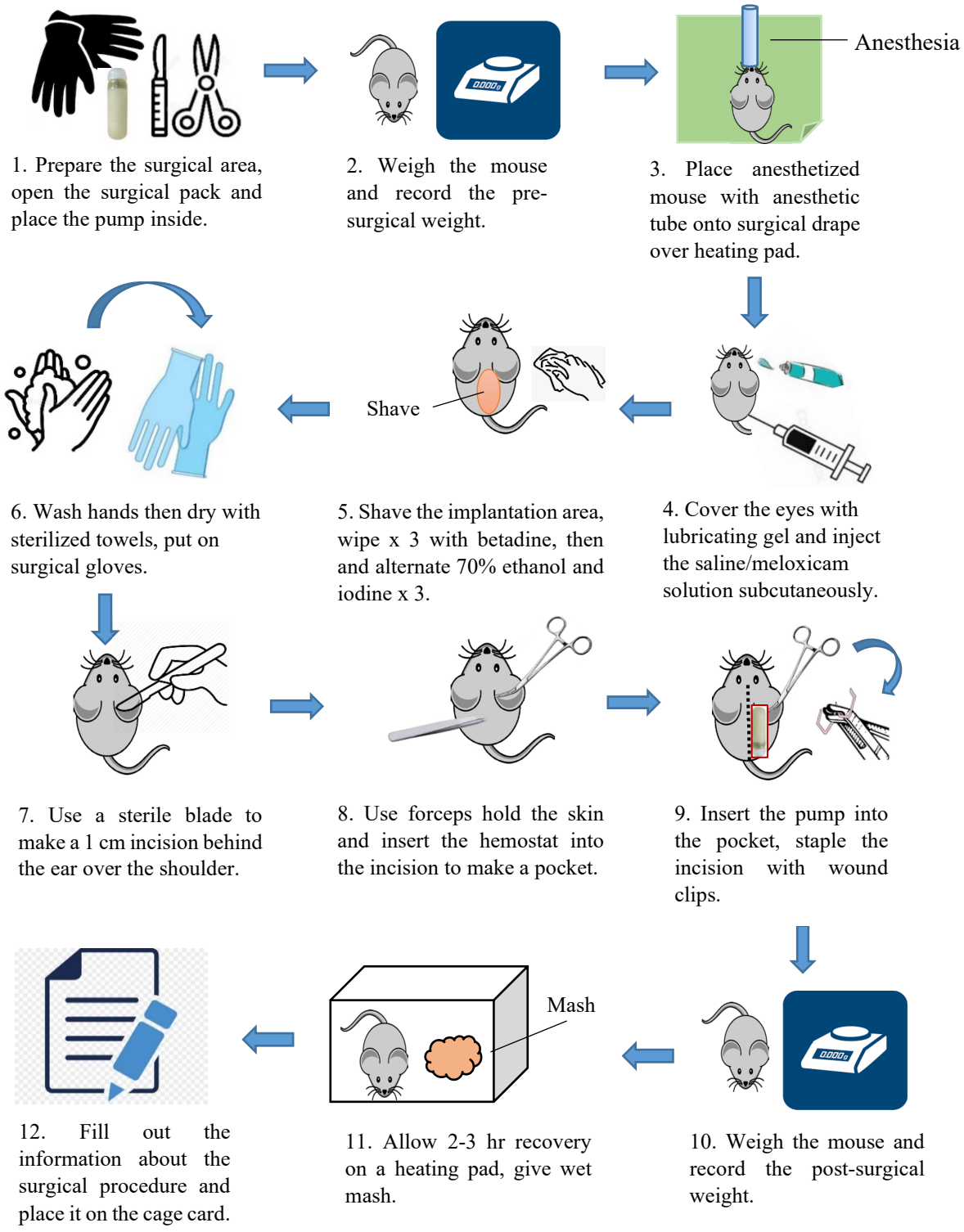

Figure 2.3. A step-by-step flow chart that illustrated the osmotic mini-pump implantation procedure. Each step is described in detail in the methods section.

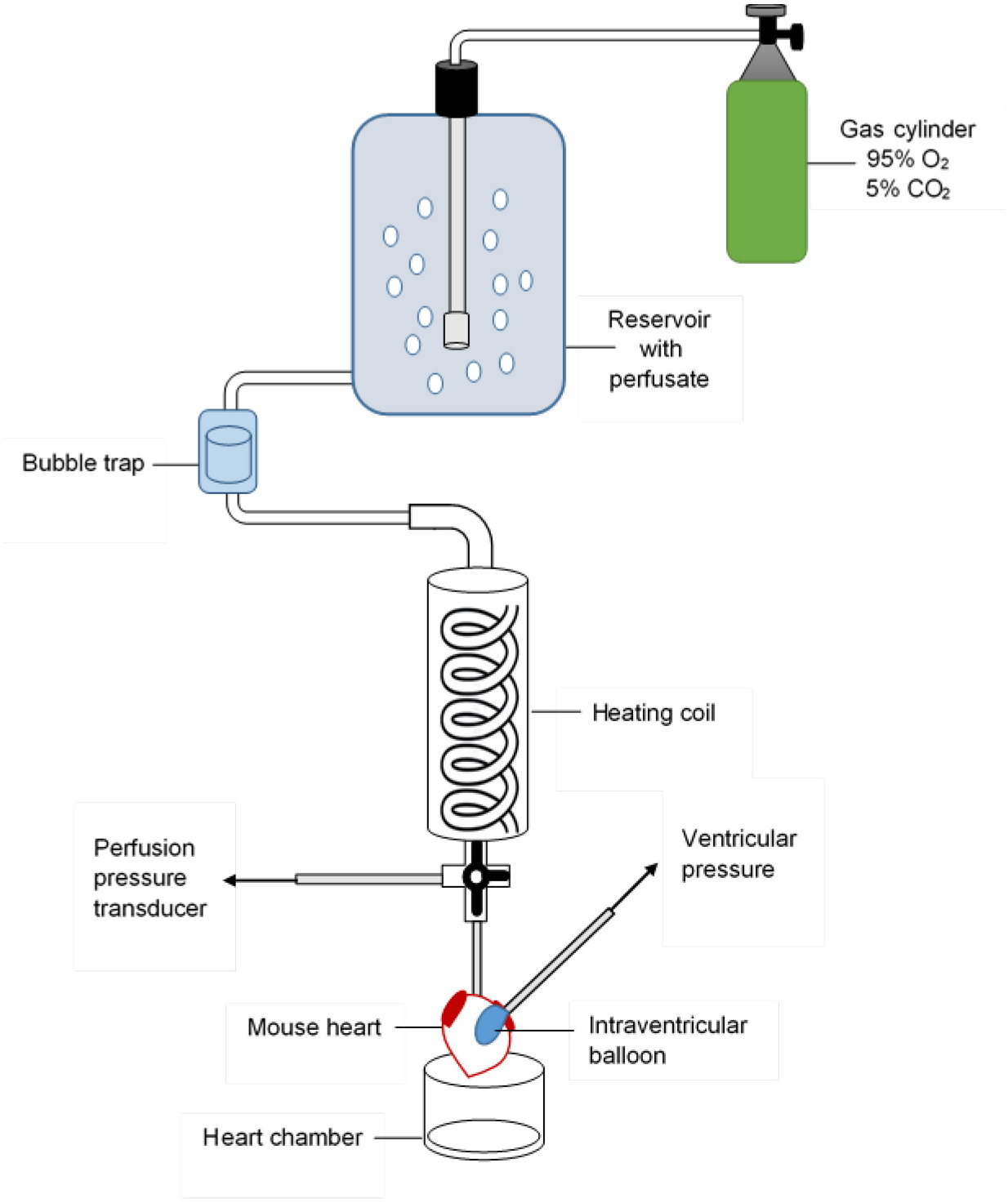

Figure 2.4. A schematic of the Langendorff apparatus used to assess left ventricular function in the mouse heart. The experiment is described in detailed in the methods section.

Chapter 3: Results

3.1 The impact of Ang II infusion on blood pressure

The first series of experiments investigated whether Ang II infusion increased blood pressure over the timeframe of this study. Systolic and diastolic blood pressure were measured using the tail-cuff method at baseline, midpoint (week 3), and endpoint (week 6). Figures 3.1A and 3.1B show representative examples of blood pressure recorded from a male mouse in the absence of Ang II (at baseline) and in the presence of Ang II (at endpoint). In each figure, the top panel shows the amount of pressure applied to the tail-cuff over time, and the bottom panel shows the blood pressure recording from the tail pulse. Systolic blood pressure, indicated by the green line, is the point at which the pulse envelop starts to amplify on the blood pressure recording. The mean arterial pressure (MAP), indicated by the red line, is the point at which the pulse begins to flatten after the first highest pulse. The diastolic blood pressure is automatically calculated by the software from the systolic blood pressure and MAP. Mean (± SEM) data for systolic blood pressure in both sexes are shown in Figures 3.2A and 3.2B. Results showed that Ang II infusion caused significant increases in systolic blood pressure in mice of both sexes compared to midpoint and endpoint controls, as well as compared to baseline data. There were no sex differences among any group. Similar results were seen with diastolic blood pressure (Figures 3.3A and 3.3B) and MAP (Figures 3.4A and 3.4B). These results indicate that Ang II infusion induced hypertension in both males and females.

3.2 Changes in *in vivo* cardiac structure in response to Ang II infusion

To investigate the effects of Ang II infusion on *in vivo* cardiac morphology and function, two-dimensional M-mode echocardiography was used to measure cardiac changes. Figures 3.5A and 3.5B show representative M-mode images of the LV of treated male mice at baseline (before treatment) and at endpoint (after treatment) respectively. Figure 3.5A also shows many of the measurements made from the M-mode images including LV wall thickness and LV chamber dimensions. Figure 3.5B shows LV dilation when compared to Figure 3.5A. Figures 3.6 and 3.7 show mean (± SEM) for LVAW and LVPW at systole respectively in control and treated mice of both sexes. Figures 3.6A and 3.7A show that Ang II infusion had no effect on systolic LVAW and LVPW thickness in female animals. By contrast, moderate thinning of systolic LVAW and LVPW occurred over time in Ang II-infused male mice, although the effect was small and treated mice were not significantly different than controls (Figures 3.6B and 3.7B). There were also sex differences between the treated mice at midpoint and endpoint, where Ang II-induced hypertension caused male mice to have thinner systolic LV walls compared to females (denoted by the # symbol in Figures 3.6A and 3.7A). The results of the M-mode echocardiography statistical analysis are summarized in Table 3.1.

Interestingly, different results were seen where LV wall thickness was examined in diastole. Diastolic LV wall thickness was unaffected by Ang II-induced hypertension in males, while cardiac wall thickening occurred in females (Figures 3.8 and 3.9). Figures 3.8A and 3.9A show that diastolic LVAW and LVPW thickness increased over time in females, and this effect was significant compared to female controls at midpoint and endpoint. Furthermore, treated females had thicker diastolic LVAW than treated males at

midpoint and endpoint. In contrast, Ang II infusion had no effect on diastolic LVAW and LVPW in males (Figures 3.8B and 3.9B). Overall, Ang II-induced hypertension caused LV walls to become thinner in males, whereas the walls became thicker in females.

Changes in the LV wall thickness can affect the size of the LV inner chamber. Indeed, results from the present study show that LV inner diameters at systole increased over time in Ang II-infused male and female animals (Figures 3.10A and 3.10B). This effect was also significant for males and females when compared to corresponding same-sex controls at midpoint and endpoint. Similarly, Ang II infusion caused dilation of the LV diameter in diastole over time in treated male mice, but this was significantly higher than control at endpoint only (Figure 3.11B). In contrast, there was only a minor effect of Ang II-induced hypertension on diastolic diameters in female hearts. A significant increase in diastolic diameter compared to control occurred only at midpoint, and there were no changes over treatment time (Figure 3.11A). There were also sex differences in the size of the inner LV chamber. Both treated and control male mice had larger LV diameters when compared to respective female groups at baseline, midpoint and endpoint (Figure 3.11A). This sex difference also occurred for systolic diameters but only at midpoint and endpoint (Figure 3.10A). These observations demonstrate that Ang II-induced hypertension led to LV dilation that was more pronounced in males than females.

As wall thickening and/or chamber dilation can result in higher LV mass (Drazner, 2011), we explored whether corrected LV mass increased in Ang II-treated mice. Corrected LV mass (LV mass x 0.8) was used since M-mode overestimates uncorrected LV mass in normal hearts (Kuhl et al., 2003) as well as in heart failure (Gopal et al., 1997) and hypertensive heart disease (Stewart et al., 1999). The value of uncorrected LV mass

measured by M-mode corresponds to ~80% of the value by 3-D imaging (Kuhl et al., 2003). The results in Figures 3.12A and 3.12B show that corrected LV mass increased in Ang II-infused mice of both sexes. This effect occurred over time and was significant compared to control mice at both midpoint and endpoint. Control male mice also had larger hearts than control females at all three time points (Figure 3.12A). Overall, these results indicate that Ang II-induced hypertension led to enlargement of the heart in both sexes, with male mice having greater chamber dilation.

The impact of Ang II-induced pressure overload on LV remodelling was further evaluated by comparing additional cardiac parameters including LV wall distensibility. LV wall distensibility is used to estimate LV wall stiffness (Takeda et al., 2009; Kawaguchi et al., 2003). LV wall distensibility was calculated from the difference between systolic LVPW and diastolic LVPW divided by systolic LVPW. Figures 3.13A and 3.13B show that LV wall distensibility decreased over time in both male and female mice, and this was significant compared to corresponding same-sex controls. In addition, female treated and control mice had greater LV wall distensibility compared to corresponding male data at midpoint only. These data indicate that male and female mice developed stiffer LV wall, as seen by reduced LV wall distensibility, following Ang II infusion.

The LV mass/end-diastolic volume ratio is a parameter used to identify LV concentric remodeling and hypertrophy in hypertensive patients (Lembo et al., 2019). The LV mass/end-diastolic volume ratio is a better indicator of LV concentric remodeling than LV wall thickness in hypertensive patients (Lembo et al., 2019). Here, the corrected LV mass/diastolic volume ratios identified from M-mode echocardiography were adapted from parameters used in humans to evaluate the degree of concentric remodeling in mice. Figure

3.14A shows that Ang II-infused female mice underwent concentric remodeling over time as seen by increased corrected LV mass/diastolic volume ratio over treatment time. This effect was significantly different from same-sex controls. In contrast, concentric remodeling did not occur in treated males, since corrected LV mass/diastolic volume ratio was unaffected by Ang II infusion (Figure 3.14B). These results illustrate that pressure overload induced by Ang II infusion caused concentric remodeling in hearts from females only.

3.3 Changes in *in vivo* cardiac function in response to Ang II infusion

M-mode echocardiography was also employed to evaluate heart rate and systolic function (EF and FS). Figure 3.15A shows that Ang II infusion had no effect on heart rate in female mice. In treated males, heart rate moderately declined over time, but this change was not significant when compared to same-sex controls. The impact of Ang II infusion on systolic function was investigated by examining effects on EF and FS. Figures 3.16 and 3.17 show that Ang II infusion caused EF and FS to decline over time in both male and female animals. These declines were significant when compared to corresponding same-sex controls. There were also sex differences, but these were present only in the control groups. Male controls had lower EF and FS compared to females at the midpoint and at the endpoint (Figures 3.16A and 3.17A). These findings suggest that Ang II infusion promoted systolic dysfunction in both sexes, and that both EF and FS may decline with age in control males when compared to females.

Pulse wave Doppler was used to further assess systolic and diastolic function. E/A ratios and IVRT are indicators of diastolic function in both preclinical and clinical studies

(Yuan et al., 2010). Prolonged IVCT is an indicator of systolic dysfunction (Garcia et al., 2006; Kono et al., 2010) and a novel predictor of HF in humans (Alhakak et al., 2020). Both IVCT and IVRT are prolonged in patients with CHF (Garcia et al., 2006). Figures 3.18A and 3.18B show representative pulse wave Doppler images in a treated male mouse at baseline (before Ang II infusion) and at midpoint (after Ang II infusion) respectively. The latter image shows that the late filling wave (A) decreased in amplitude while the early wave E was not affected. Figures 3.19A and 3.19B show that the E wave was unaffected by Ang II treatment in mice of both sexes. However, a sex difference was present where treated females had lower E wave values than males at the endpoint. In contrast, Ang II-induced hypertension caused the A wave to decline in amplitude over time in mice of both sexes (Figures 3.20A and 3.20B). Interestingly, this was more pronounced in males, as the decline in the A wave was significant when compared to male controls at midpoint and endpoint. By contrast, this did not occur in females. This sex difference translated to the results observed for the E/A ratios. Although E/A ratios in the treated female group increased slightly at midpoint and endpoint, this effect was not significant over time and when compared to the corresponding control group (Figure 3.21A). In males however, the E/A ratio increased, and this was significant over time and when compared to same-sex controls (Figure 3.21B). Thus, severe diastolic dysfunction was observed in treated males but not treated females.

Diastolic function was further examined using IVRT. Figures 3.22A and 3.22B show that Ang II-induced hypertension caused impaired relaxation in both males and females as seen by the prolongation of IVRT over time. In males, this adverse effect was significant compared to same-sex controls at midpoint and endpoint (Figure 3.22B).

However, diastolic dysfunction was less evident in females since IVRT prolongation was significant compared to female controls at midpoint only (Figure 3.22A). The impact of pressure overload caused by Ang II infusion on IVCT was also examined. IVCT prolongation was more profound in male mice than in female mice. Figure 3.23A and 3.23B show that Ang II-induced hypertension had no effect on IVCT in females, but caused marked IVCT prolongation in males at endpoint. This change was significant when compared to values at baseline and midpoint, male endpoint control, and endpoint treated females. Together, these results suggest that Ang II-induced hypertension caused diastolic dysfunction in both sexes, but this was more marked in male mice. IVCT prolongation in treated males but not females suggests that male mice exhibited worse systolic dysfunction in response to Ang II infusion when compared to females. A summary of the p values for all the cardiac parameters assessed using pulse wave Doppler echocardiography is shown in Table 3.2.

3.4 The impact of Ang II-infusion on contractile function in isolated whole hearts

At the endpoint, Langendorff-perfused heart experiments were performed to investigate the effects of Ang II infusion on baseline contractile function in *ex vivo* hearts. Due to differences in heart weights among the animals, RPP and flow rate were normalized to heart weight. Figures 3.28 shows that Ang II infusion had no effect on baseline heart rate, LVDP, rate of contraction (+dP/dt), and rate of relaxation (–dP/dt) in any group, and there were no sex differences in hearts from the treated groups. Although Ang II treatment did not have an effect on these parameters, hearts from male control mice did have higher baseline +dP/dt and –dP/dt when compared to females (Figures 3.24C and 3.24D).

Similarly, Ang II treatment had no effect on RPP in either male or female hearts, but RPP in control hearts from male mice was higher when compared to female controls (Figure 3.25A). RPP is a product of LVDP and heart rate and is used as an indicator of cardiac work and myocardial oxygen consumption in both animals and humans (Pal et al., 2014, Aksentijevic et al., 2016). Interestingly, the impact of Ang II on cardiac work in Langendorff-perfused hearts was apparent when RPP was normalized to heart weight. Figure 3.25B shows that normalized RPP decreased significantly in hearts from treated male mice when compared to same-sex controls, but this was not seen in females. To determine whether the effects were attributable to differences in coronary perfusion, coronary flow rate were compared in treated and control mice of both sexes. Figure 3.26 shows that coronary flow rate and normalized coronary flow rate in hearts from treated male and female mice were not affected by Ang II treatment. There were no sex differences in coronary flow rate in any group. Together, these results illustrate that Ang II treatment had little impact on contractile properties of Langendorff-perfused hearts from female animals, although it did reduce cardiac work in hearts from male mice.

3.5 The impact of Ang II infusion on tissue morphology and fibrosis

Following Langendorff studies, heart weights were recorded to determine the impact of Ang II treatment on *ex vivo* cardiac morphology. Figure 3.27 shows that Ang II-treated female mice exhibit cardiac hypertrophy in *ex vivo* heart. The hypertrophied heart, shown on the right, was isolated from an Ang II-infused female mouse (Figure 3.27B). The control heart, shown on the left, is smaller in size in comparison (Figure 3.27A). Body weights of controls and treated mice were also recorded at the end of the experiment to

assess whether Ang II infusion affects body weights. Figure 3.28A shows that Ang II-treated male mice had markedly reduced body weights compared to same-sex controls, but this did not occur in females. In addition, treated and control male mice had larger body weights than treated and control females respectively (Figure 3.28A). Since Ang II infusion induced alterations in body weight, it was not used to normalize measures of tissue hypertrophy. Fluid retention in animals with HF can affect actual body weight and introduce error in cardiac measures normalized by body weight (Hagdorn et al., 2019). To avoid such error, tibia length has been recommended for indexing cardiac measures, since it normalizes for animal size independently of changes in body compositions (Hagdorn et al., 2019). As shown in figure 3.28B, control male mice also had larger heart weights than control females. Figure 3.28 also shows that Ang II-induced hypertension resulted in larger heart weights in female treated mice when compared to same-sex control. However, this was not seen in males (Figure 3.28B). Similar results were seen when heart weight was normalized to tibia length (Figure 3.28C).

The lung was isolated from each mouse and its weight was recorded to examine whether Ang II-infusion resulted in changes in lung morphology. The amount of fluid in the lung was also measured to determine the extent of pulmonary edema, a common manifestation of HF (Miglioranza et al., 2017). Figures 3.29A-C show that Ang II-treated females had larger wet lung weights, increased lung weight to tibia length ratios, and elevated pulmonary fluid respectively, and this was not seen in males. There were no sex differences in any group (Figures 3.29A-C).

Previous results in *in vivo* heart indicated that Ang II-treated mice of both sexes exhibited diastolic dysfunction and increased LV wall stiffness. In the hypertrophied heart,

increased cardiac wall stiffness is due to fibrosis or deposition of extracellular collagen (Roe et al., 2017). Thus, increased cardiac wall stiffness in Ang II-infused mice may be due high levels of fibrosis in the heart. In order to quantify the levels of fibrosis in hearts from mice used in this study, the fibrosis assay measuring hydroxyproline concentrations was performed. The hydroxyproline concentration is associated with collagen level and is a marker of fibrosis (Qiu et al., 2014). Figure 3.30 shows that Ang II-infused mice had higher collagen content on average than the corresponding control groups, but this was not statistically significant. Overall, these findings suggest that lower body weight and greater cardiac hypertrophy was seen in Ang II-treated male mice, while increased pulmonary hypertrophy and elevated pulmonary edema was seen in treated females only. The levels of fibrosis in hearts isolated from both males and females were not affected by Ang II infusion. Results for *in vivo* and *ex vivo* overall cardiac changes in treated mice of both sexes were summarised in Table 3.3.

3.6 Effects of Ang II infusion on frailty and mortality in mice of both sexes

The results presented thus far show that older male and female mice developed signs of HF in response to Ang II infusion. The next series of experiments aimed to determine the effects of Ang II-induced HF on frailty and mortality in aging mice of both sexes. FI scores and mortality were assessed at baseline and at weekly intervals after Ang II infusion in mice of both sexes. Figure 3.31 shows Kaplan-Meier survival curves, which illustrate survival for the mice used in this study. Mortality was recorded when an animal died unexpectedly or was euthenized due to illness or low HEP weight. Treated male and female mice had higher mortality rates than corresponding same-sex controls, but analysis

with log-rank tests showed no significant differences between groups (Figure 3.31). Next we assessed the impact of Ang II-induced HF on frailty measured as FI scores. FI scores were normalized to percent of baseline control (mean ± SEM) for males and females (Figures 3.32A and 3.32B). Results showed that FI scores of Ang-II infused male and female mice progressively increased over time to levels that were significantly higher than corresponding same-sex controls. Interestingly, this difference in FI scores between treated and control mice was more marked in males than in females (Figure 3.32B). For example, a sex difference between FI scores for treated mice was seen at week 5, where males had higher FI scores than females (Figure 3.32A). These data indicate that Ang II infusion worsened frailty in mice of both sexes, with males being more severely affected than females.

To determine whether the differences in FI scores between Ang II-infused and control mice were due to effects on a single deficit or to more widespread effects on multiple deficits, the proportion of mice with each deficit were determined. Figure 3.33A, B, and C show the proportion of treated and control female mice with specific deficits at baseline, midpoint, and endpoint respectively. Figure 3.34 shows these proportions in males. The results show that Ang II infusion caused increases in the proportions of deficits across treatment time in both males and females. In addition, a wide variety of deficits were affected. Interestingly, some deficits differed significantly between control and Ang II-treated mice. For example, at baseline the female control group showed more kyphosis than the treated group, while at midpoint the treated group showed more menace reflex and vision loss deficits than control (Figure 3.33A and 3.33B). At endpoint, the proportions of treated female mice with deficits in breathing rate, vision loss, hearing loss, body condition

score, and kyphosis were higher compared to the control group (Figure 3.33C). For male mice, there was a higher proportion of control mice with deficits in piloerection at baseline (Figure 3.34A). At midpoint, the proportion of mice with deficits in breathing rate, tail stiffening, kyphosis, and coat condition was higher in treated compared to control mice (Figure 3.34B). The treated male group also showed more deficits than control group at endpoint in grimace scale, breathing rate, hearing loss, gait disorders, and tail stiffening (Figure 3.34C). These data suggest that the differences in FI scores in treated versus control mice arose from a combination of multiple deficits rather than effects on a single deficit or system.

Next, the FRIGHT and AFRAID clock scores, as predictors of biological age and life expectancy respectively, were determined for treated and control mice of both sexes. Figures 3.35A and 3.35B show that Ang II-induced hypertension increased estimated biological age in mice of both sexes. For example, FRIGHT clock ages progressively increased over time in Ang II-treated female mice, and this was significantly different from controls at weeks 3 and 6 (Figure 3.35A). An even more striking increase in biological age was seen for male mice, as the difference was also significant at week 5 (Figure 3.35B). Ang II infusion also caused estimated life expectancy, indicated by the AFRAID clock, to decline over time in both sexes (Figures 3.36A and 3.36B). Interestingly, this decline in treated males was significant compared to same-sex controls at midpoint (week 3), but this did not occur in females. It is also interesting to note that females had a longer life expectancy at baseline than males. These data suggest that Ang II infusion caused accelerated aging and reduced life expectancy in male and female mice, with the impact being more severe in males.

It is possible that Ang II-infused mice with highest levels of frailty at baseline were more susceptible to adverse cardiac outcomes including signs of HF. Thus, the relationship between *in vivo* cardiac parameters at endpoint and the baseline frailty scores in treated mice was investigated by plotting all cardiac parameters measured immediately prior to an animal's death as a function of individual baseline FI scores. Specific examples for females and males are shown in Figures 3.37 and 3.38 respectively. Figures 3.37A-H show that endpoint cardiac parameters including corrected LV mass, LV diameter at systole, LVAW at systole, LVPW at diastole, EF, IVCT, IVRT, and E/A ratios respectively were not correlated with baseline FI scores in treated female mice. These results were similar in male mice (Figures 3.38A-H). These results suggest that baseline frailty may not predict adverse cardiac outcomes in Ang II-infused mice, regardless of their sex.

A. Baseline Ang II Male

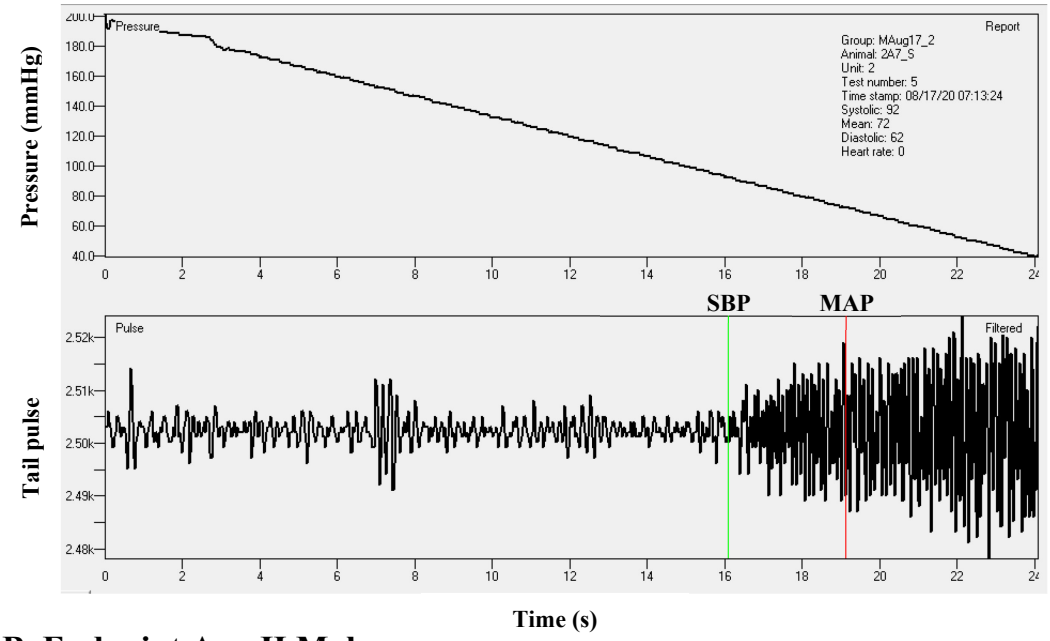

B. Endpoint Ang II Male

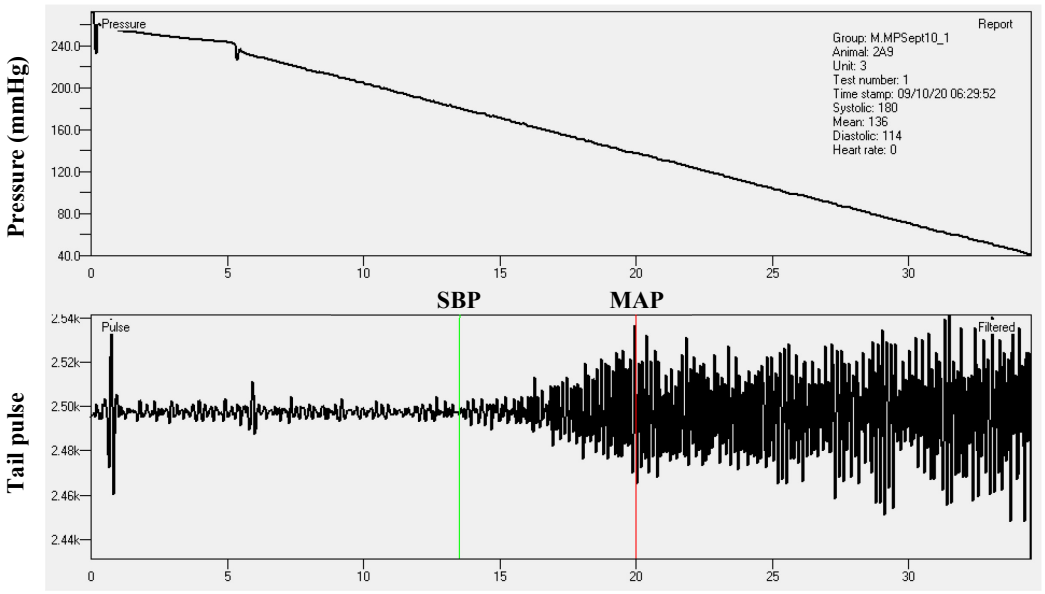

Figure 3.1. Representative examples of blood pressure show that an Ang II-treated male mouse developed hypertension at endpoint compared to baseline. The trace on the pressure panel (top) shows the amount of pressure being applied to the cuff on the mouse's tail. On the tail pulse panel (bottom), the green line indicates where the pulse envelop begins, indicating the systolic blood pressure (SBP). The red line indicates where there is a fairly even drop-off of pulses after the highest pulse. This is the mean arterial pressure (MAP). The diastolic blood pressure is calculated from the SBP and MAP.

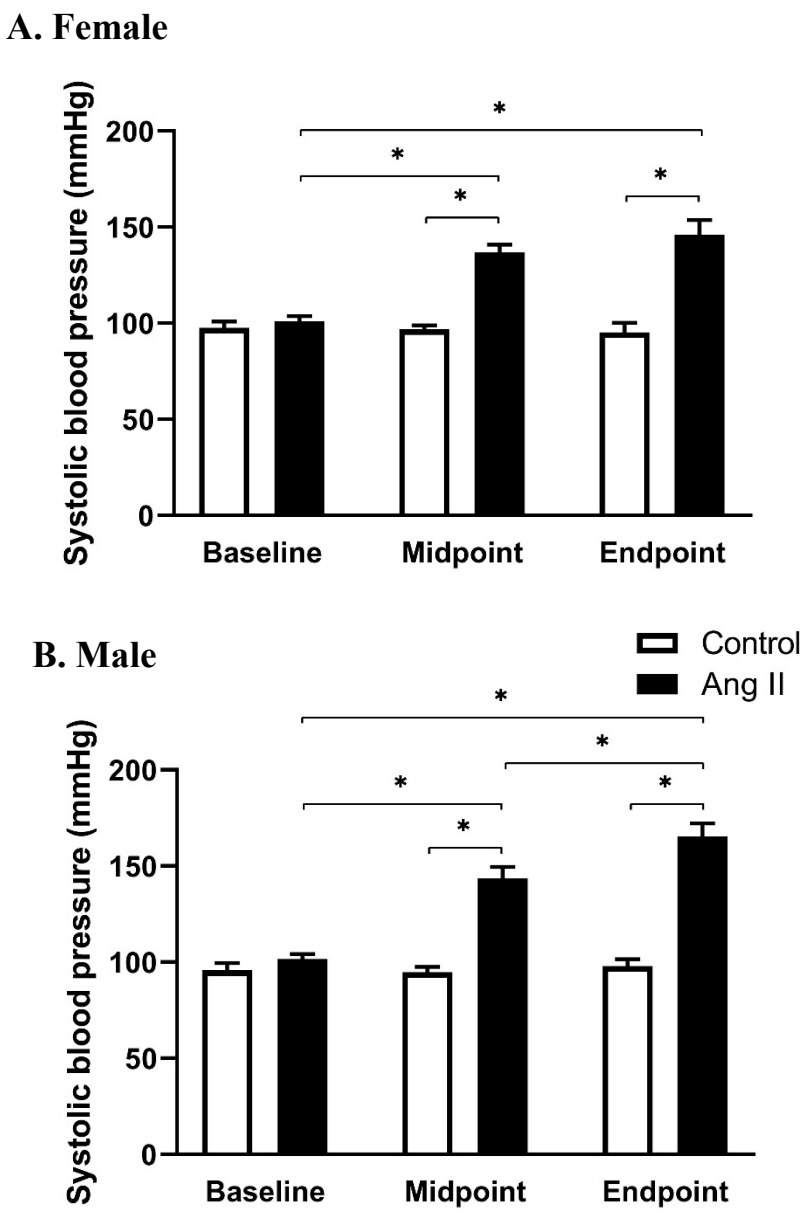

Figure 3.2. Ang II infusion increased systolic blood pressure in mice of both sexes. A. Systolic blood pressure increased over time in treated female mice, and this was significant compared to same-sex controls. B. Similar results were seen in males. Sample sizes for females were n = 9 control, n = 10 treated and males were n = 6 control and n = 11 treated. Data were analysed with mixed-effects analysis and a Fisher's LSD post-hoc test. The symbol * denotes P <0.05.

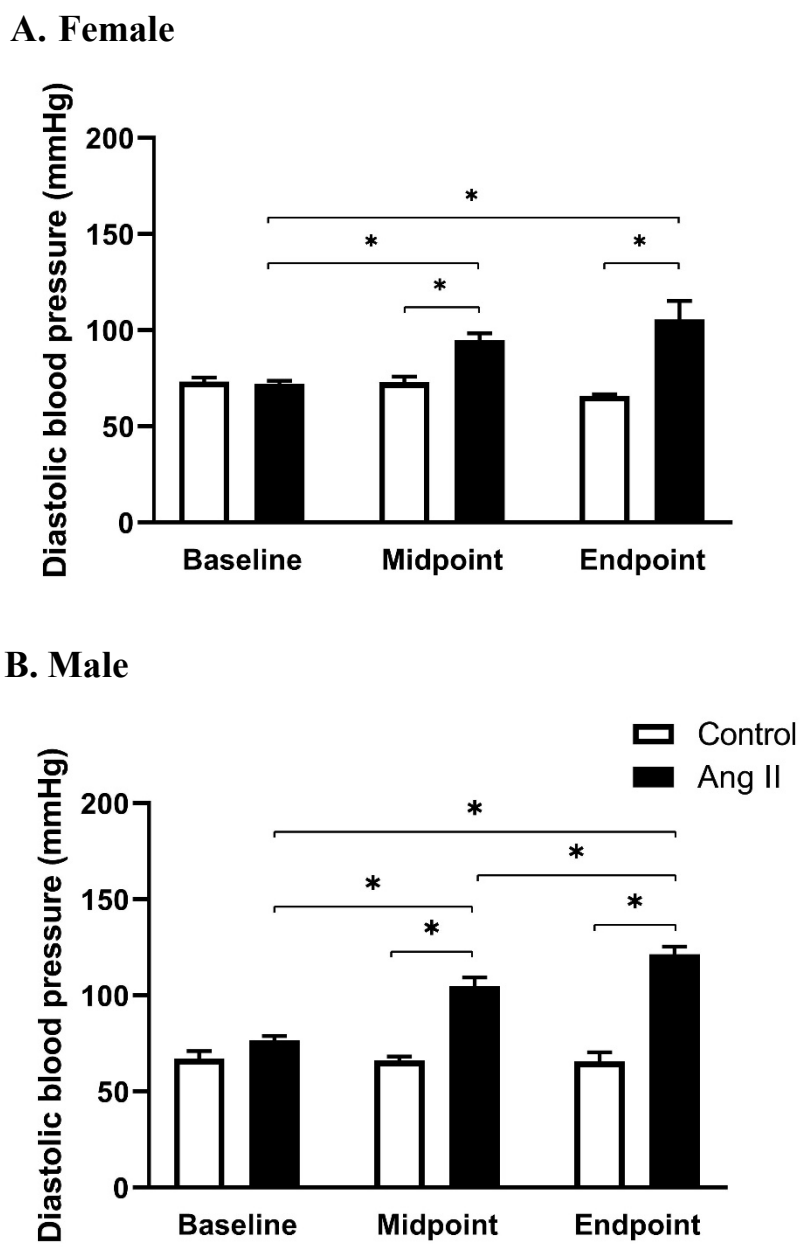

Figure 3.3. Ang II infusion increased diastolic blood pressure in mice of both sexes. A. Diastolic blood pressure increased over time in treated female mice, and this was significant compared to same-sex controls. B. Similar results were seen in males. Sample sizes for females were n = 9 control, n = 10 treated and males were n = 6 control and n = 11 treated. Data were analysed with mixed-effects analysis and a Fisher's LSD post-hoc test. The symbol * denotes $P < 0.05$.

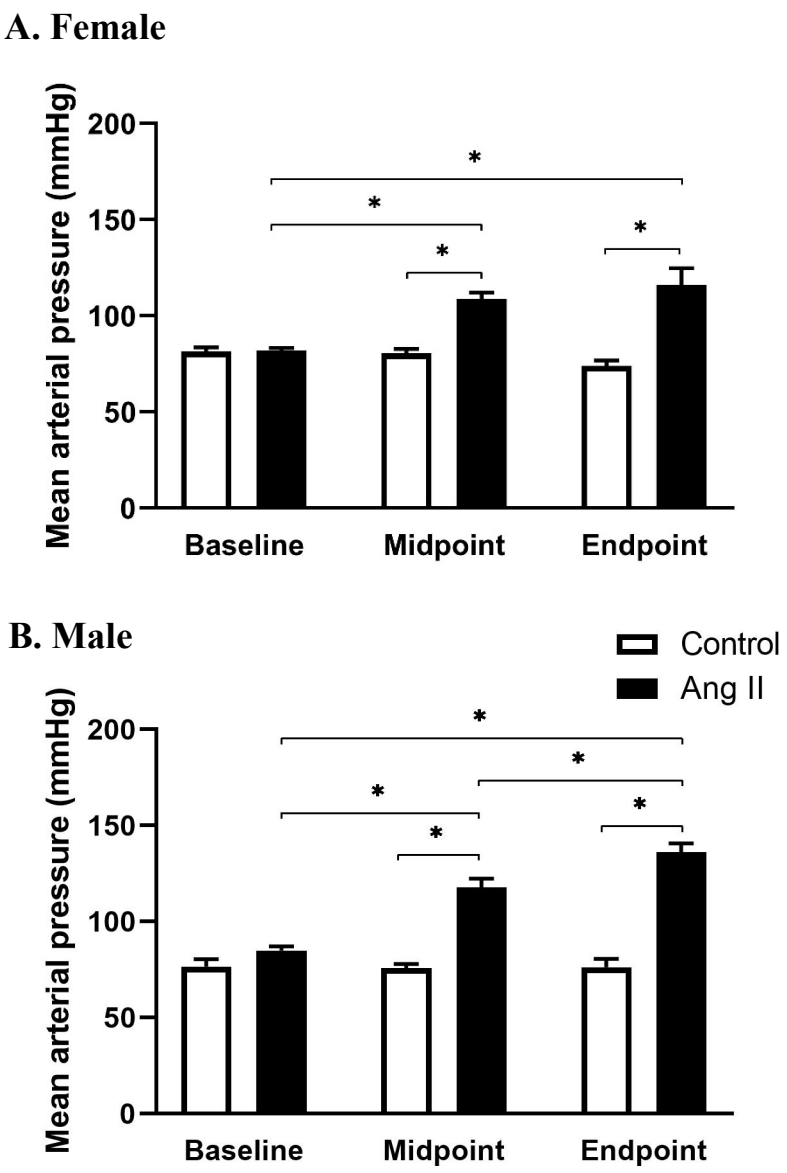

Figure 3.4. Ang II infusion led to hypertension in mice of both sexes. A. Mean arterial pressure increased over time in treated female mice, and this was significant compared to same-sex controls. B. Similar results were seen in males. Sample sizes for females were n = 9 control, n = 10 treated and males were n = 6 control and n = 11 treated. Data were analysed with mixed-effects analysis and a Fisher's LSD post-hoc test. The symbol * denotes $P < 0.05$.

A. Baseline Ang II Male

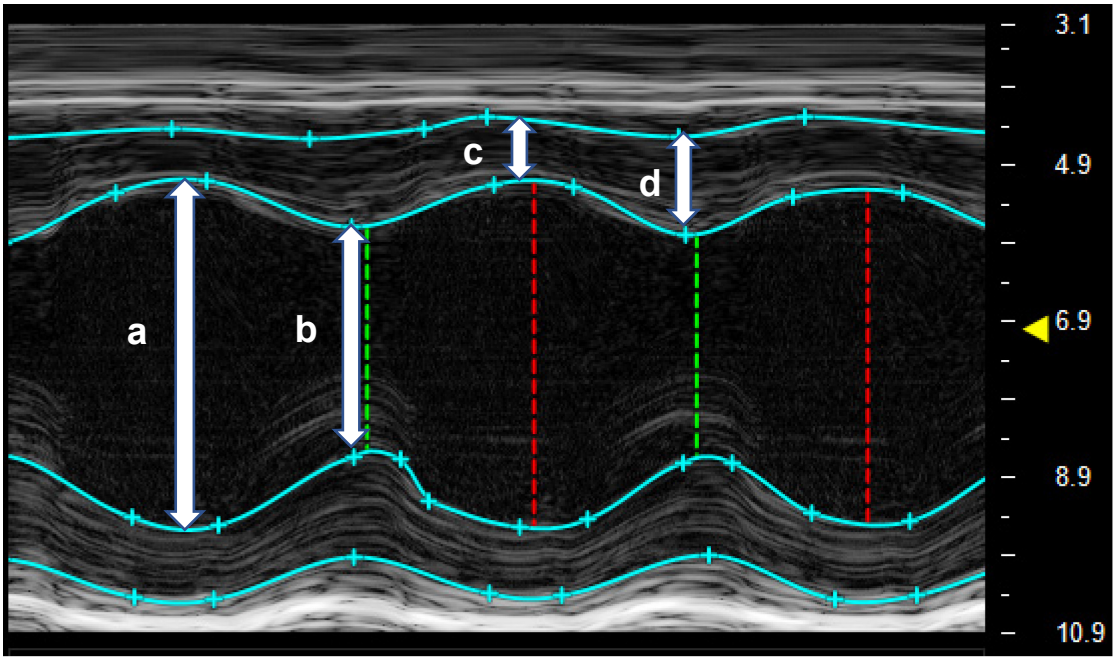

B. Endpoint Ang II Male

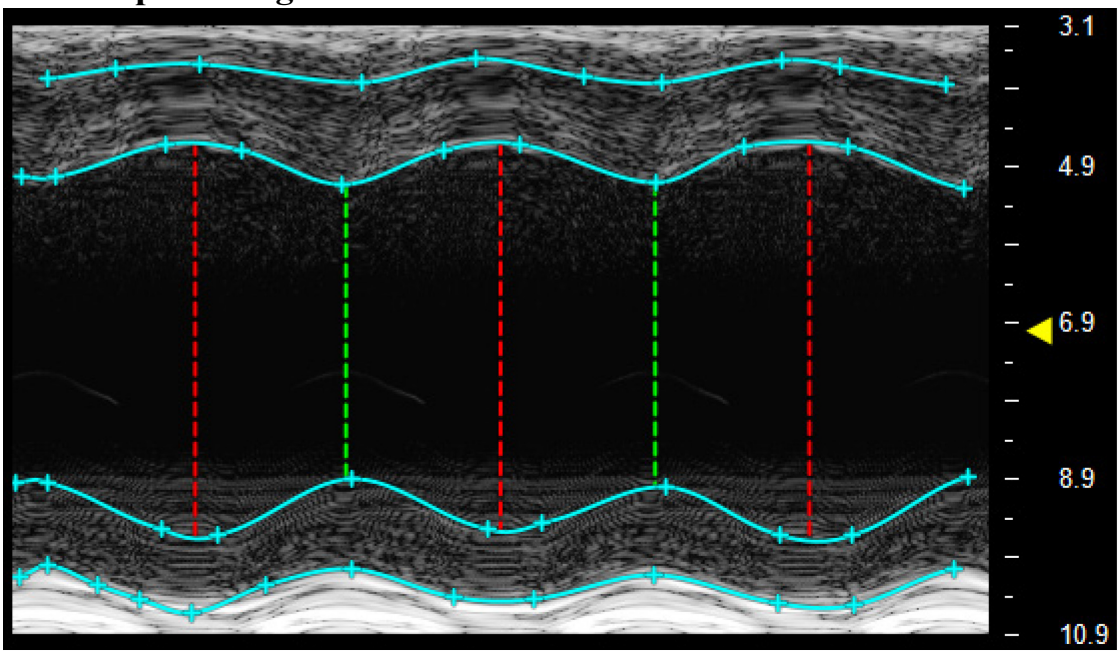

Figure 3.5. Representative M-mode echocardiography images of *in vivo* LV structure in male mice before (baseline) and after Ang II infusion (endpoint). A. The top image shows normal LV structure. The letters a, b, c, d represent diastolic diameter, systolic diameter, systolic diameter of left ventricular anterior wall, and diastolic diameter of left ventricular anterior wall respectively. B. The bottom image shows LV chamber dilation.

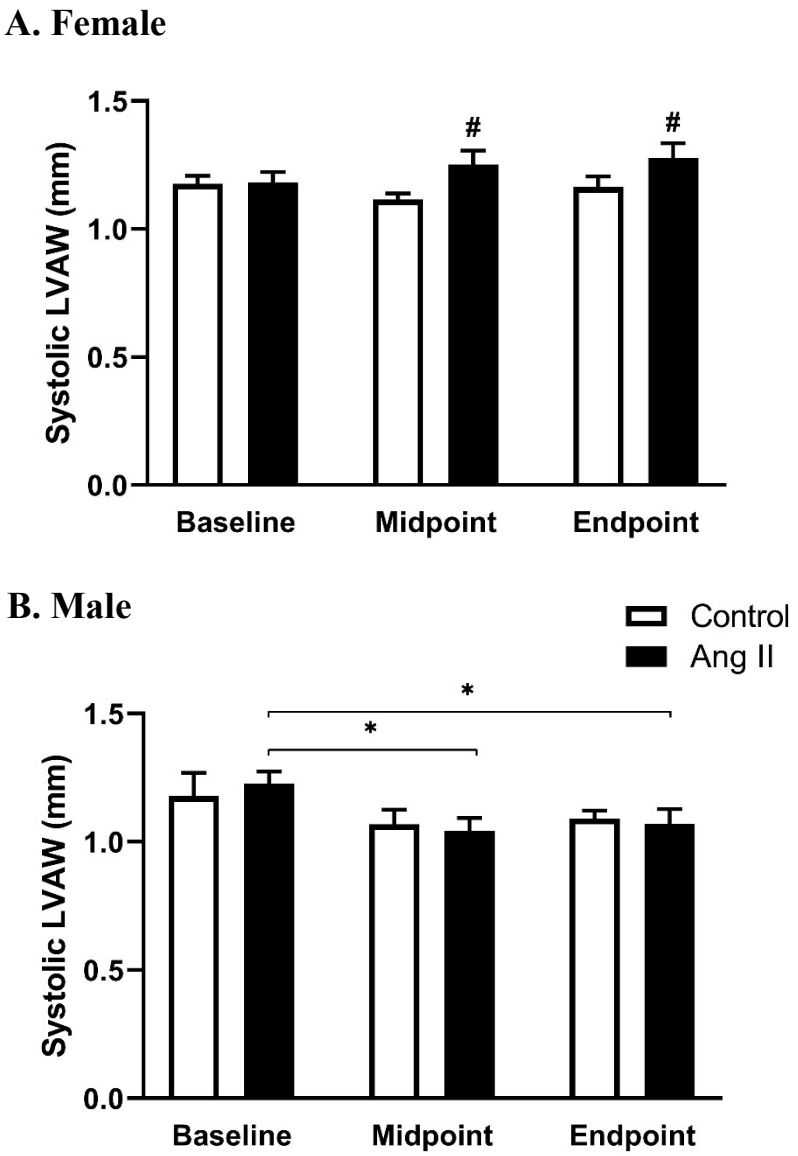

Figure 3.6. Ang II-induced hypertension decreased systolic LVAW thickness male mice, and the walls were thinner than in females. A. Ang II-induced hypertension had no effect on systolic LVAW female mice compared to same-sex controls. B. Systolic LVAW in treated males decreased moderately over time and was significantly lower than in treated females at midpoint and endpoint. Sample sizes for females were n = 9 control, n = 10 treated and males were n = 6 control and n = 11 treated. Data were analysed with mixed-effects analysis and a Fisher's LSD post-hoc test. The symbol * denotes $P < 0.05$ and # denotes significant difference from corresponding data in males, $P < 0.05$.

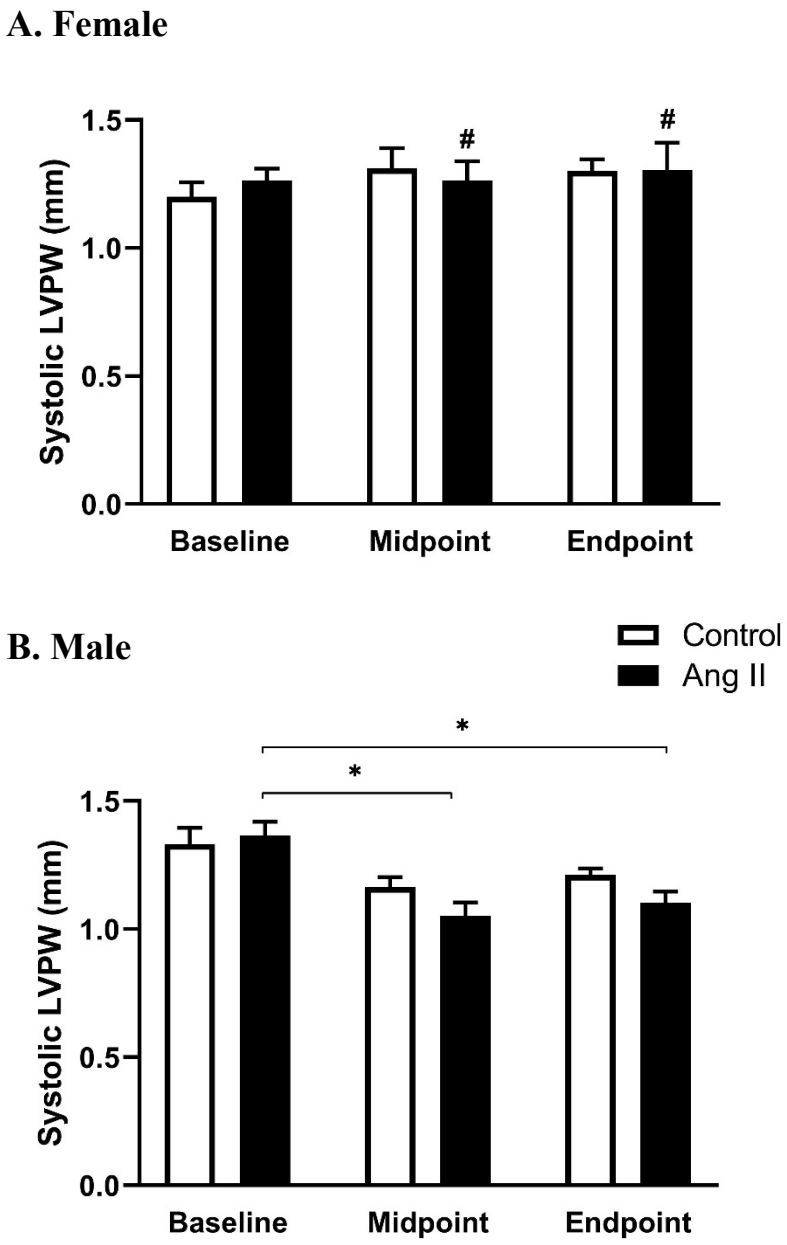

Figure 3.7. Ang II-induced hypertension reduced systolic LVPW thickness in male mice, and this was smaller than in females. A. Ang II-induced hypertension had no effect on systolic LVPW female mice compared to same-sex controls. B. Systolic LVPW in treated males decreased moderately over time and was significantly lower than in treated females at midpoint and endpoint. Sample sizes for females were n = 9 control, n = 10 treated and males were n = 6 control and n = 11 treated. Data were analysed with mixed-effects analysis and a Fisher's LSD post-hoc test. The symbol * denotes $P < 0.05$ and # denotes significant difference from corresponding data in males, $P < 0.05$.

Table 3.1. P-values from mixed-effects analysis for cardiac parameters measured by M-mode echocardiography.

Parameter, unit	Time	Sex	Treatment	Time x Sex	Time x Treatment	Sex x treatment
LVAWs, mm	0.0775	0.0507	0.2641	**0.0493**	0.8894	0.3152
LVPWs, mm	0.2477	0.1237	0.3147	**0.0386**	0.1114	0.2865
LVAWd, mm	0.2993	0.1338	**0.0027**	0.3736	0.1089	0.0617
LVPWd, mm	0.1294	0.6661	**0.0046**	0.3762	0.387	**0.0409**
Ds, mm	**<0.0001**	**<0.0001**	**<0.0001**	0.1527	**0.0033**	0.4488
Dd, mm	**0.0144**	**<0.0001**	**0.0052**	0.2199	**0.0276**	0.4537
Corrected LV mass, mg	**0.02**	**<0.0001**	**0.0008**	**0.0255**	0.0605	**0.0002**
HR, bpm	**0.0068**	**0.0266**	0.4798	0.5833	0.2909	0.6855
EF, %	**<0.0001**	**0.01**	**<0.0001**	0.134	**0.0005**	0.4119
FS, %	**<0.0001**	**0.0221**	**<0.0001**	0.1229	**0.0006**	0.183

Abbreviations: LVAWs, systolic left ventricular anterior wall; LVPWs, systolic left ventricular posterior wall; LVAWd, diastolic left ventricular anterior wall; LVPWd, diastolic left ventricular posterior wall; Ds, systolic diameter; Dd, diastolic diameter; HR, heart rate; bpm, beats per minute; EF, ejection fraction; FS, fractional shortening.

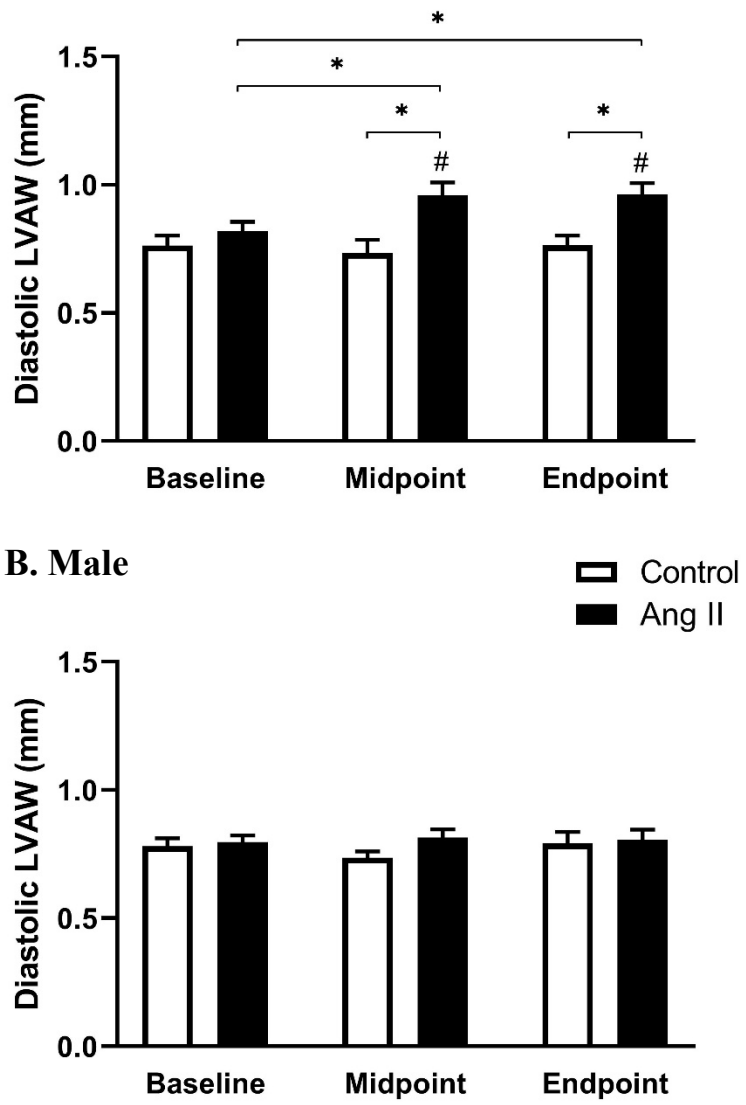

Figure 3.8. Ang II-induced hypertension markedly increased diastolic LVAW thickness in female mice but not in male mice. A. Diastolic LVAW increased over time in treated female mice, and this was significant compared to female controls and treated males at midpoint and endpoint. B. Ang II-induced hypertension had no effect on diastolic LVAW in males. Sample sizes for females were n = 9 control, n = 10 treated and males were n = 6 control and n = 11 treated. Data were analysed with mixed-effects analysis and a Fisher's LSD post-hoc test. The symbol * denotes $P < 0.05$.

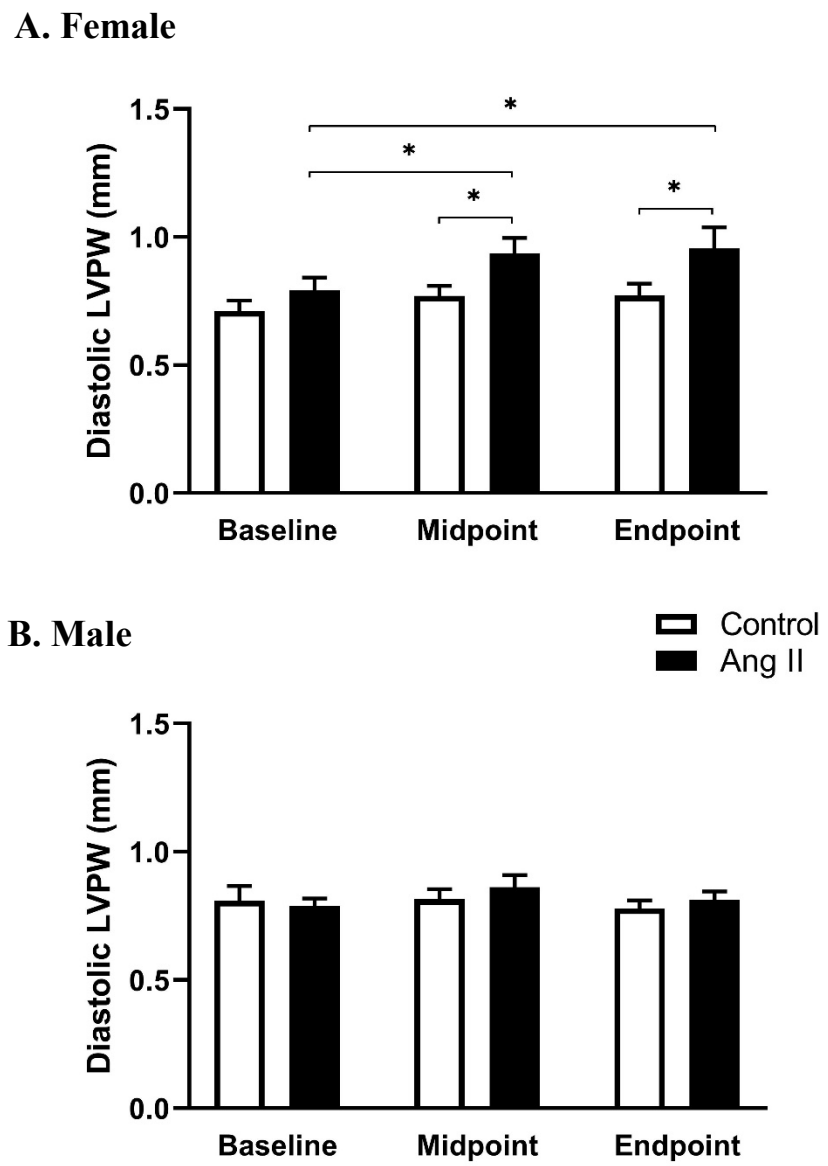

Figure 3.9. Ang II-induced hypertension increased diastolic LVPW thickness in female mice but not in male mice. A. Diastolic LVPW increased over time in treated female mice, and this was significant compared to female controls. B. Ang II-induced hypertension had no effect on diastolic LVPW in males. Sample sizes for females were n = 9 control, n = 10 treated and males were n = 6 control and n = 11 treated. Data were analysed with mixed-effects analysis and a Fisher's LSD post-hoc test. The symbol * denotes $P < 0.05$.

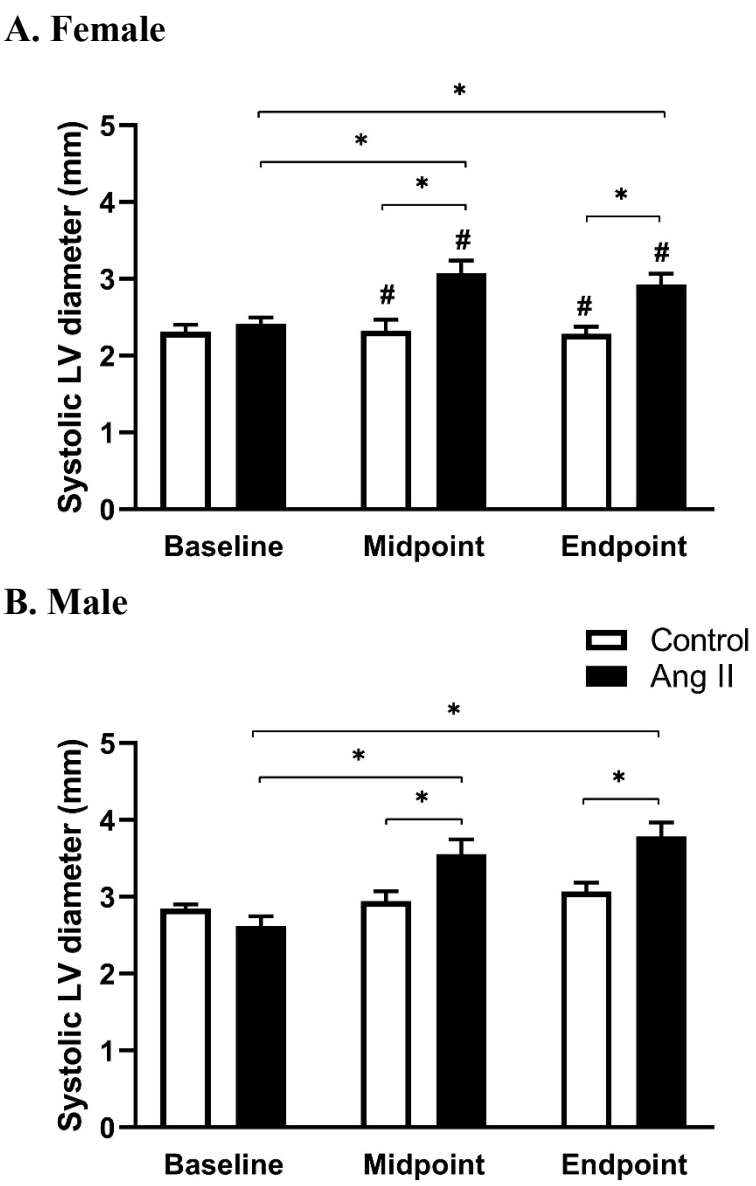

Figure 3.10. Ang II-induced hypertension dilated the LV in systole in mice of both sexes. A. Systolic LV diameter in treated female mice increased over time, and this was significant compared to same-sex controls. B. Similar results were seen in males. Both male treated and control mice had larger systolic diameters compared to corresponding females at midpoint and endpoint. Sample sizes for females were n = 9 control, n = 10 treated and males were n = 6 control and n = 11 treated. Data were analysed with mixed-effects analysis and a Fisher's LSD post-hoc test. The symbol * denotes $P < 0.05$ and # denotes significant difference from corresponding data in males, $P < 0.05$.

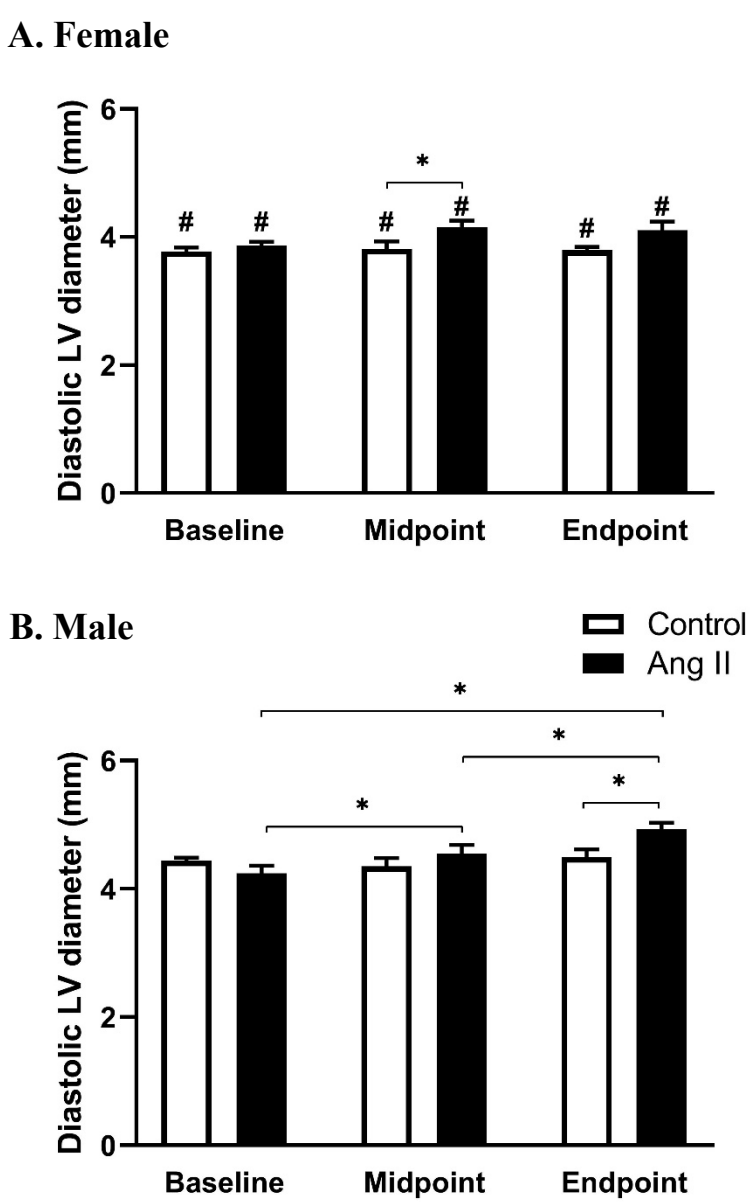

Figure 3.11. Ang II-induced hypertension dilated the LV in diastole in males more than in females. A. Diastolic diameter in treated female mice increased at midpoint only. B. Diastolic diameter in treated male mice increased over time and was significantly larger than male controls at endpoint. Both male treated and control mice had larger diastolic diameters than females at all time points. Sample sizes for females were n = 9 control, n = 10 treated and males were n = 6 control and n = 11 treated. Data were analysed with mixed-effects analysis and a Fisher's LSD post-hoc test. The symbol * denotes $P < 0.05$ and # denotes significant difference from corresponding data in males, $P < 0.05$.

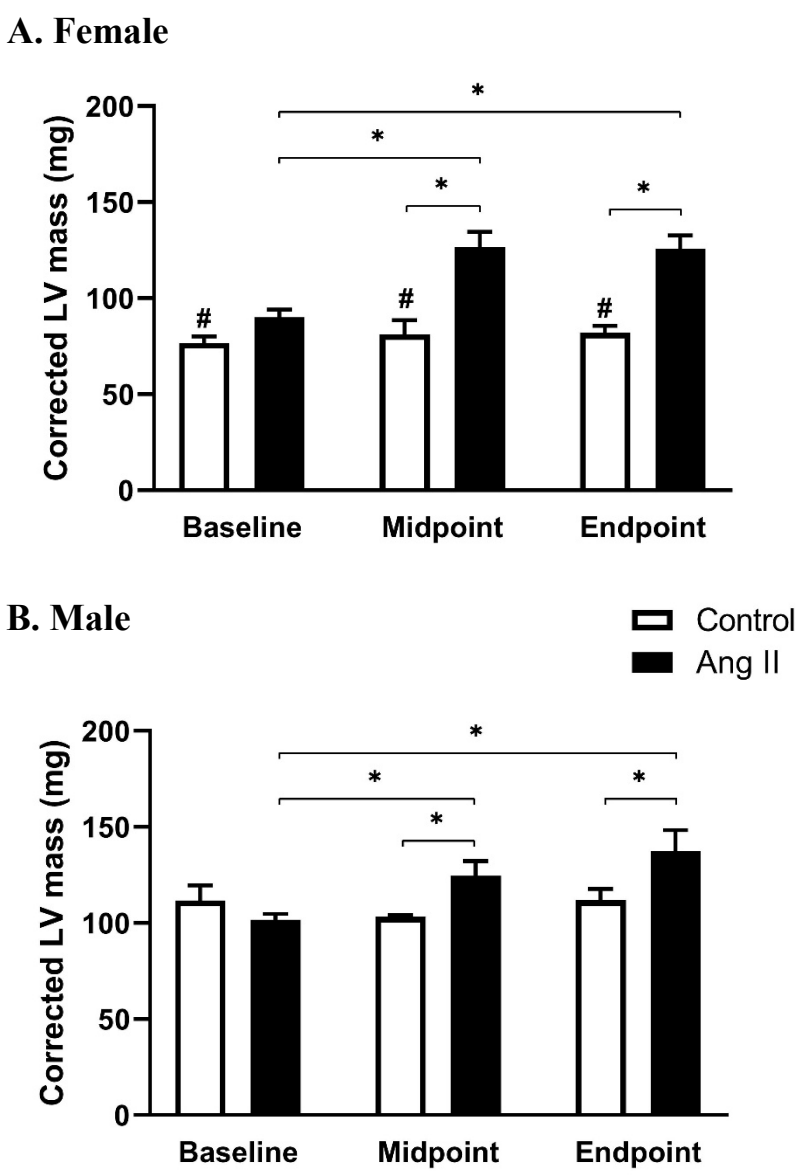

Figure 3.12. Pressure overload induced by Ang II increased LV mass in mice of both sexes. A. Corrected LV mass in treated female mice increased over time, and this was significant compared to same-sex controls. B. Similar results were seen in males. Male controls also had larger hearts than female controls at all time points. Sample sizes for females were n = 9 control, n = 10 treated and males were n = 6 control and n = 11 treated. Data were analysed with mixed-effects analysis and a Fisher's LSD post-hoc test. The ymbol * denotes P <0.05 and # denotes significant difference from corresponding data in males, P <0.05.

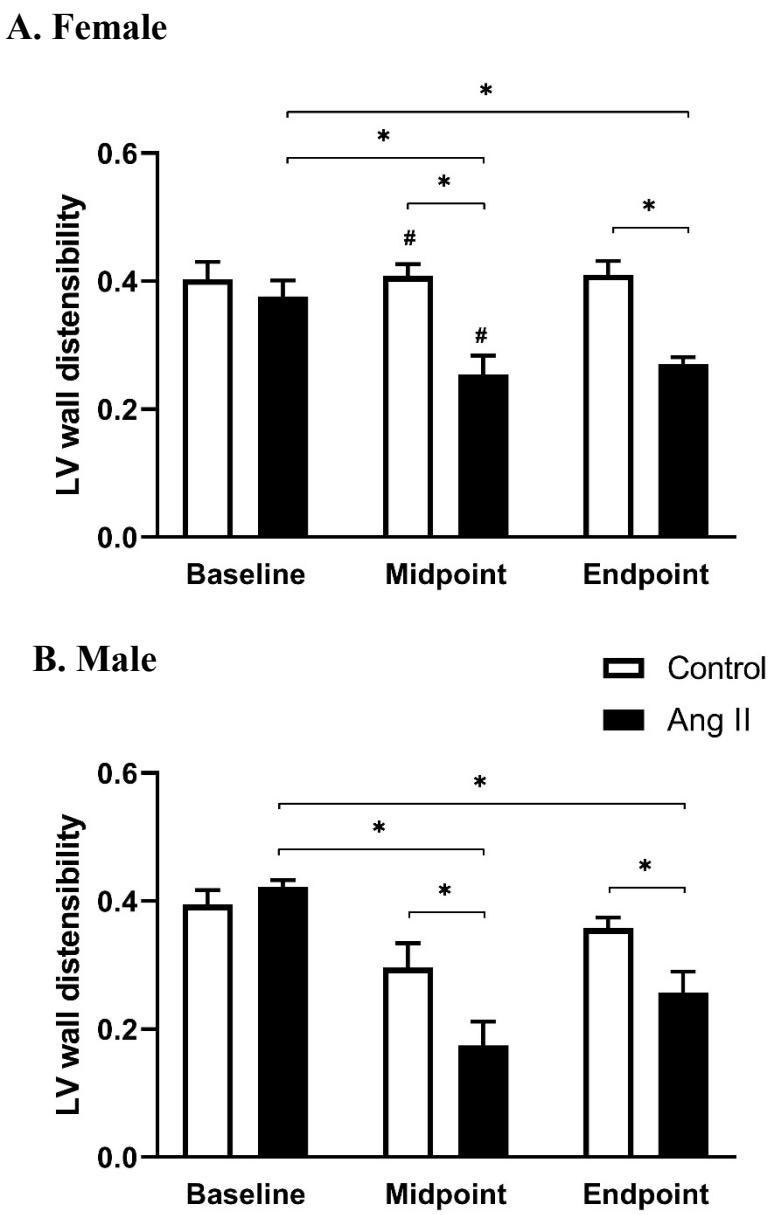

Figure 3.13. Ang II-induced hypertension caused increased wall stiffness in mice of both sexes. A. LV wall distensibility decreased over time in treated females, and this was significant compared to same-sex controls. B. Similar results were seen for male mice. Both control and treated male mice also had lower LV wall distensibility when compared to corresponding data in females, indicating that LV stiffness was greater in males than females at midpoint. Sample sizes for females were n = 9 control, n = 10 treated and males were n = 6 control and n = 11 treated. Data were analysed with mixed-effects analysis and Fisher's LSD post-hoc. Symbol * denotes $P < 0.05$ and # denotes significant difference from corresponding data in males, $P < 0.05$.

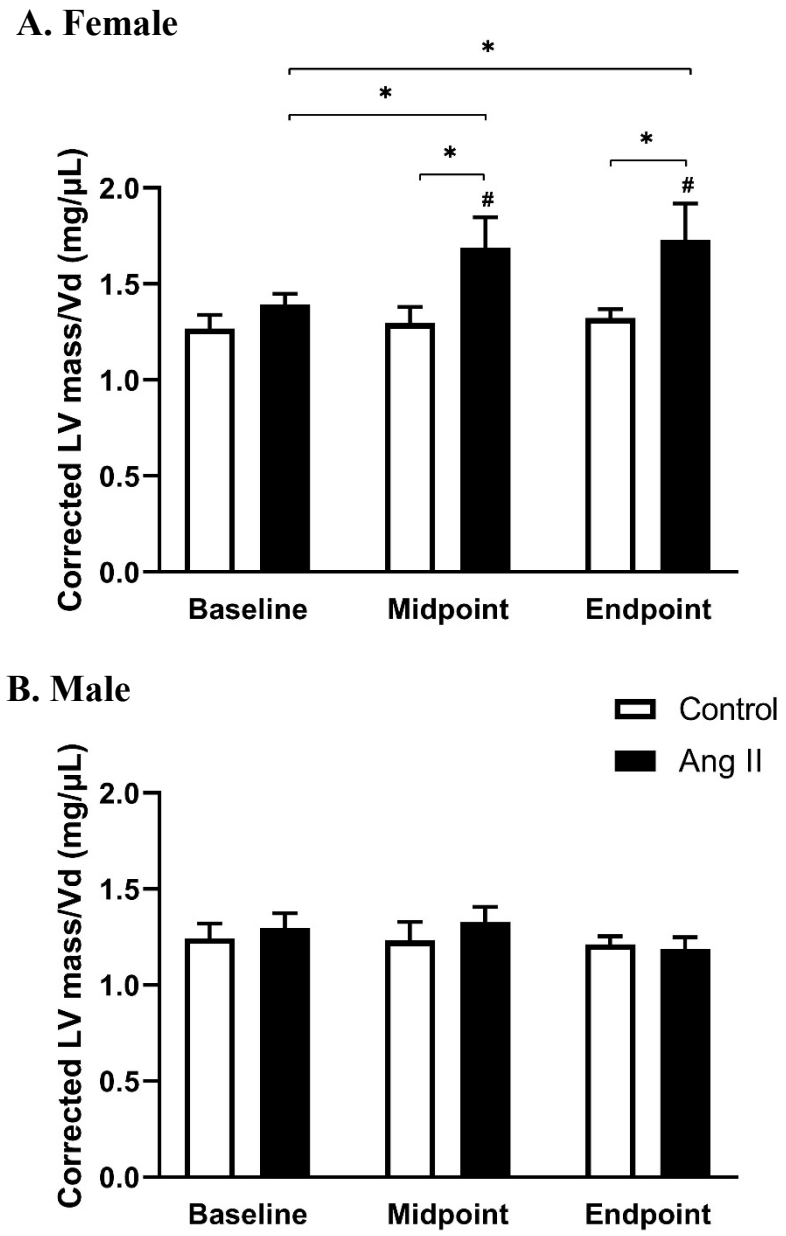

Figure 3.14. Ang II-induced pressure overload promoted concentric remodeling in female mice but not in male mice. A. Corrected LV mass/diastolic volume ratios increased over time in treated female mice, and this was significant compared to same-sex controls. B. Ang II infusion did not have an effect on corrected LV mass/diastolic volume ratio in males. Sample sizes for females were n = 9 control, n = 10 treated and males were n = 6 control and n = 11 treated. Data were analysed with mixed-effects analysis and a Fisher's LSD post-hoc test. The symbol * denotes $P < 0.05$ and # denotes significant difference from corresponding data in males, $P < 0.05$

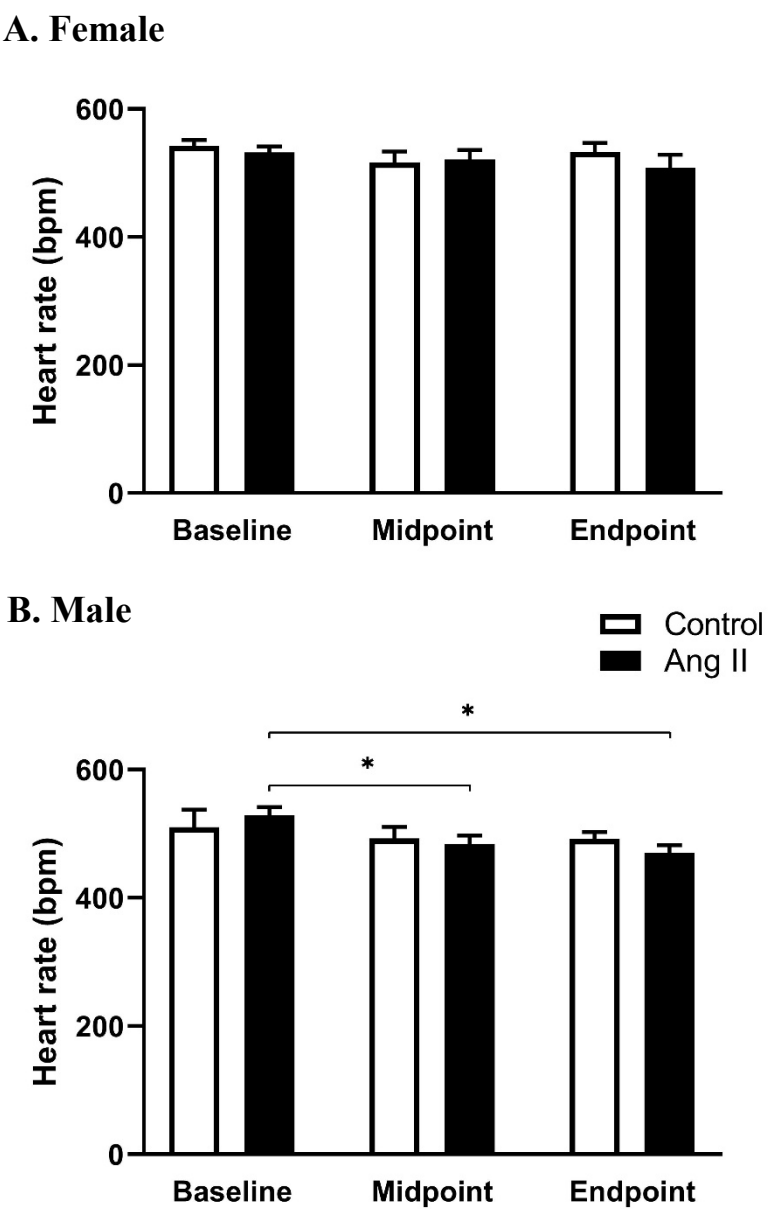

Figure 3.15. Ang II-induced hypertension caused a moderate decline in heart rate in males but had no effect in females. A. Heart rate was not affected by Ang II infusion in females. B. Heart rate in Ang II-infused male mice declined moderately over time, but this was not significant compared to same-sex controls Sample sizes for females were n = 9 control, n = 10 treated and males were n = 6 control and n = 11 treated. Data were analysed with mixed-effects analysis and a Fisher's LSD post-hoc test. The symbol * denotes P <0.05.

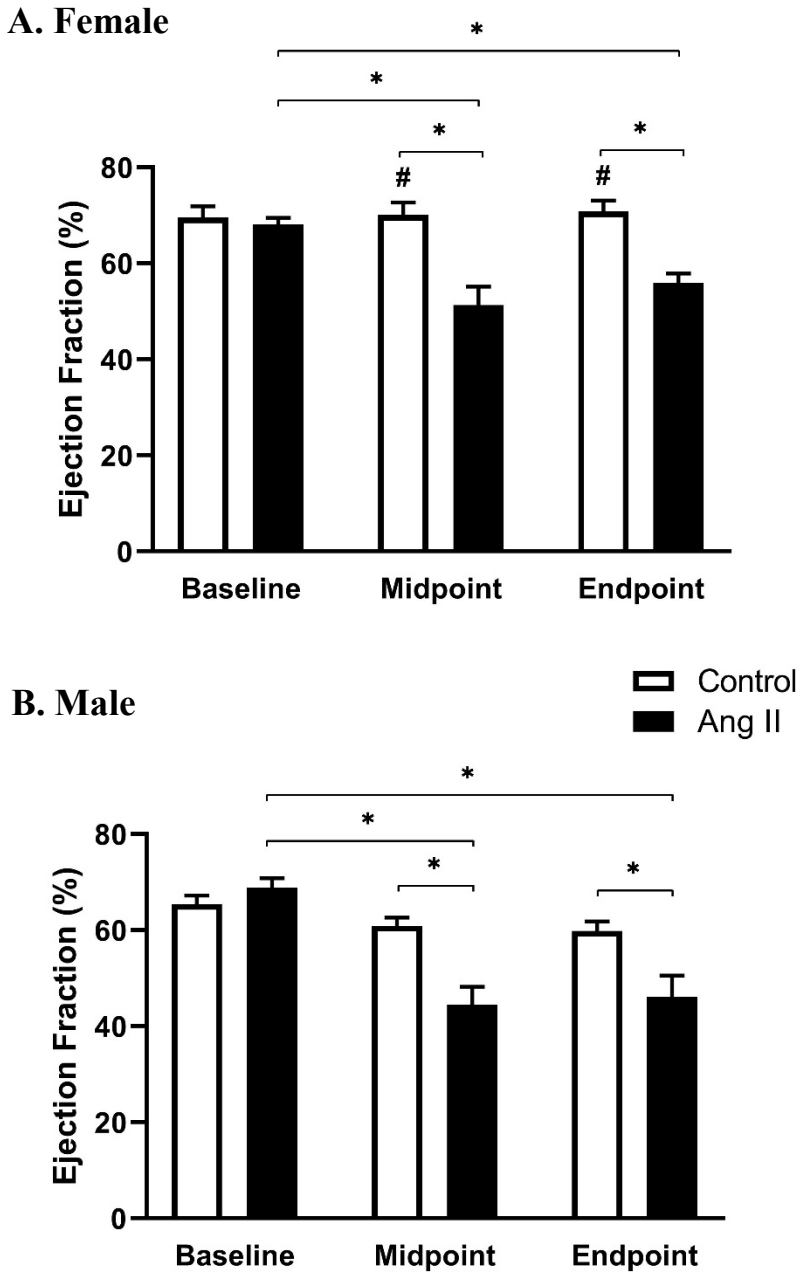

Figure 3.16. Pressure overload caused by Ang II infusion reduced ejection fraction in mice of both sexes. A. Ejection fraction decreased over time in treated female mice, and this was significant compared to same-sex controls. B. Similar results were seen in males. Male controls also had lower ejection fraction than female controls at midpoint and endpoint. Sample sizes for females were n = 9 control, n = 10 treated and males were n = 6 control and n = 11 treated. Data were analysed with mixed-effects analysis and a Fisher's LSD post-hoc test. The symbol * denotes $P < 0.05$ and # denotes significant difference from corresponding data in males, $P < 0.05$.

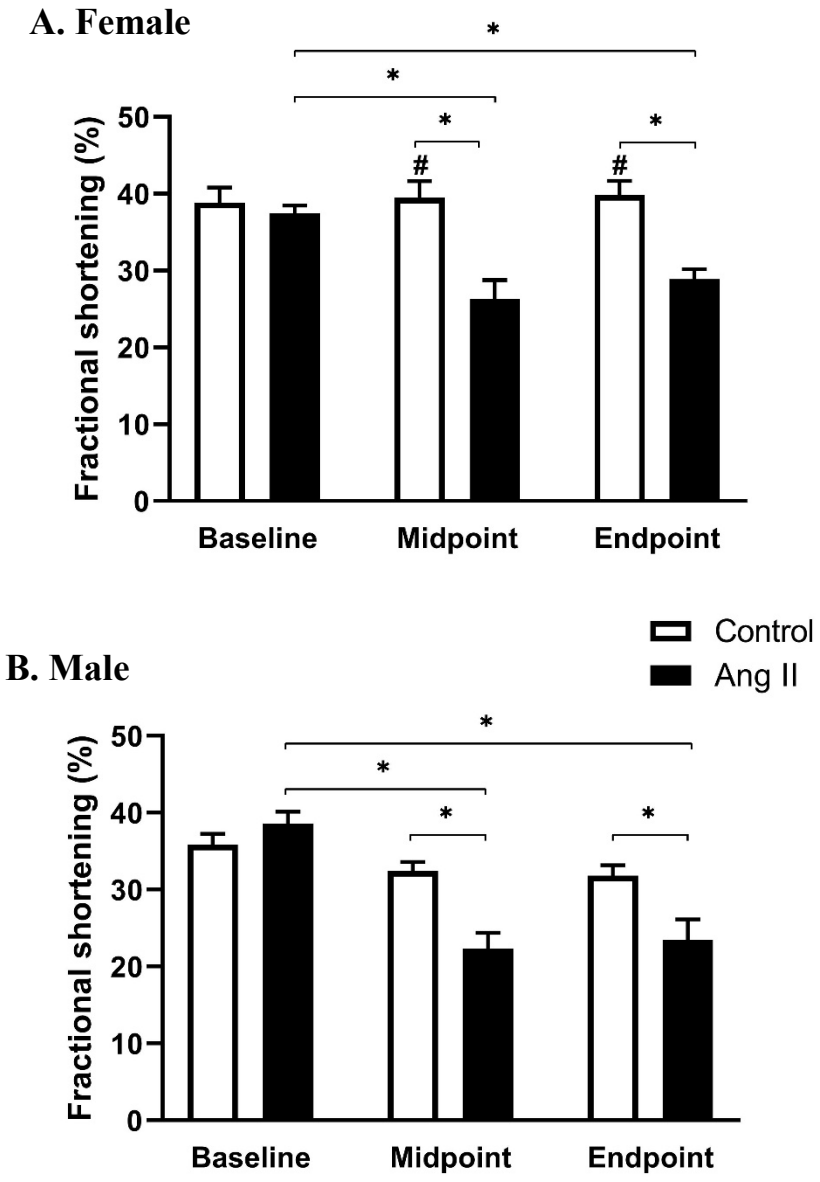

Figure 3.17. Pressure overload caused by Ang II infusion reduced fractional shortening in mice of both sexes. A. Fractional shortening decreased over time in treated female mice, and this was significant compared to same-sex controls. B. Similar results were seen in males. Male controls also had lower fractional shortening than female controls at midpoint and endpoint. Sample sizes for females were n = 9 control, n = 10 treated and males were n = 6 control and n = 11 treated. Data were analysed with mixed-effects analysis and a Fisher's LSD post-hoc test. The symbol * denotes $P < 0.05$ and # denotes significant difference from corresponding data in males, $P < 0.05$.

A. Baseline Ang II Male

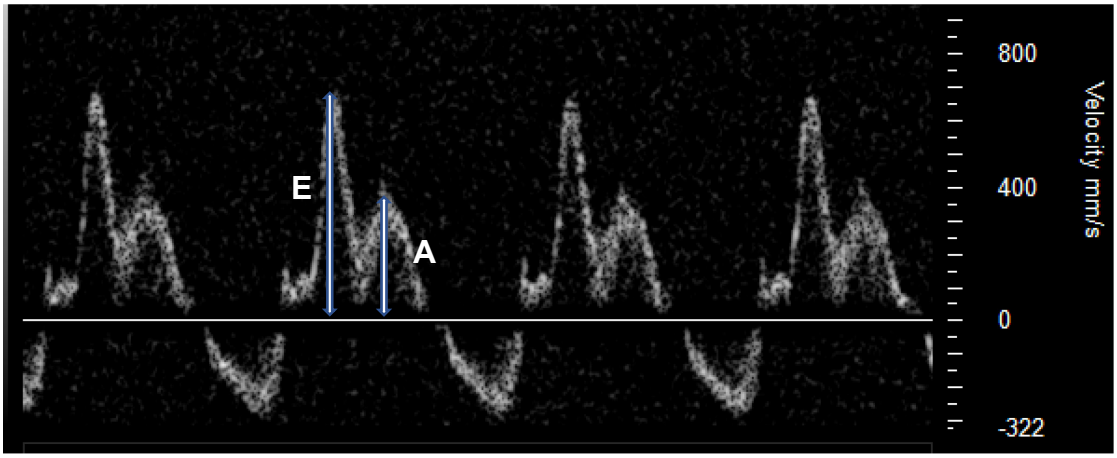

B. Midpoint Ang II Male

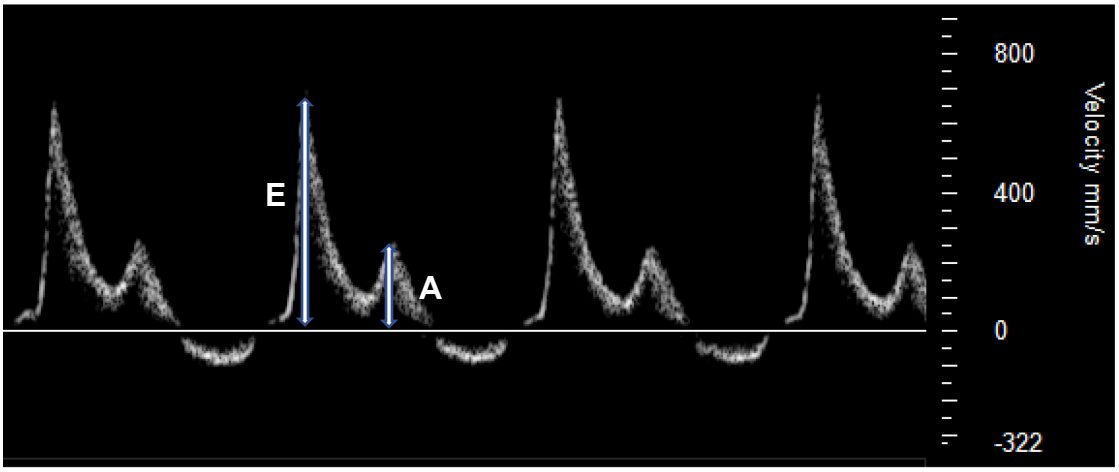

Figure 3.18. Representative Doppler echocardiography images of *in vivo* LV function in male mice before (baseline) and after Ang II infusion (midpoint). The top image (A) shows normal E (early filling velocity) and A (late filling velocity) waves. The bottom image (B) shows a lower A wave. The resulting E/A ratio in panel B is higher than the E/A ratio in panel A, indicating diastolic dysfunction in this male mouse treated with Ang II.

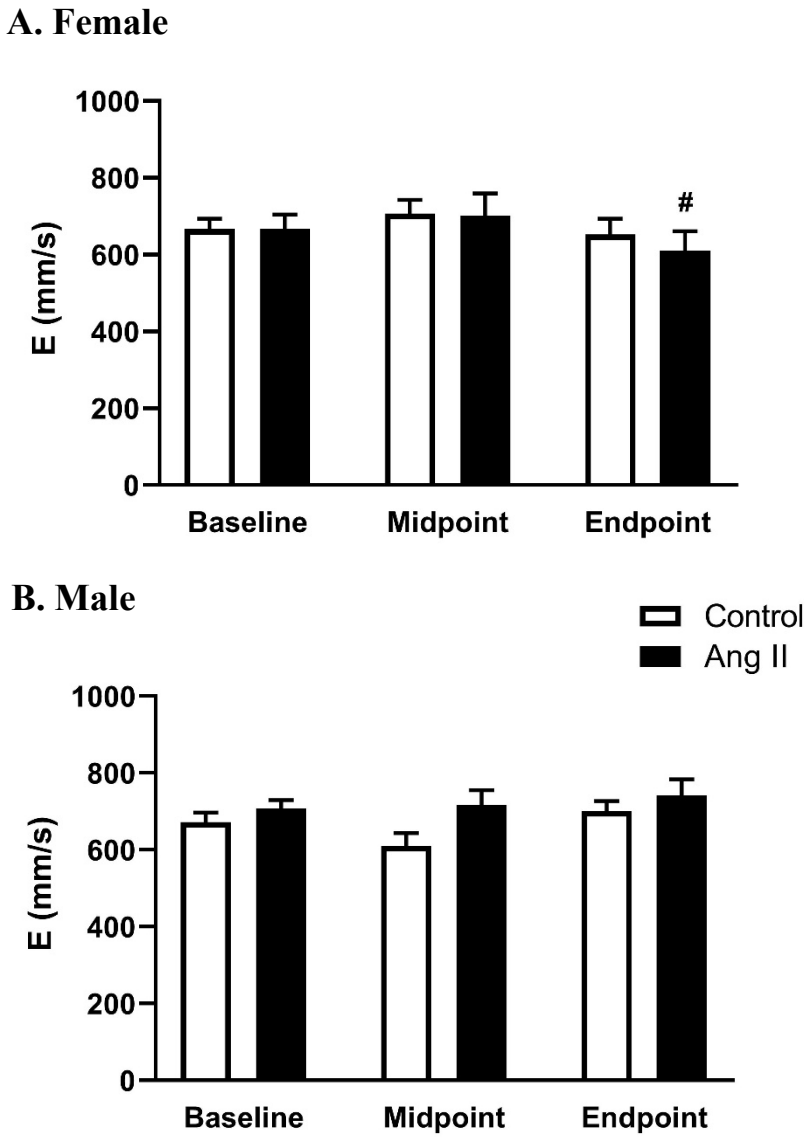

Figure 3.19. Ang II-induced hypertension had little effect on late filling velocity in mice of both sexes. E waves in females (A) and males (B) were not affected by Ang II infusion, but treated males had higher values than females at endpoint. Sample sizes for females were n = 9 control, n = 10 treated and males were n = 6 control and n = 11 treated. Data were analysed with mixed-effects analysis and a Fisher's LSD post-hoc test. The symbol # denotes significant difference from corresponding data in males, $P < 0.05$.

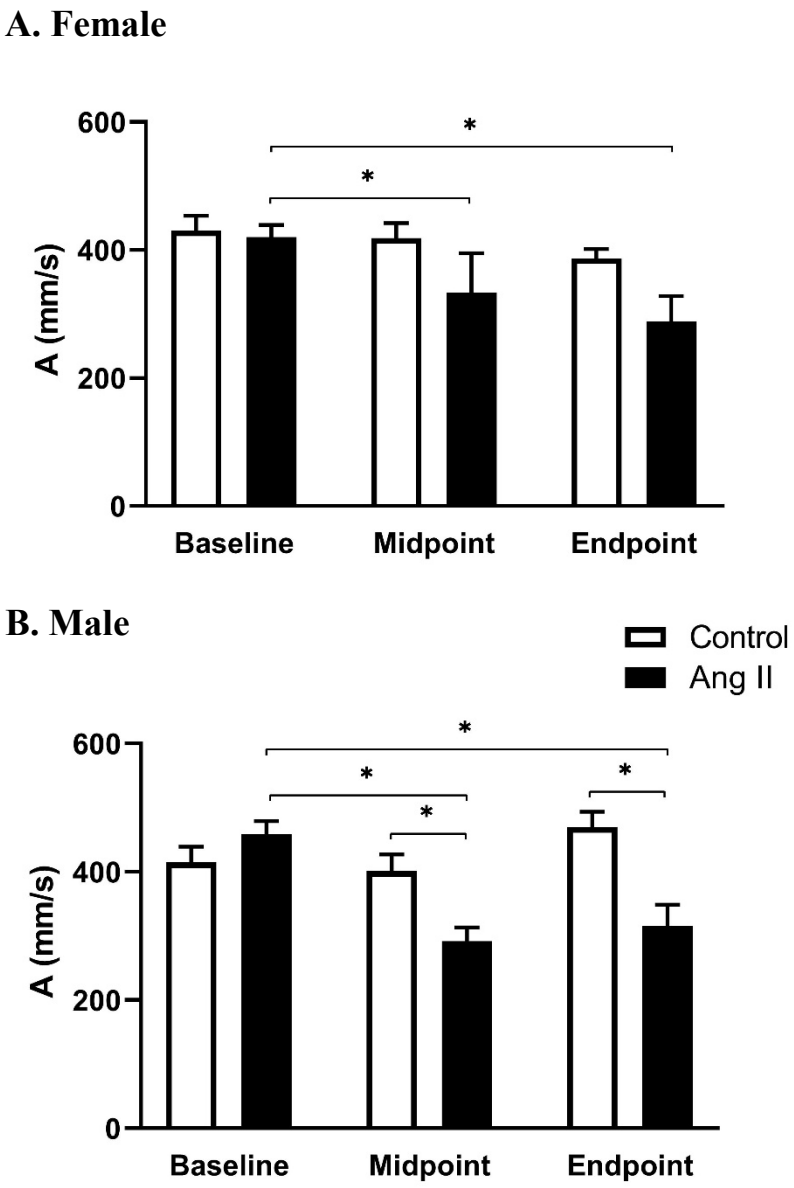

Figure 3.20. Ang II-induced hypertension reduced late filling velocity in male and female mice, but this was more pronounced in males. A waves in treated females (A) and treated males (B) declined over time after Ang II infusion. This was significantly different from same-sex controls in males but not females. Sample sizes for females were n = 9 control, n = 10 treated and males were n = 6 control and n = 11 treated. Data were analysed with mixed-effects analysis and a Fisher's LSD post-hoc test. The symbol # denotes significant difference from corresponding data in males, $P < 0.05$.

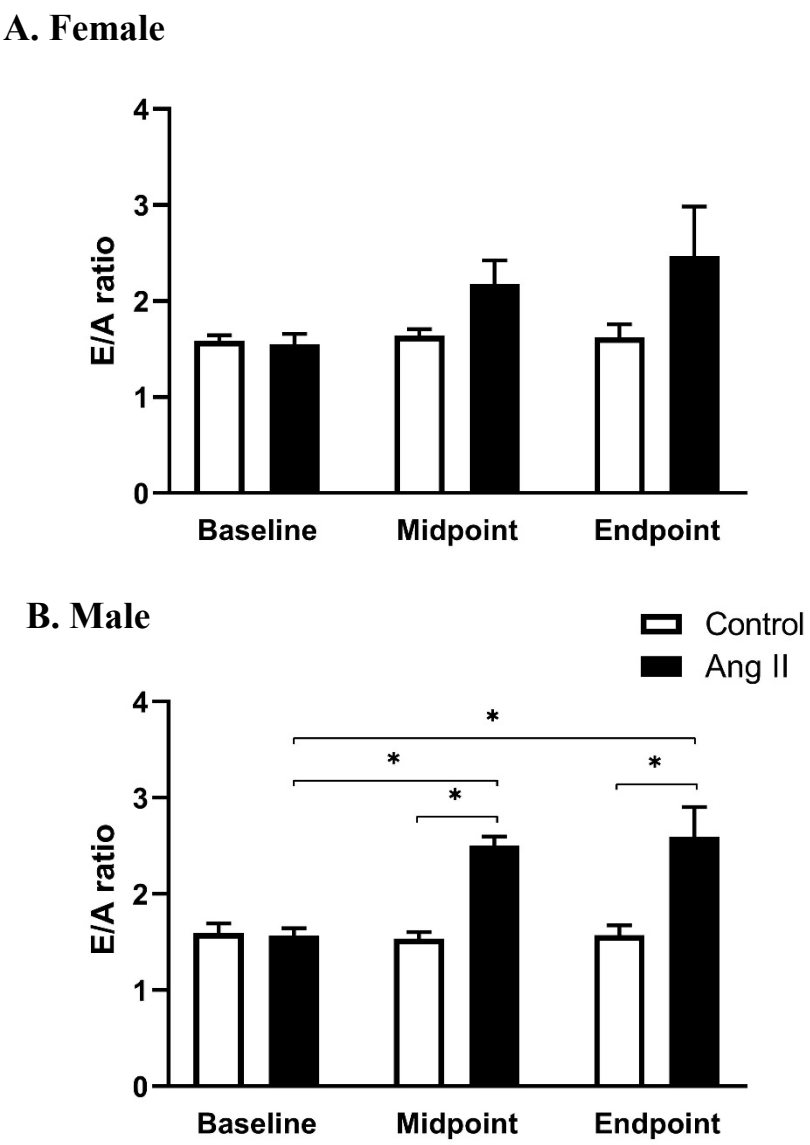

Figure 3.21. Ang II-induced hypertension promoted abnormal diastolic filling in males but not in females. A. E/A ratios in treated females were not significantly different from same-sex controls. B. E/A ratios increased over time in males, and this was significantly different from male controls. Sample sizes for females were n = 9 control, n = 10 treated and males were n = 6 control, n = 11 treated. Data were analysed with mixed-effects analysis and a Fisher's LSD post-hoc test. The symbol * denotes $P < 0.05$.

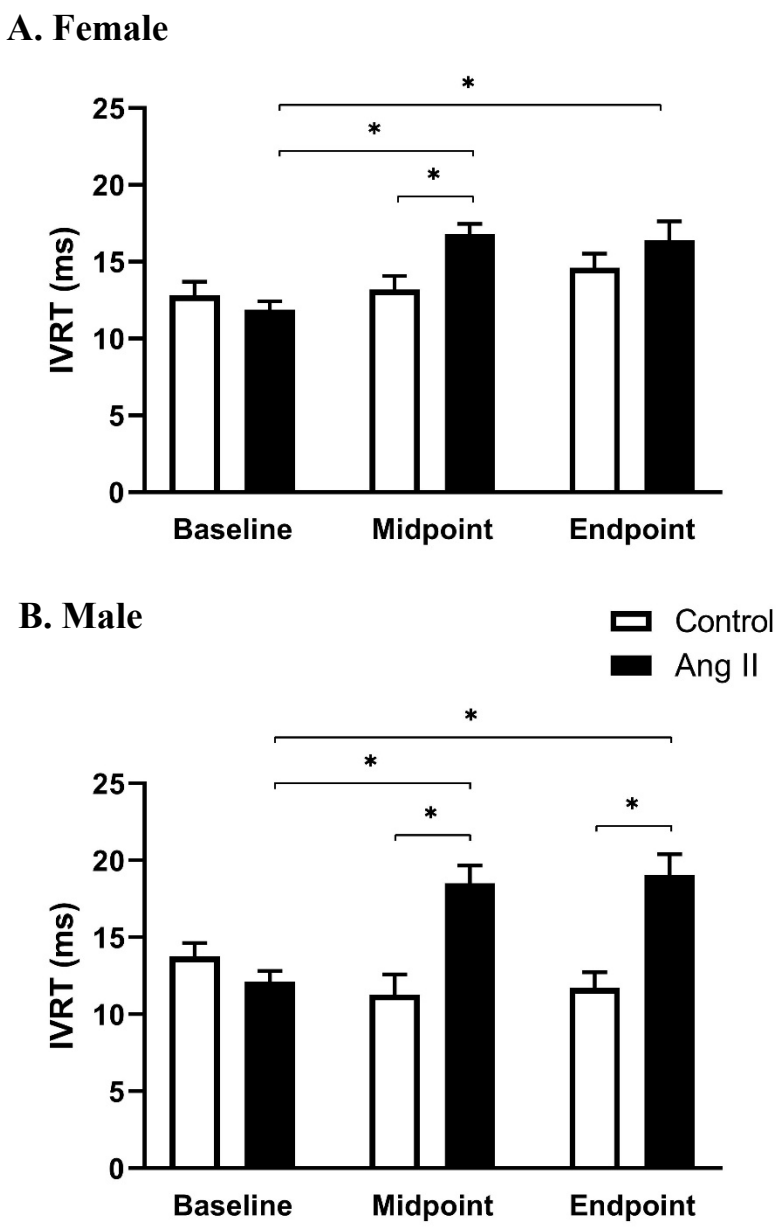

Figure 3.22. Ang II-induced hypertension resulted in diastolic dysfunction in male and female mice, but this was more prominent in males. A. IVRT increased over time in females but this was significant compared to female controls at midpoint only. B. Similar results were seen for male mice, but large differences from control occurred at both midpoint and endpoint. Sample sizes for females were n = 9 control, n = 10 treated and males were n = 6 control and n = 11 treated. Data were analysed with mixed-effects analysis and a Fisher's LSD post-hoc test. The symbol * denotes $P < 0.05$ and # denotes significant difference from corresponding data in males, $P < 0.05$.

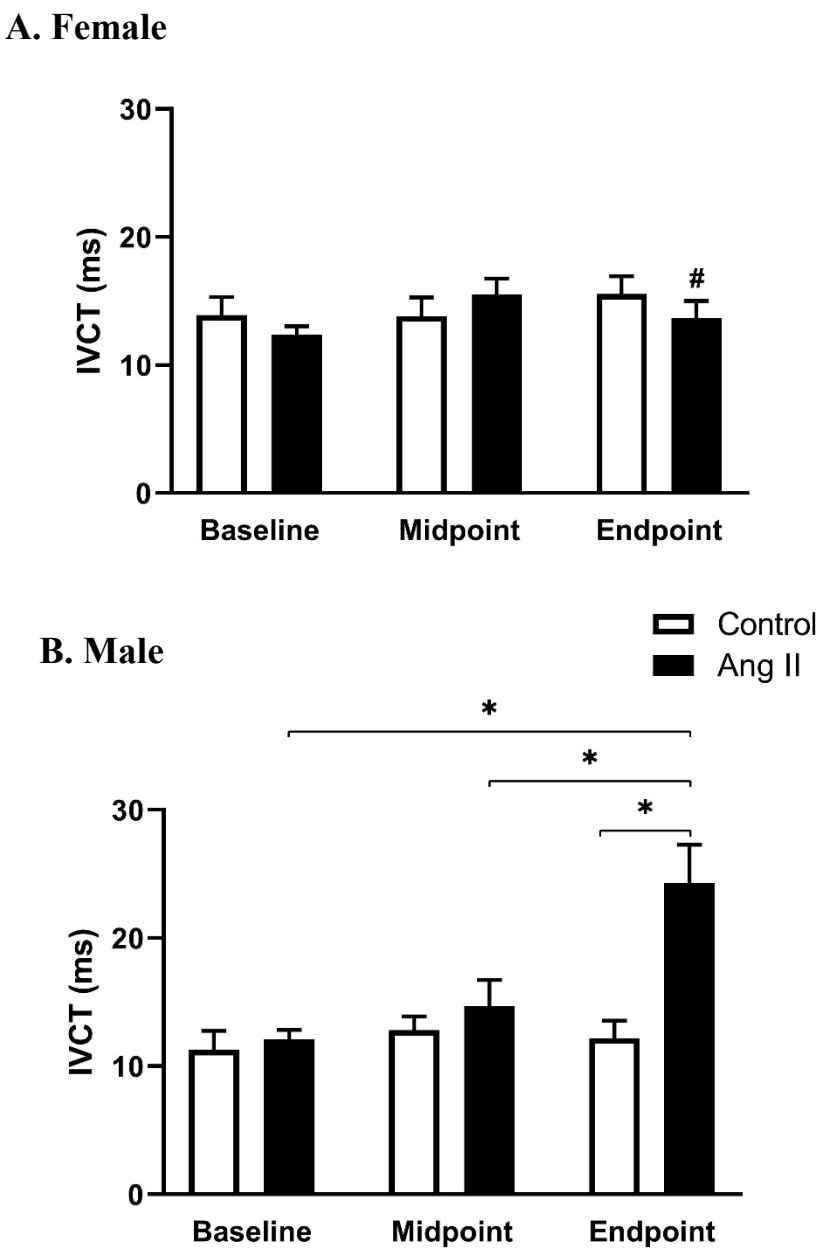

Figure 3.23. Ang II-induced hypertension resulted in abnormal LV contractility in males when compared to females. A. IVCT in treated females was not affected by Ang II infusion. B. IVCT increased over time in males, and this was significantly different from both male controls and treated females at endpoint. Sample sizes for females were n = 9 control, n = 10 treated and males were n = 6 control, n = 11 treated. Data were analysed with mixed-effects analysis and a Fisher's LSD post-hoc test. The symbol * denotes P <0.05.

Table 3.2. P-values from mixed-effects analysis for cardiac parameters measured by doppler echocardiography.

Parameter	Time	Sex	Treatment	Time x Sex	Time x Treatment	Sex x treatment
IVRT PW, ms	**0.0003**	0.8451	**<0.0001**	0.8275	**<0.0001**	**0.0246**
IVCT PW, ms	**0.0006**	0.7512	**0.0475**	0.0814	**0.0483**	**0.0273**
E, mm/s	0.9751	0.3937	0.3544	0.1425	0.686	0.1606
A, mm/s	**0.0017**	0.5021	**0.0002**	0.1793	**0.0033**	0.803
E/A ratio	**0.0004**	0.7369	**<0.0001**	0.9163	0.223	0.4484

Abbreviations: IVRT PW, isovolumic relaxation time pulse wave; IVCT PW, isovolumic contraction time pulse wave; E, early filling velocity; A, late filling velocity.

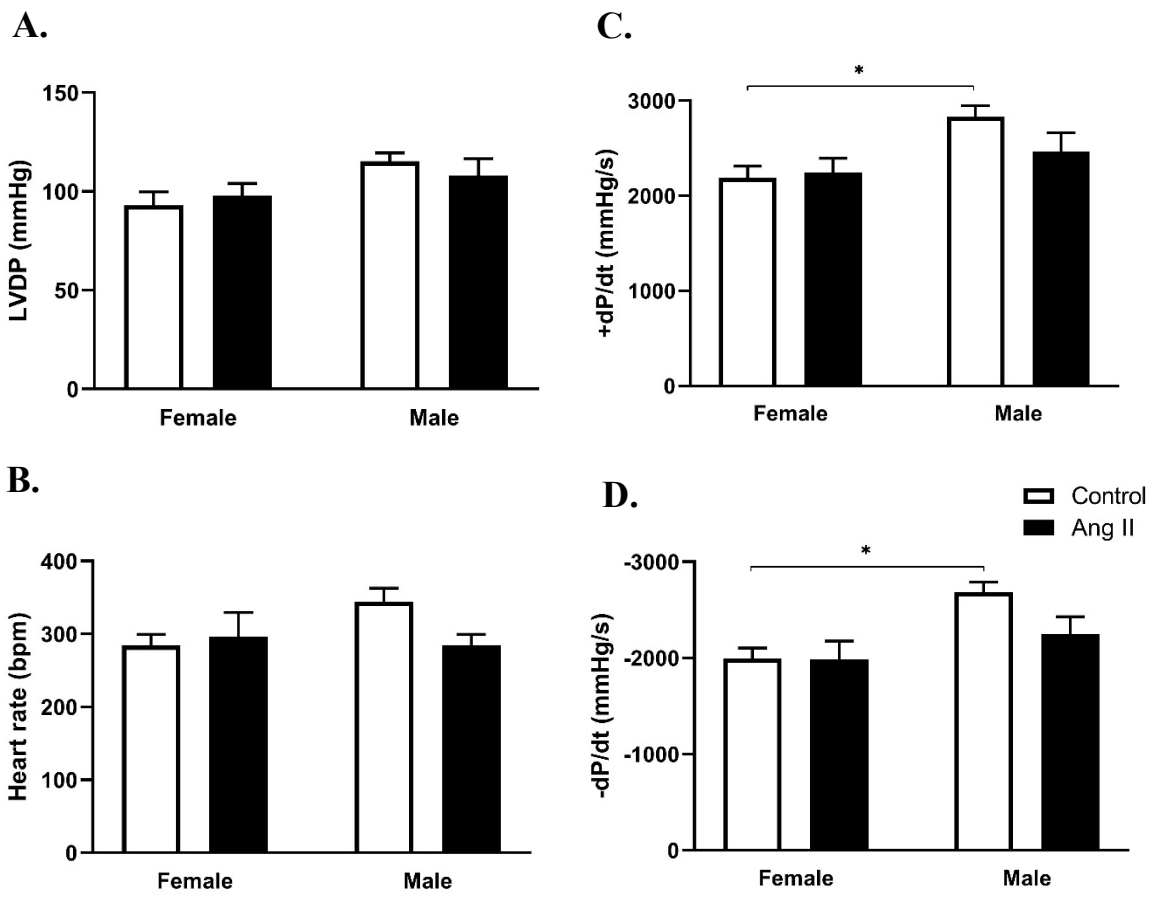

Figure 3.24. Chronic Ang II-induced hypertension did not affect baseline chronic contractile function in Langendorff-perfused hearts from mice of both sexes. A. Ang II infusion had no effect on baseline LVDP or (B) baseline heart rate in male and female hearts. Similar results were seen for baseline +dP/dt (C) and –dP/dt (D), but these values for male control hearts were higher compared to female controls. Sample sizes for females were n = 10 control and n = 9 treated and males were n = 9 control, n = 11 treated. Data were analyzed with 2-way ANOVA and a Tukey's post-hoc test. The symbol * denotes $P < 0.05$.

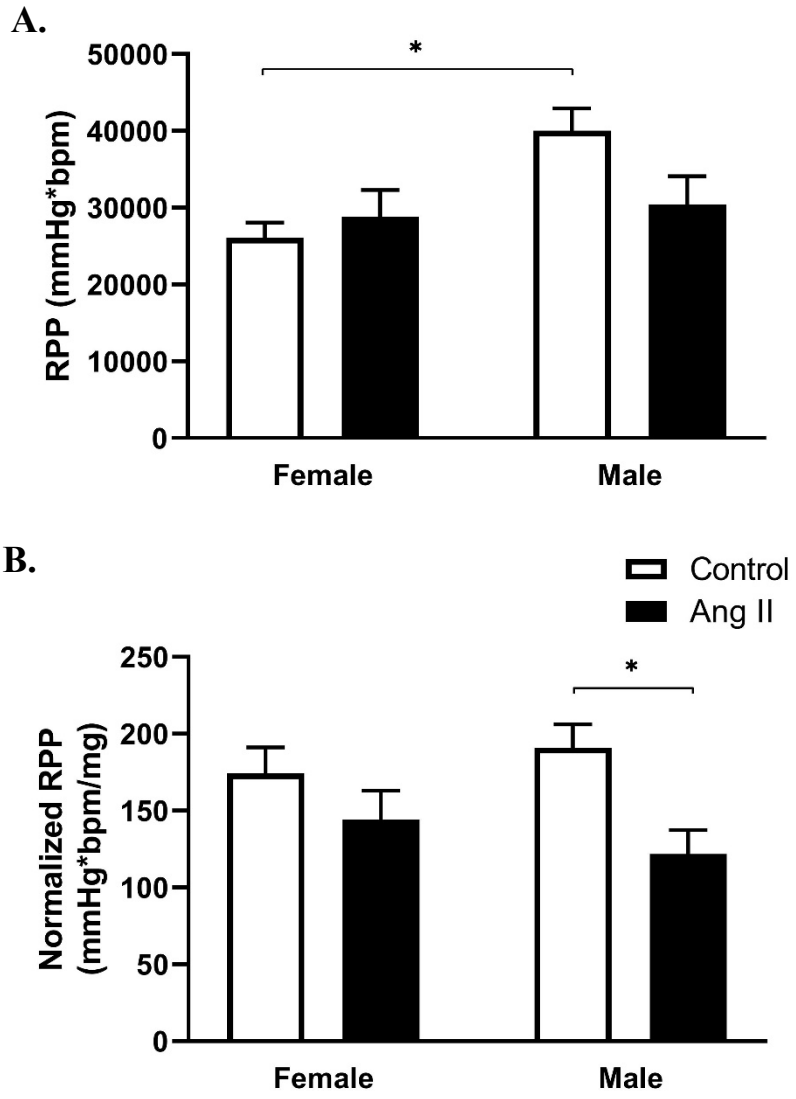

Figure 3.25. Ang II-induced hypertension reduced cardiac work in Langendorff-perfused hearts from male but not female mice. A. Ang II infusion did not affect the rate pressure product (RPP) in hearts from males and females, but values for control males were higher than for female controls. B. RPP normalized to heart weight decreased in hearts from treated male mice when compared to male controls, but this did not occur in females. Sample sizes for females were n = 10 control, n = 9 treated and males were n = 9 control, n = 11 treated. Data were analyzed with 2-way ANOVA and a Tukey's post-hoc test. The symbol * denotes $P < 0.05$.

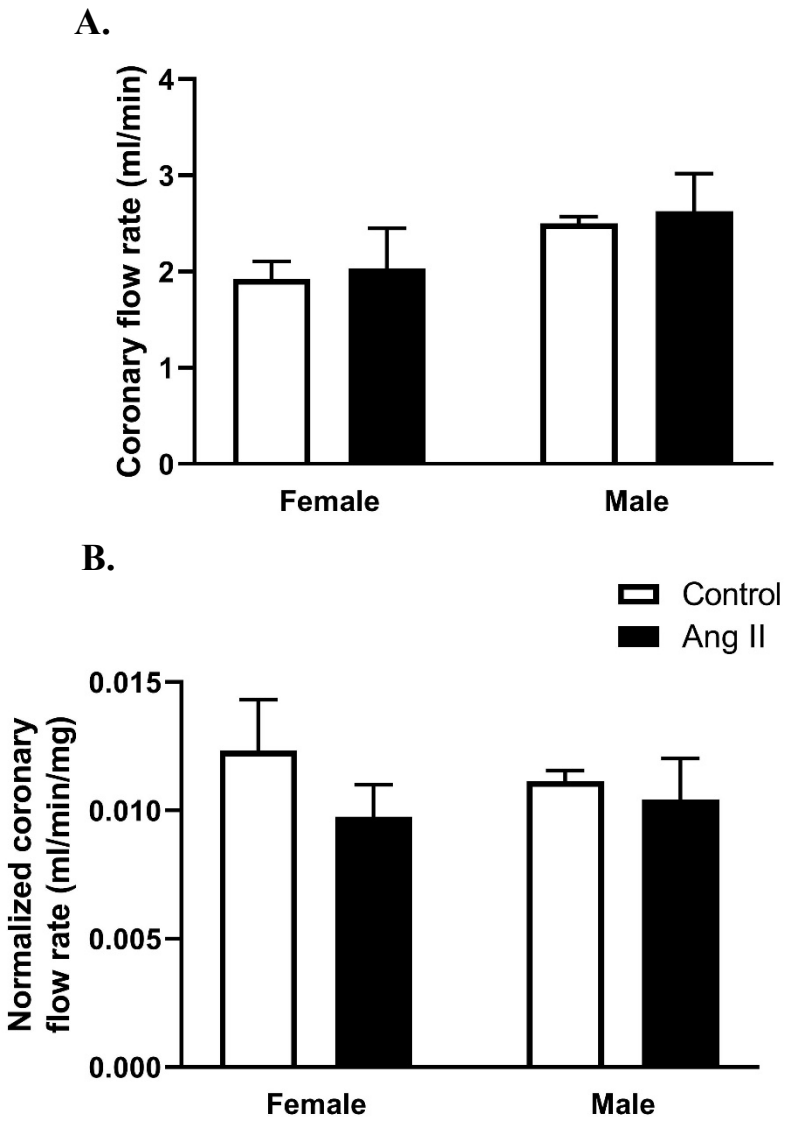

Figure 3.26. Ang II-induced hypertension had no effect on baseline coronary flow rate in Langendorff-perfused hearts from mice of both sexes. A. Ang II-induced hypertension did not affect baseline coronary flow rate or B. baseline coronary flow rate normalized to heart weight in male and female hearts. Sample sizes for females were n = 4 control, n = 3 treated and males were n = 4 control, n = 9 treated. Data were analyzed with 2-way ANOVA and a Tukey's post-hoc test.

A. Female control

B. Female Ang II

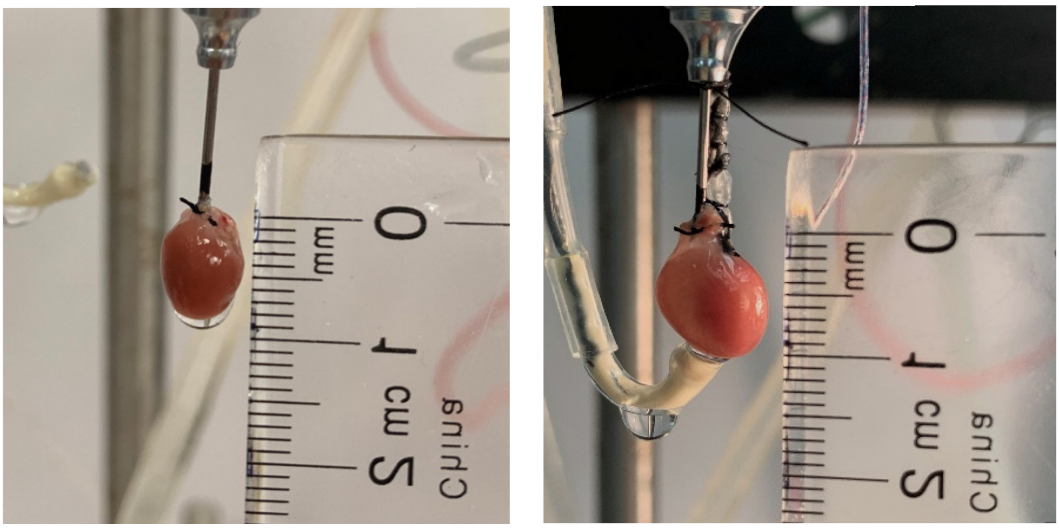

Figure 3.27. Cardiac hypertrophy in an intact heart isolated from Ang II-infused female mice. The picture on the right shows a heart isolated from an Ang II-infused female mouse. The picture on the left shows a normal heart isolated from a control female mouse. The right heart is greater in size compared to the left control heart.

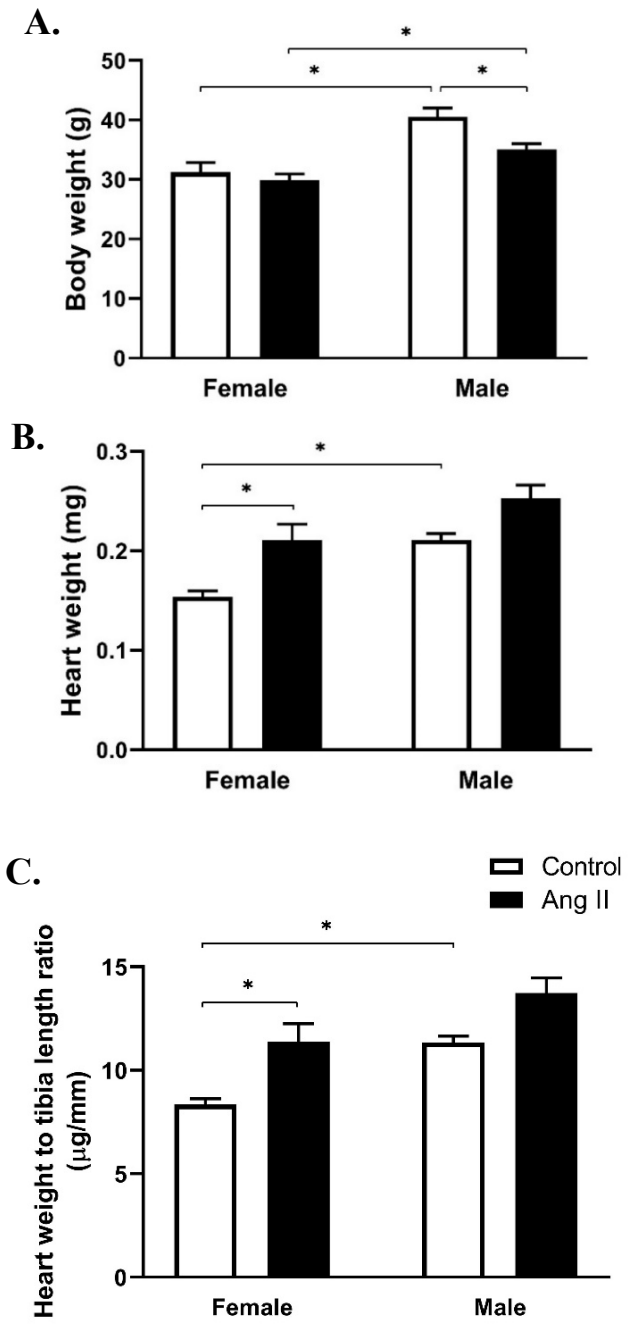

Figure 3.28. Ang II-induced hypertension resulted in lower body weights in males but greater cardiac hypertrophy in females. A. Ang II-induced hypertension reduced body weights in male more than in male controls. Male treated and control mice had larger body weight than corresponding females. Treated females had larger heart weights (B) and heart weights to tibia length ratios (C) than female controls. Female controls had lower heart weights (B) and heart weights to tibia length ratio (C) than male controls. Sample sizes for females were n = 9 control, n = 10 treated and males were n = 6 control, n = 11 treated. Data were analysed with 2-way ANOVA and a Tukey post-hoc's test. The symbol * denotes $P < 0.05$.

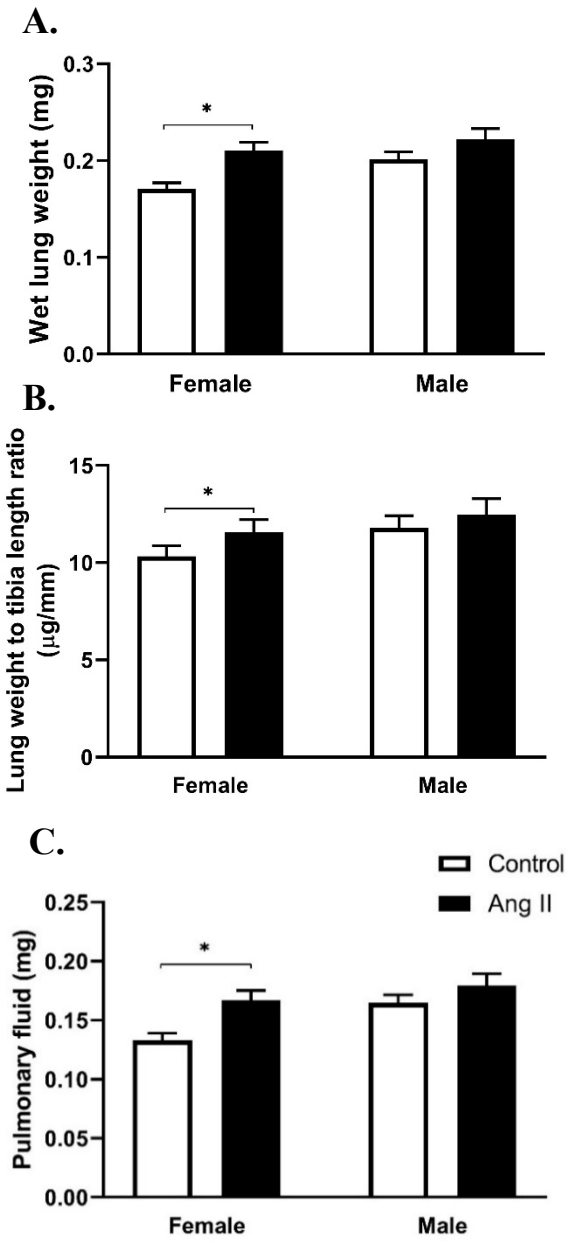

Figure 3.29. Ang II-induced hypertension resulted in lung hypertrophy and pulmonary edema in female mice but not in males. A. Ang II-induced hypertension increased wet lung weight (A), increased lung weight to tibia length ratio (B), and elevated amount of pulmonary fluid (C) in female mice compared to same-sex controls, but this did not occur in male mice. Sample sizes for females were n = 9 control, n = 10 treated and males were n = 6 control, n = 11 treated. Data were analysed with 2-way ANOVA and a Tukey post-hoc's test. The symbol * denotes $P < 0.05$.

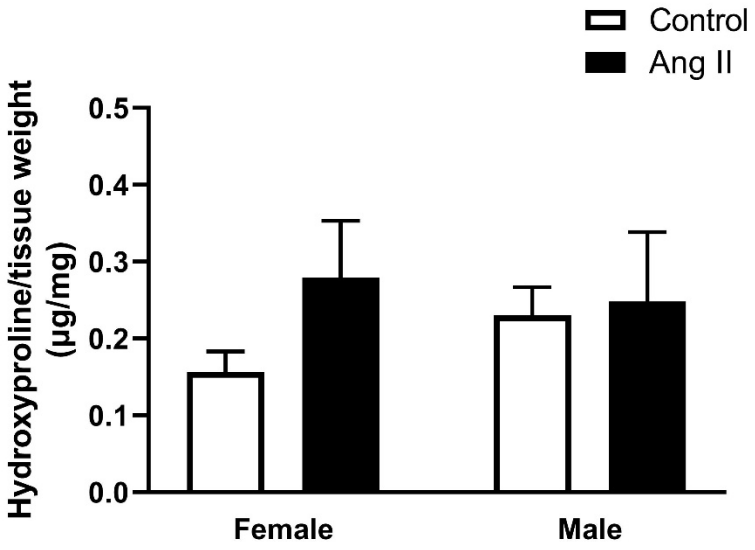

Figure 3.30. Ang II-induced hypertension did not affect fibrosis levels in hearts isolated from male and female mice. Hydroxyproline levels in hearts from females (A) and males (B) did not change after Ang II infusion. Sample sizes for females were n = 5 control, n = 6 treated and males were n = 5 control, n = 9 treated. Data were analysed with 2-way ANOVA and Tukey post-hoc's test.

Table 3.3. Summary of results of overall changes in the cardiovascular system for Ang II-treated mice of both sexes compared to same-sex controls. Sex differences for overall changes were compared among treated animals. Arrows ↑, ↓ , ↔ represent increase, decrease, and no change respectively.

Parameter, unit	Male	Female	Significant sex differences
Blood pressure, mmHg	↑	↑	No
Systolic LV wall thickness, mm	↓	↔	Thinner walls in males
Diastolic LV wall thickness, mm	↔	↑	Thicker walls in females
Systolic LV diameter, mm	↑	↑	Chambers more dilated in males
Diastolic LV diameter, mm	↑	↔	Chambers more dilated in males
Corrected LV mass, mg	↑	↑	No
LV wall distensibility	↓	↓	No
Corrected LV mass/Vd, mg/µL	↑	↔	Concentric hypertrophy in females
Heart rate, bpm	↓	↔	No
EF and FS, %	↑	↑	No
E/A	↑	↔	No
IVRT, ms	↑	↑	No
IVCT, ms	↑	↔	Prolonged IVCT at endpoint in males
LVDP, mmHg	↔	↔	No
+dP/dt, mmHg/s	↔	↔	No
-dP/dt, mmHg/s	↔	↔	No
Langendorff heart rate, bpm	↔	↔	No
Normalized RPP, mmHg*bpm	↓	↔	No
Normalized flow rate, ml/min	↔	↔	No
Heart weight/tibia length, µg/mm	↑	↔	No
Pulmonary edema	↑	↔	No
Fibrosis levels	↔	↔	No

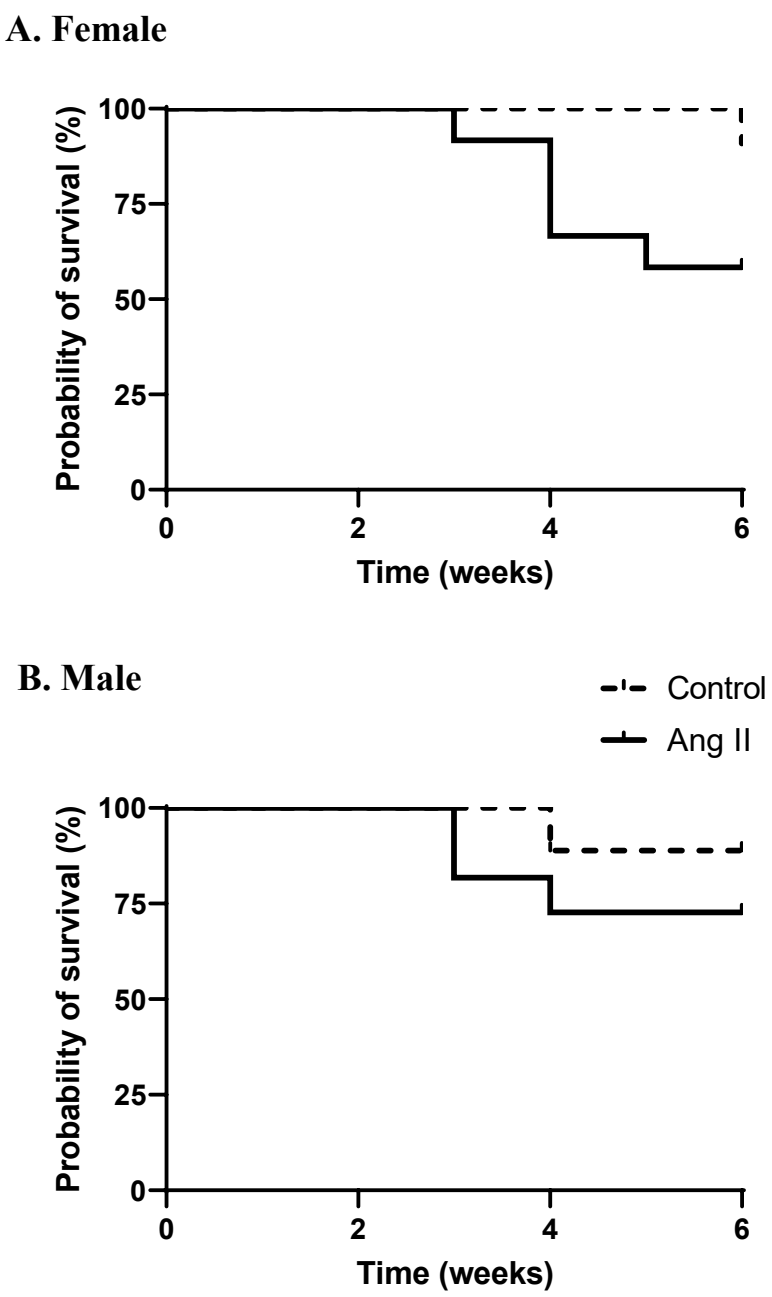

Figure 3.31. Kaplan Meier survival curves show no significant differences in mortality in Ang II-infused versus control mice of both sexes. A. Ang II-infused female mice had a lower probability of survival compared to same-sex controls, but this difference was not statistically significant. B. Similar results were seen with male mice. Mortality occurred when mice died unexpectedly or were euthanized due to illness or low humane endpoint weight. Mice that were euthanized at the end of the experiment were censored. Sample sizes for females were n = 11 control, n = 12 treated and males were n = 9 control, n = 11 treated. Data were analyzed with a Log-rank test.

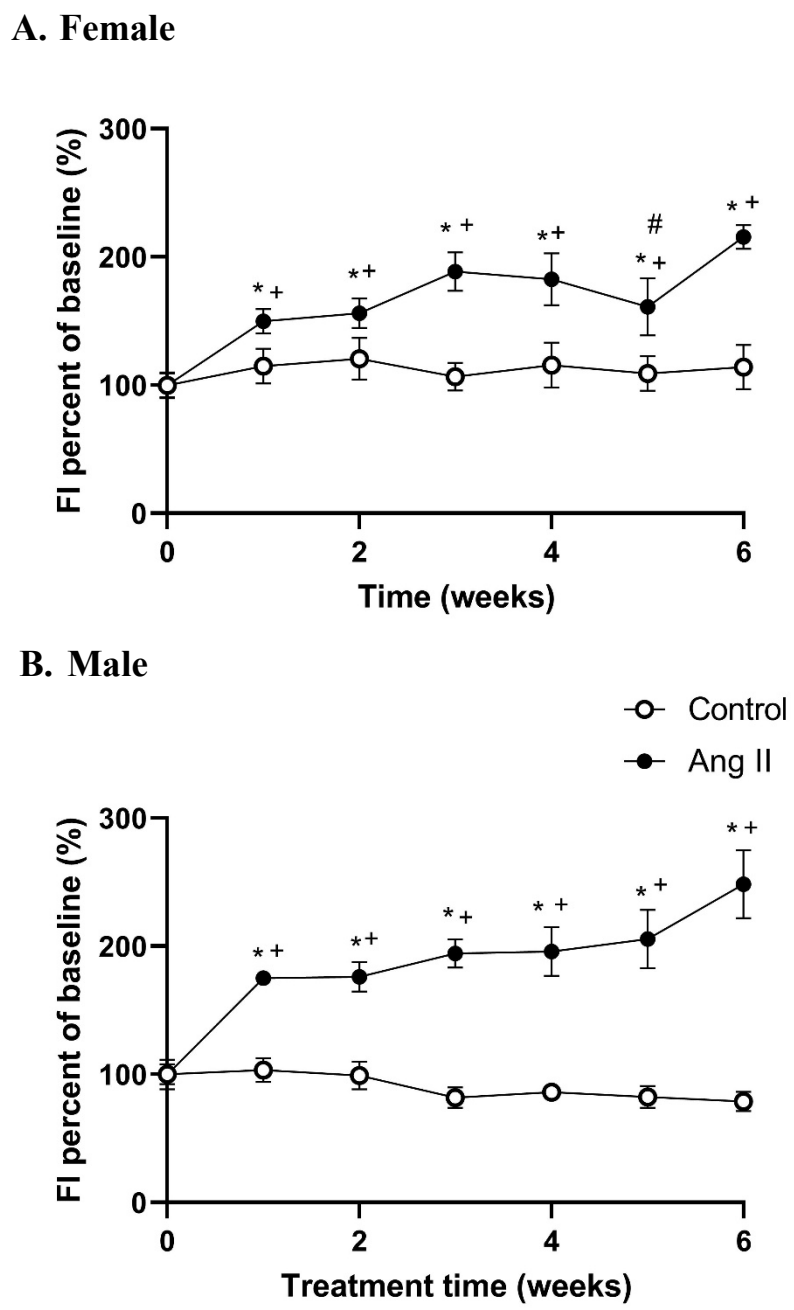

Figure 3.32. Frailty scores increased in mice of both sexes following Ang II infusion. A. Female treated mice had higher frailty index (FI) scores than female controls. B. Similar results were seen for male mice. FI scores in treated males were higher than treated females at week 5. Sample sizes for females were n = 11 control, n = 12 treated and males were n = 9 control, n = 11 treated. Data was analyzed with mixed effect analysis and a Fisher's LSD post-hoc test. The symbols #, *, and + indicate P <0.05 compared to corresponding male data, corresponding same-sex controls, and corresponding baseline data respectively.

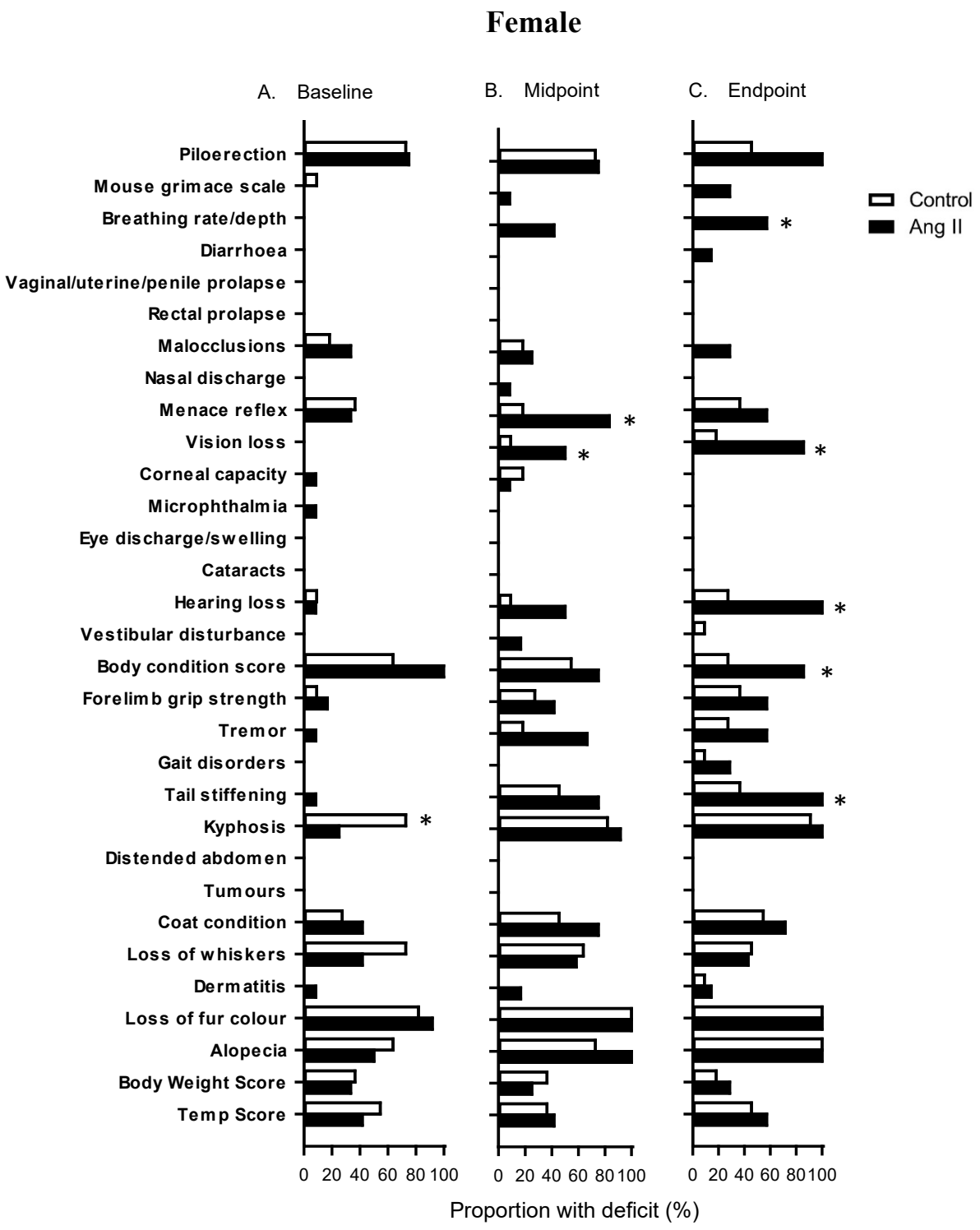

Figure 3.33. Proportions of female mice with deficits increased after Ang II treatment. Panels A, B, and C show proportions of treated versus control female mice with deficits at baseline, midpoint, and endpoint respectively. Sample sizes were n = 11 control and n = 12 treated. Data was analyzed with a Chi square analysis test. The symbol * indicates P <0.05 compared to corresponding data of the same deficit.

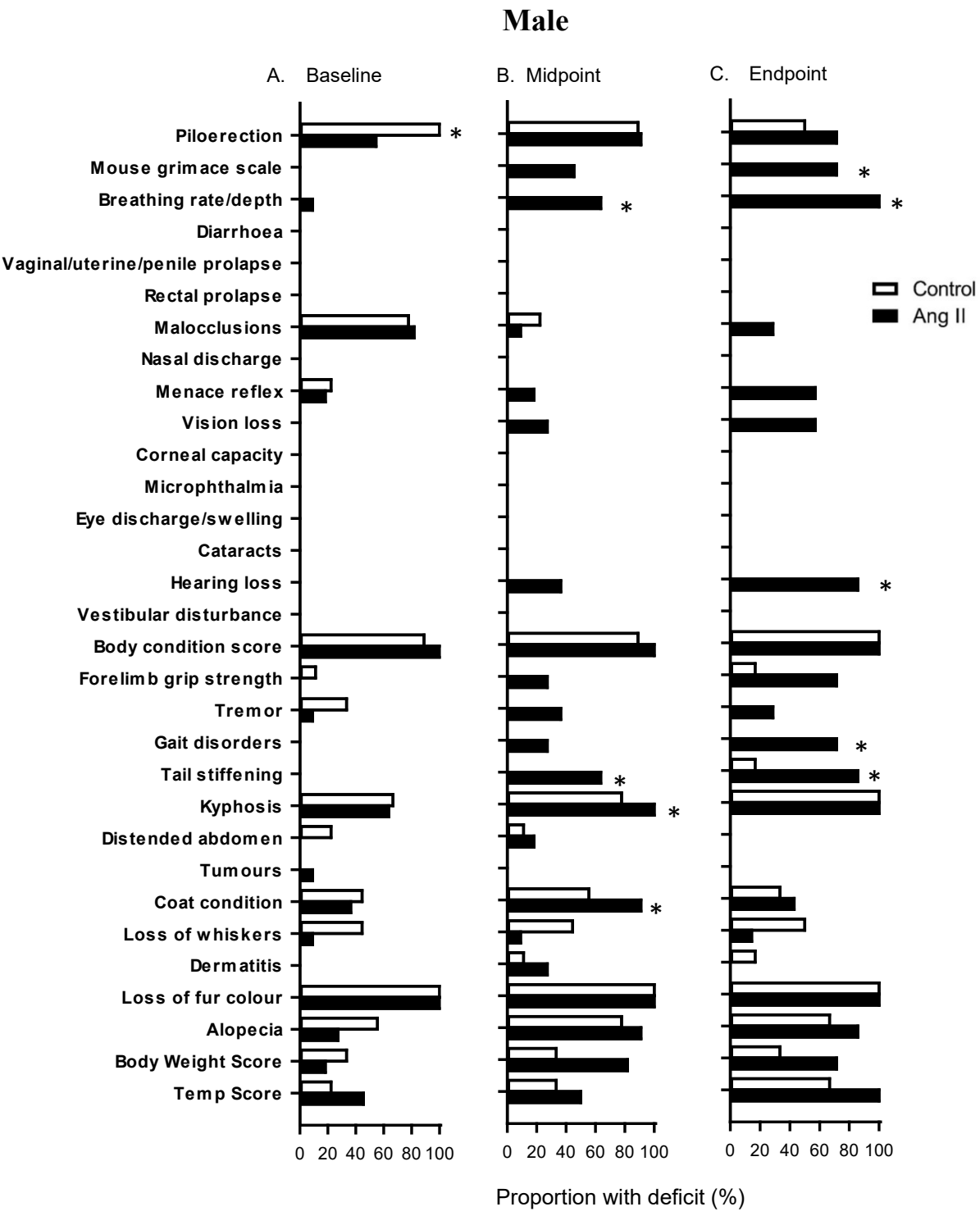

Figure 3.34. Proportions of male mice with deficits increased after Ang II treatment. Panels A, B, and C show proportions of male treated versus control mice with deficits at baseline, midpoint, and endpoint respectively. Sample sizes were n = 9 control and n = 11 treated. Data was analyzed with a Chi square analysis test. The symbol * indicates $P < 0.05$ compared to corresponding data of the same deficit.

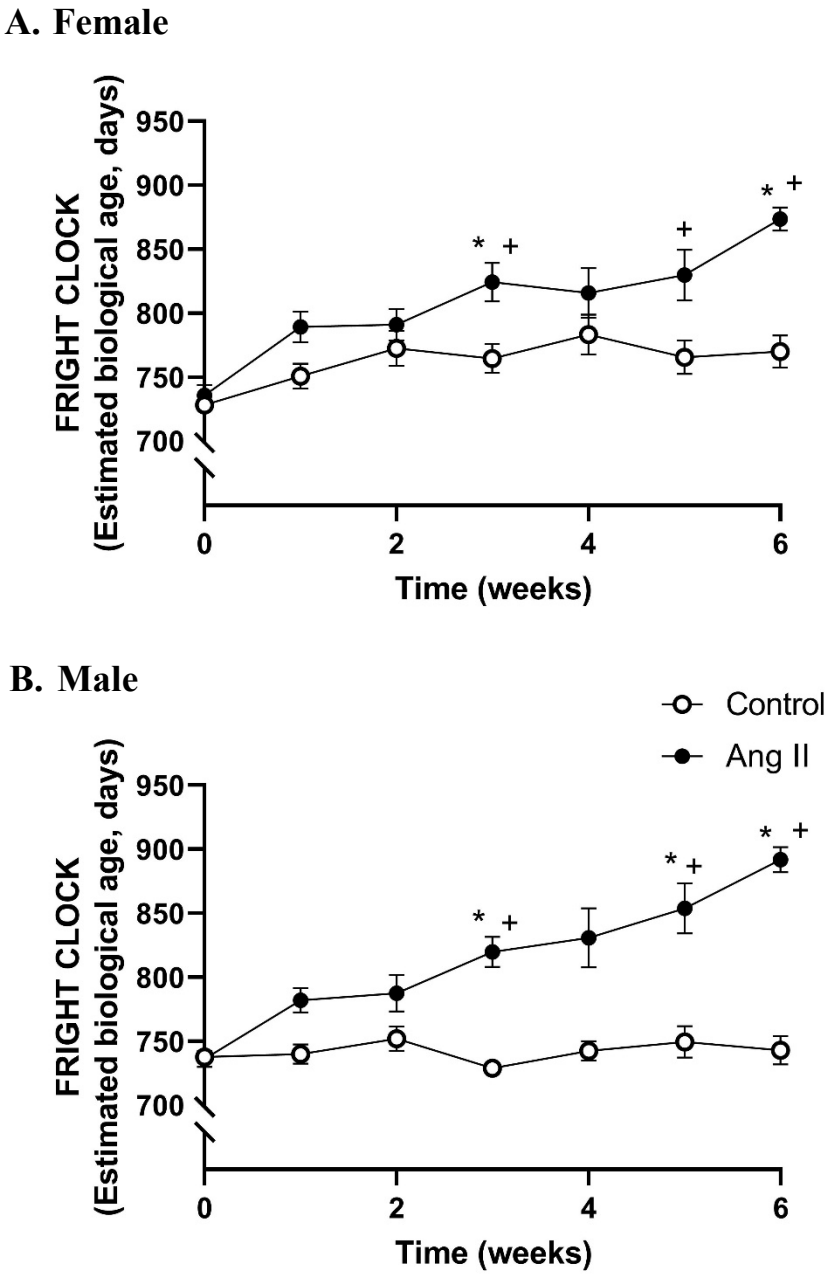

Figure 3.35. Ang II-treatment accelerated aging in Ang II-treated male and female mice, but this was more pronounced in male mice. A. Female treated mice had older FRIGHT CLOCK ages over time, and this was significantly higher than female controls at weeks 3 and 6. B. Similar results were seen for male mice, but significant differences compared to controls occurred at weeks 3, 5, and 6. Sample sizes for females were n = 11, control and n = 12, Ang II and for males were n = 9, control, n = 11, Ang II. Data was analyzed with mixed effect analysis and a Fisher's LSD post-hoc test. The symbols * and + indicate $P < 0.05$ compared to corresponding same-sex controls and corresponding baseline data respectively.

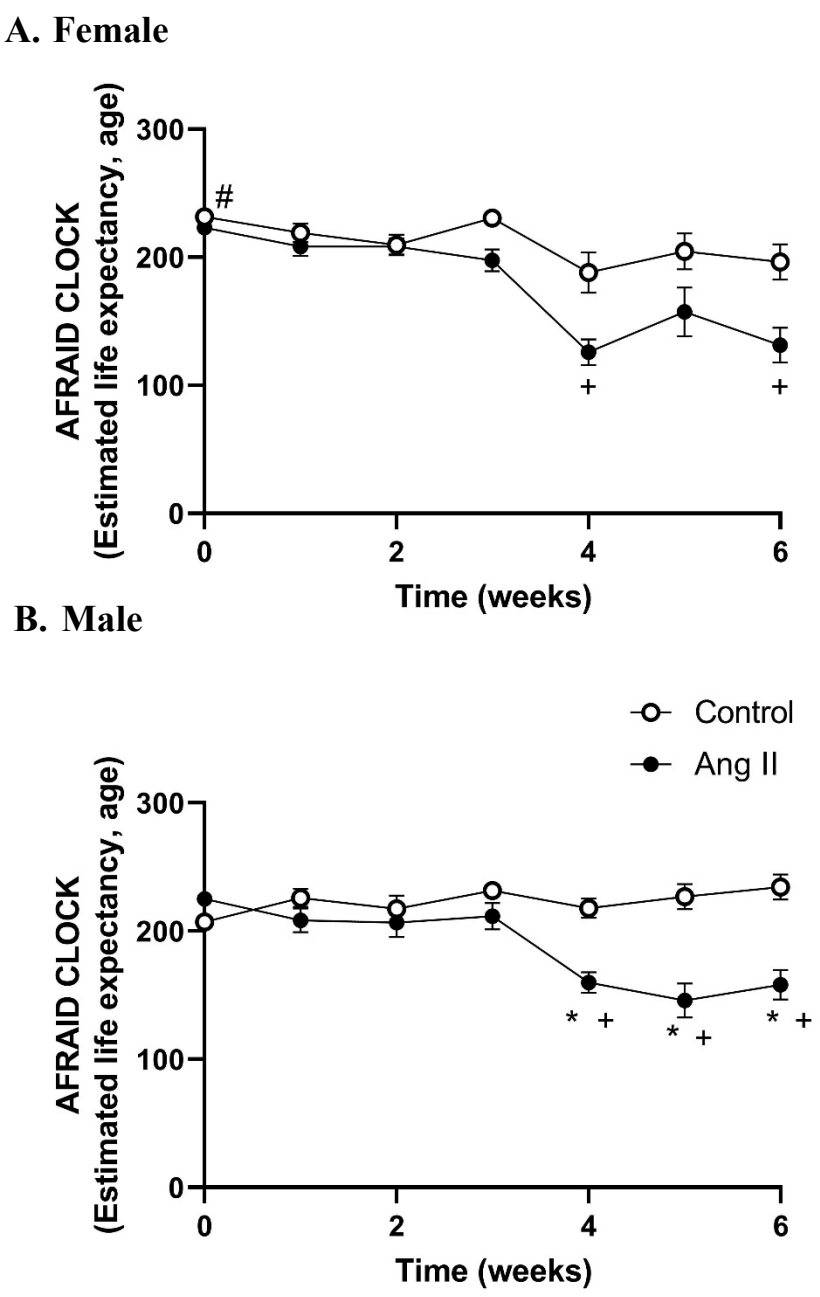

Figure 3.36. Estimated life expectancy declined in Ang II-treated male and female mice, but this effect was more pronounced in male mice. A. Female treated mice had lower AFRAID CLOCK over time when compared to control, but this was not significantly different. B. Values in treated males also increased over time when compared to controls, and this was significant from controls after week 3. Sample sizes for females were n = 11, control and n = 12, Ang II and for males were n = 9, control and n = 11, Ang II. Data was analyzed with mixed effect analysis and a Fisher's LSD post-hoc test. The symbols #, *, and + indicate $P < 0.05$ compared to corresponding male data, same-sex controls, and baseline data respectively.

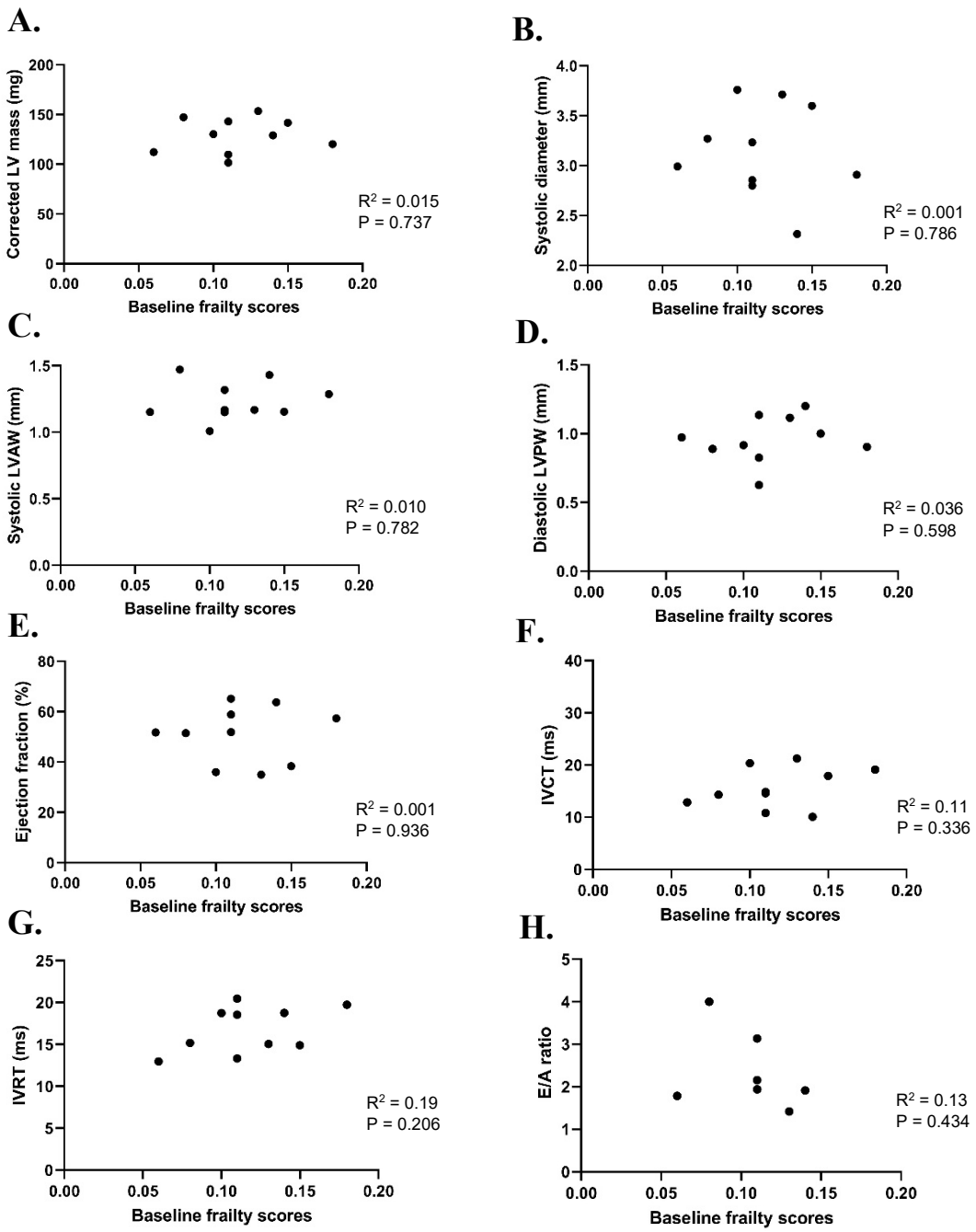

Figure 3.37. Sample endpoint LV echocardiography structural parameters in Ang II-treated female mice did not correlate with baseline frailty scores. Panel A shows no correlation between endpoint corrected LV mass and baseline frailty scores in Ang II-infused female mice. Panel B, C, D, E, F, G, and H show similar results in systolic diameter, systolic LVAW, diastolic LVPW, ejection fraction, IVCT, IVRT, and E/A ratios respectively. Sample size was n = 10. Data were analyzed with linear regression analysis.

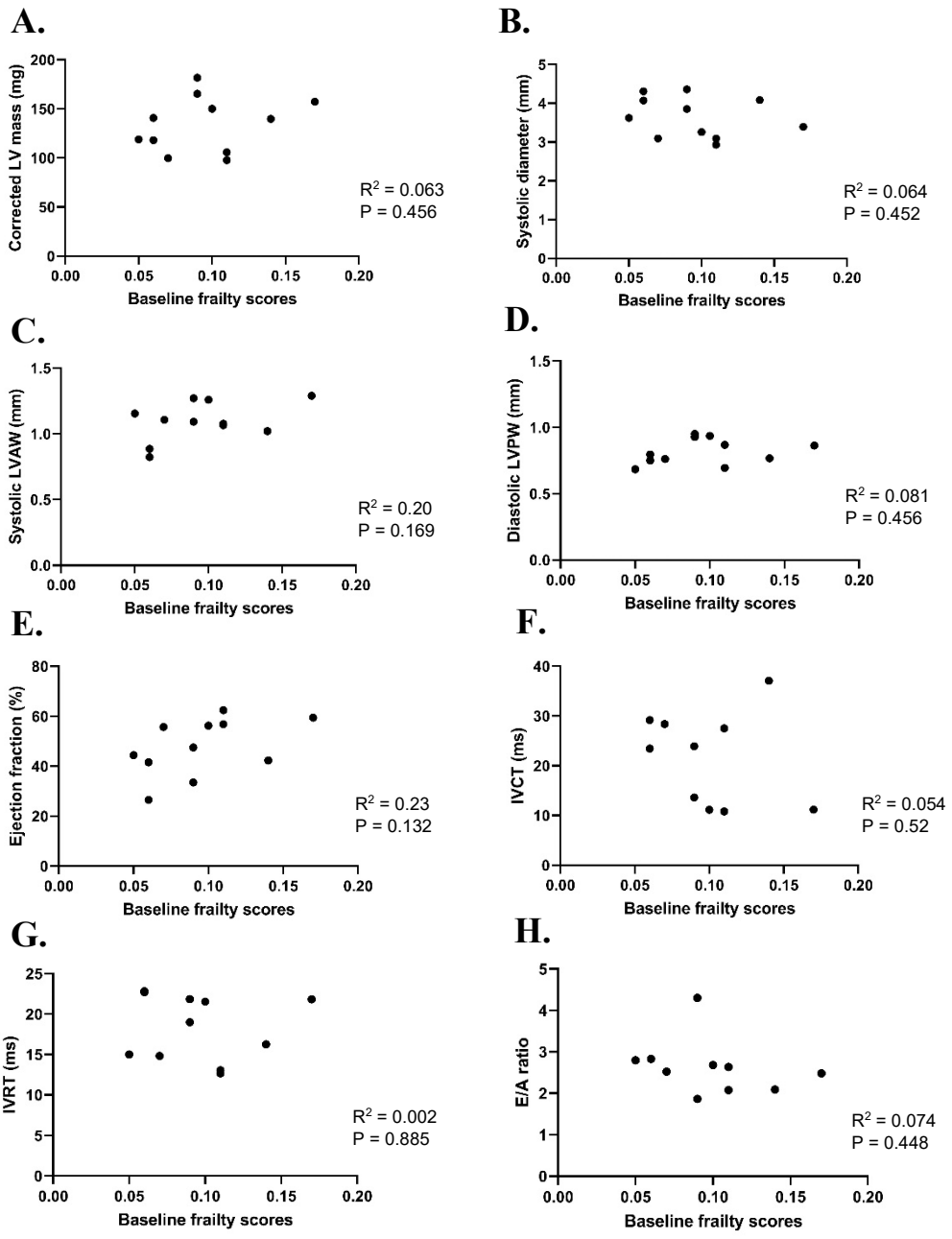

Figure 3.38. Sample endpoint LV echocardiography structural parameters in Ang II-treated male mice did not correlate with baseline frailty scores. Panel A shows no correlation between endpoint corrected LV mass and baseline frailty scores in Ang II-infused male mice. Panel B, C, D, E, F, G, and H show similar results in systolic diameter, systolic LVAW, diastolic LVPW, ejection fraction, IVCT, IVRT, and E/A ratios respectively. Sample size was n = 10. Data were analyzed with linear regression analysis.

Chapter 4: Discussions

4.1 Overview of key findings

The first two objectives of this study were to determine the effects of Ang II infusion on the cardiovascular system in C57BL/6 mice and to explore sex differences in Ang II-induced cardiac remodeling. Following Ang II infusion, both male and female mice developed hypertension that remained until the end of the experiment. Ang II-induced hypertension resulted in LV hypertrophy (increased corrected LV mass) and stiffening of the cardiac walls (elevated LV wall distensibility) in mice of both sexes. Pressure overload caused by Ang II infusion also resulted in sex differences in cardiac structural and functional remodelling. Ang II-infused male mice had thinner LV walls and greater chamber dilation, which are characteristics of eccentric remodelling when compared to treated females. On the other hand, increased wall thickness and concentric hypertrophy were more prominent in Ang II-infused females. Treated females also showed some LV dilation, but to a lesser extent than males. These changes in cardiac structural remodeling are illustrated in Figure 4.1.

Other changes also occurred in Ang II-infused mice. Both male and female mice developed systolic and diastolic dysfunction, but this was more severe in males. For instance, Ang II-induced hypertension resulted in reduced EF and FS in mice of both sexes, but prolonged IVCT was seen only in treated males. Furthermore, prolonged IVRT was seen in both male and female animals, but only males had markedly higher E/A ratios. Despite evidence of diastolic dysfunction, fibrosis levels in treated male and female animals were not different when compared to respective same-sex controls. Although increased LV mass was observed with echocardiography in treated mice of both sexes,

cardiac hypertrophy in isolated hearts was evident in females only. Ang II-infused female mice also had larger lungs and more pulmonary fluid compared to same-sex controls, an effect not seen in male mice. Langendorff contractile parameters (LVDP, +dP/dt, -dP/dt, flow rate, and normalized flow rate) in males and females were also unaffected by Ang II-induced hypertension and cardiac remodeling. Interestingly, Ang II-induced hypertension caused a reduction in cardiac work, indicated by normalized RPP, in males but not females. These results suggest that Ang II-induced hypertension caused adverse cardiac remodelling in a sex-specific manner. The impact on cardiac systolic and diastolic function was more severe in male mice, while the impact on cardiac hypertrophy and pulmonary congestion was worse in females.

The third objective of this study was to determine if Ang-II induced HF would accelerate frailty in mice of both sexes. Results showed that FI scores progressively increased with treatment time in Ang II-infused mice of both sexes, and this was significant compared to same-sex controls. Similar results were seen for FRIGHT and AFRAID CLOCKS, which indicates that Ang II-induced HF increased biological age and reduced life expectancy in aging mice. Interestingly, the differences in frailty and clock scores between Ang II-infused male mice and male controls were greater than in females. These findings show that Ang II-induced adverse cardiac remodeling increased frailty and accelerated aging in mice of both sexes, and that this effect was more pronounced in males than females.

This study also aimed to determine whether baseline frailty was associated with adverse cardiac outcomes in Ang II-infused mice. The relationship between endpoint *in vivo* cardiac parameters and baseline FI scores for each treated mouse was explored using

regression analysis. Results showed that there were no correlations between cardiac structural and functional parameters and baseline FI scores in mice of both sexes. These findings show that baseline frailty may not predict adverse cardiac remodeling that leads to HF in male and female mice treated with Ang II.

4.2 Ang II infusion induced hypertension in mice of both sexes

It has been well established that Ang II induces hypertension via constriction of the blood vessels (Touyz et al., 2003). In both humans and animals, Ang II-induced hypertension is associated with negative cardiovascular remodelling and fibrosis that leads to HF (Touyz et al., 2003). Thus, it was important to measure blood pressure in this study to determine if changes in blood pressure were associated with negative cardiac changes. The results show that Ang II infusion caused mice of both sexes to develop hypertension that was sustained throughout the experiment. There were no sex differences in blood pressure levels following Ang II infusion. The hypertensive effect of Ang II infusion was not surprising as this has been well established in the literature (Tsukamoto et al., 2013; Harding et al., 2011; Xu et al., 2008). However, some previous studies have observed sex differences in blood pressure response to Ang II infusion in mice. For example, Xue et al. (2005) infused young C57BL/6 mice of both sexes with 800 ng/kg/min Ang II for one week, at which point male mice developed higher MAP than females. The study also compared blood pressure in Ang II-infused gonadectomised mice of both sexes and found that gonadectomy attenuated hypertension in males but augmented hypertension in females (Xue et al., 2005). This finding suggests that sex differences may occur Ang II-induced

hypertension in younger mice, although sex differences in blood pressure were not seen in the present study.

Other studies have shown that sex hormones are implicated in Ang II-induced hypertension in rodents. For example, Ang II infusion (120 ng/kg/min) for 28 days induced hypertension, increased LV to body weight ratios, and enhanced cardiac fibrosis in both young male Wistar rats and in castrated male rats given testosterone, but not in castrated male rats without testosterone (Mishra et al., 2019). Androgens increase oxidative stress and blood pressure via the pathways through which Ang II activates NADPH oxidases, a major generator of ROS in vascular cells (Reckelhoff et al., 2003). In contrast, estrogens decrease the production of Ang-II induced ROS in peripheral cardiovascular tissue (Xue et al., 2008, Strehlow et al., 2003) and NADPH oxidase and nitric oxide synthase in the endothelium (Gragasin et al., 2003). Nickenig et al. (2000) showed that Ang II increased the production of free oxygen radicals in vascular smooth muscle cells, but this was suppressed by estrogen. Furthermore, Ang II infusion (0.7 mg/kg/day) in young ovariectomized female C57BL/6 mice for 3 weeks promoted hypertension, cardiac hypertrophy and cardiac fibrosis (Pedram et al., 2013). These effects were all prevented in mice receiving an estrogen receptor β agonist, suggesting that estrogen plays a role in preventing adverse cardiac outcomes associated with Ang II-induced hypertension (Pedram et al., 2013).

Estrogen also plays a role in the interaction of Ang II with angiotensin type 2 (AT_2) receptors, a regulator of blood pressure and sodium excretion (Gillis and Sullivan, 2016). The expression of AT_2 receptors is dependent on estrogen levels, and these receptors are present at a higher level in female mice than in males (Pessoa et al., 2015).

AT_2 receptor agonist treatment increases renal blood flow and sodium excretion in female spontaneous hypertensive rats but does not affect these parameters in male rats (Hilliard et al., 2014). In addition, Ang II infusion (600 ng/kg/min for 10 days) induced hypertension in young male C57BL/6 mice and AT_2 receptor knockout male and female mice (Brown et al., 2012). However, young female C57BL/6 mice did not develop hypertension, suggesting they may be protected via estrogen-AT_2 receptor interaction pathways (Brown et al., 2012). As estrogen (Frick, 2009) and testosterone (Hashimoto et al., 2019) decline with age in rodents, the older mice used in this study may have had somewhat lower levels of sex hormones. This may explain why sex differences in blood pressure were not observed in this study.

4.3 Ang II-induced hypertension promoted concentric hypertrophy in female mice and eccentric hypertrophy in males

To determine the effects of Ang II on the heart, and whether there were sex differences in cardiac changes induced by Ang II infusion, *in vivo* cardiac changes were examined by echocardiography at baseline, midpoint and endpoint. Results showed that Ang II-induced hypertension resulted in marked changes in cardiac structure in older mice of both sexes. Treated mice of both sexes exhibited LV hypertrophy, dilation of LV inner diameters, and LV wall stiffening (reduced LV distensibility). There were also sex differences in the cardiac changes promoted by Ang II-induced hypertension. Treated females exhibited concentric hypertrophy (thicker LV walls and increased corrected LV mass/diastolic volume ratio), while males had eccentric hypertrophy (thinner LV walls and greater dilation of the LV chambers). Reduced distensibility indicates increased wall

stiffening to resist wall deformation during diastole (Takeda et al., 2009). Thus, LV wall distensibility is linked to impairments in cardiac walls in diastole and is inversely related to wall stiffness (Takeda et al., 2009). In both humans and animals, pressure overload is often associated with concentric hypertrophy and wall stiffening, which help to minimize wall stress (Schiattarella and Hill, 2015). In hypertensive patients, elevated LV mass/end-diastolic volume ratio is not only an indicator of concentric hypertrophy but is also associated with increased myocardial fibrosis and LV dysfunction (Lembo et al., 2019). In addition, older women with hypertension are more likely to develop concentric LV hypertrophy when compared to older men with hypertension (Drazner, 2011), which corresponds to the results seen in the present study. More investigation is required to understand the mechanisms underlying sex differences in Ang II-induced cardiac changes.

Obesity in the presence of severe hypertension often leads to eccentric cardiac hypertrophy (Smalcelj et al., 2000). In the present study, concentric cardiac hypertrophy was more prominent in Ang II-treated females and eccentric remodeling (thinner walls and dilated chambers) was seen in males. There were also sex differences in body weight where control and treated male mice had higher body weights than respective females. Treatment with Ang II also resulted in increased body weight in treated male mice when compared to control males, which was not seen in females. Reynolds et al. (2019) demonstrated that aged male C57BL/6 mice (18 mos) were more susceptible to obesity than age-matched female mice. Aged male mice have greater body mass and fat mass as well as lower glucose tolerance than young male mice (6 mos) and aged females (Reynolds et al., 2019). Aged females had higher body mass, but not fat mass when compared to young females (Reynolds et al., 2019). In humans, those who are hypertensive and obese are more likely

to exhibit cardiac eccentric hypertrophy (Zabalgoitia et al., 2001; Gottdiener et al., 1994). In particular, individuals who are middle aged and markedly obese with moderate or severe hypertension are most likely to develop eccentric hypertrophy (Smalcelj et al., 2000). Moreover, female obese hypertensive patients exhibit eccentric hypertrophy more than male obese hypertensive individuals (Akintunde et al., 2013). It is possible that eccentric hypertrophy in Ang II-treated male mice in the present study was due to obesity and hypertension.

Hypertension increases afterload to the ventricles, which often results in compensatory concentric hypertrophy to reduce wall stress (De Simone, 2004). Obesity increases preload which leads to increased ventricular wall tension and subsequently ventricular dilatation (Csige et al., 2018). Obesity in the presence of hypertension eventually leads to LV hypertrophy with diastolic and systolic ventricular dysfunction (De Simone et al., 2002). Previous studies examining cardiac changes in Ang II-infused young male mice (8-12 weeks) found that Ang II-induced hypertension resulted in concentric cardiac hypertrophy (Tsukamoto et al., 2013; Xu et al., 2008; Peng et al., 2011). The use of old versus young mice, which have different body compositions, may explain the differences in cardiac remodeling in these studies in comparison to the present study. It is likely that obesity plays a role in promoting eccentric cardiac remodeling in the Ang II-infused older male mice in the present study. More studies are required to explore markers of obesity in older mice treated with Ang II, and whether these markers are associated with Ang II-induced cardiac remodeling.

4.4 Ang II-induced hypertension promoted diastolic dysfunction in mice of both sexes

The present study found that both treated male and female mice exhibited diastolic dysfunction, but this was more severe in males. Ang II-treated male and female mice also had prolonged IVRT, but only males had increased E/A ratios that were significantly different from same-sex controls. There are several grades of diastolic dysfunction. Grade I or early dysfunction is represented by reduced E/A ratio < 0.9 (Panesar and Burch, 2017). As diastolic function worsens, grade II or a pseudonormalization pattern can be observed where E/A ratio increases (0.9-1.5) and may appear normal (Panesar and Burch, 2017). Grade III or restrictive filling pattern is characterized by an elevated E/A > 2 (Panesar and Burch, 2017). Thus, the markedly elevated E/A ratio in treated male mice indicated restrictive LV filling and severe diastolic dysfunction.

A previous study treating young male C57BL/6 mice with Ang II (2.0 μg/kg/min) for 4 weeks also found markedly prolonged IVRT compared to control mice treated with saline (Xu et al., 2008). Other studies looking at the effects of Ang II-induced hypertension on younger male mice also reported signs of diastolic dysfunction (Mori et al., 2012; Jia et al., 2010; Li et al., 2013). The impact of Ang II-induced hypertension on diastolic function in females is unclear as no previous studies looked at this relationship, but the results presented here suggest that effects are less dramatic than seen in males.

Concentric hypertrophy occurs as a compensatory mechanism in response to increased afterload due to hypertension (Oktay et al., 2014). Increased wall thickness is an

adaptive response in order to decrease wall stress (Plitt et al., 2020). Over time, this remodeling process results in wall stiffening, leading to impaired relaxation, characteristic of diastolic dysfunction (Lam et al., 2007). The transition between hypertension and HF involves not only adaptive structural remodeling but also changes in the ECM (Rysa et al., 2005). Deposition of ECM proteins such as collagen in the myocardium causes the heart to stiffen which impairs relaxation and leads to diastolic dysfunction (Plitt et al., 2020). Future studies should investigate changes in ECM in Ang II-infused mice and how this affects cardiac function.

Since Ang II-infused animals exhibit increased LV wall stiffening in the present study, we expected fibrosis levels in the LV to increase. However, results of the fibrosis assay showed that there were no significant differences among any groups in fibrosis levels. This finding differs from some other studies examining fibrosis in humans and animals. Studies on the impact of Ang II on fibrosis found that Ang II increases attachment of human fibroblasts to collagens I and III, the main collagens in the heart (Kawano et al., 2000). The fibroblast-collagen adhesion promotes wound healing and scar formation (Kawano et al., 2000). Elevated serum levels of Ang II are found in patients with myocardial fibrosis and heart diseases including atherosclerosis, hypertension and HF (Kim and Iwao, 2000; Brasier et al., 2002; Zhao et al., 2004). Clinical studies looking at the effects of Ang II receptor blockers found that they attenuated cardiac remodeling associated with myocardial fibrosis (Billet et al., 2008). These findings suggest that Ang II facilitates the development of cardiac fibrosis in cardiac diseases in humans.

Studies in animals treated with Ang II also found that Ang II plays a role in promoting cardiac fibrosis. Rodents infused with Ang II exhibit cardiac changes including

hypertrophy and fibrosis similar to humans (Billet et al., 2008; Li et al., 2007; Liu et al., 2003). Sopel et al. (2011) found that young male C57BL/6 mice infused with Ang II (2.0 μg/kg/min) exhibited hypertension, cardiac hypertrophy, and extensive myocardial collagen deposition after 7 days. The study also demonstrated that Ang II promoted the infiltration of fibrocytes and inflammatory cells into the myocardium which stimulate fibrosis (Sopel et al., 2011). These studies support the role of Ang II in promoting myocardial fibrosis. The absence of marked fibrosis in Ang II infused mice in the present study may have occurred because we used older control and treated mice that may already have elevated fibrosis due to aging (Kane et al., 2021). It also could be that fibrosis can be focal and we might not have sampled the right region of the LV.

4.5 Ang II-induced hypertension promoted systolic dysfunction in mice of both sexes, but this was worse in males.

Results of the present study showed that Ang II-treated mice of both sexes exhibited systolic dysfunction as seen by decreased EF and FS. In treated female mice, systolic dysfunction was accompanied by concentric hypertrophy. In hypertensive cardiac diseases, increased blood pressure often results in concentric LV hypertrophy, followed by LV dilation and systolic dysfunction where EF is reduced (Krishnamoorthy et al., 2011). This transition from concentric LV hypertrophy to systolic dysfunction has been reported in animals and in humans (Litwin et al., 1995; Krishnamoorthy et al., 2011). Krishnamoorthy et al. (2011) demonstrated that increases in LV chamber dimensions play a role in reduced EF in individuals with concentric hypertrophy. In hypertensive patients with concentric cardiac hypertrophy, those with reduced EF have larger LV end-diastolic

diameter and LV end-systolic dimension than those with preserved EF (Krishnamoorthy et al., 2011). This suggests that dilation of the LV volume in concentric hypertrophy is part of the progression to reduced EF in this population (Krishnamoorthy et al., 2011). Among patients with HF, those with reduced EF and concentric hypertrophy are older hypertensive women (Nauta et al., 2020). The studies presented in this thesis suggest that concentric hypertrophy with dilated LV chambers is associated with reduced EF in Ang II-treated females.

Results from the present study also show that Ang II-treated male mice exhibited eccentric hypertrophy along with systolic dysfunction. This was seen as reduced EF and FS, as well as prolonged IVCT. Indeed, treated male mice had markedly prolonged IVCT when compared to same-sex controls and treated females at endpoint. Eccentric LV hypertrophy is commonly associated with HFrEF (Nauta et al., 2020). Longer IVCT is also associated with HF as it is an independent predictor of HF in the general population (Alhakak et al., 2020). In patients with HF, IVCT is markedly prolonged (Bruch et al., 2000; Janert et al., 2000; Meric et al., 2014) as seen in the treated male mice in this study. Prolonged IVCT is also used as a prognostic marker that predict the risks of HF in women aged 45 to 94 years (Alhakak et al., 2020). Further investigations are required to understand why prolonged IVCT only occurred in Ang II treated male mice but not females, and to reveal underlying mechanisms.

To investigate the influence of Ang II infusion on contractile function in isolated *ex vivo* hearts and whether there are sex differences, Langendorff-perfused hearts were investigated. Although systolic function declined in *in vivo* hearts of Ang II-treated mice, Langendorff cardiac parameters including LVDP, flow rate, heart rate, +dP/dt, and -dP/dt

did not differ between control and Ang II-infused mice of both sexes. However, normalized RPP in treated male mice was significantly lower than same-sex controls, which was not observed in females. This decline suggests that hearts from Ang II-treated male mice could perform less work and had reduced contractility when compared to same-sex controls. In patients with chronic HF, those with lower RPP exhibit more advanced stage of HF (El-Dosouky et al., 2019). On the other hand, patients with higher RPP have higher rates of concentric LV hypertrophy, which plays a compensatory role in normalizing contractile stress and total contractile force (El-Dosouky et al., 2019). Thus, the concentric geometry may explain why normalized RPP was preserved in Ang II-treated female mice.

The *in vivo* heart from Ang II-treated mice was subjected to constant hypertension, whereas this did not occur in the Langendorff-perfused heart. Thus, one reason why systolic dysfunction seen *in vivo* was not reflected in the Langendorff-perfused hearts results maybe because a constant pressure Langendorff system was used. The pressure was maintained at 80 mmHg throughout the experiment for all the Langendorff-perfused hearts which did not represent the hypertensive physiological conditions experienced *in vivo*. Since the hearts from Ang II-treated mice remodeled to adapt to pressure overload, the reduction in pressure in the Langendorff system used in this study reduced the requirement to compensate for systolic stress. Furthermore, ventricular function of the *ex vivo* Langendorff-perfused hearts is determined in the absence of neural and/or hormonal influences, which may also play a role in systolic dysfunction in the *in vivo* heart. It is possible that the *in vivo* cardiac functional changes would be reflected *ex vivo* if a constant flow Langendorff model was used and the pressure applied is changed to match that of the physiological system. Future studies performing Langendorff

experiments on hearts in hypertensive animal models should consider employing the constant flow system.

4.6 Ang II-induced hypertension promoted cardiac hypertrophy and pulmonary edema in females only

There were also sex differences in isolated tissues in Ang II-treated and control mice. Male controls had larger heart weights and heart weights normalized to tibia length compared to female controls. However, these sex differences were abolished when the mice were treated with Ang II. In addition, Ang II-treated females had larger heart weights and heart weight to tibia length ratios compared to controls, but this was not observed in males. The cardiac hypertrophy seen in isolated whole hearts from treated females reflects the *in vivo* results, where the differences in corrected LV mass between treated and control females were much larger when compared to males. Concentric LV hypertrophy in treated females but not males may also explain why hypertrophy in isolated whole hearts was more pronounced in females.

Treated females also accumulated more pulmonary fluid than female controls, but this was not seen in males. Increases in lung weight commonly occur in LV failure, and are a reliable indicator of LV dysfunction (Xu et al., 2011). In an aortic constriction-induced mouse HF model, pressure overload led to LV dysfunction accompanied by larger lung weights and increased lung fibrosis (Chen et al., 2012). The pressure overload induced by aortic constriction results in concentric LV hypertrophy via mechanical stimulation and activation of hormones including Ang II (Estrada et al., 2021). Concentric hypertrophy leads to diastolic dysfunction which, in turn, increases LV diastolic pressure

(Spier and Meurs, 2004). This increase in pressure can lead to elevated left atria and pulmonary venous pressures (Spier and Meurs, 2004). The increased pressure in the left atria causes fluid to accumulate in the lung interstitial spaces, which leads to pulmonary edema (Drake and Doursout, 2002). Concentric LV hypertrophy combined with hypertension particularly promotes acute pulmonary edema, a condition in which the pulmonary airspaces fill with liquid (Maclver et al., 2015; Gandhi et al., 2001). Chronic hypertension and concentric LV hypertrophy contribute to increased peripheral vascular resistance, which increases the demand on the LV and an inability to raise LV stroke volume appropriately (Maclver et al., 2015). On the other hand, stroke volume in the RV is relatively unchanged, which creates a mismatch in stroke volume between RV and LV (Maclver et al., 2015). Acute pulmonary edema occurs when a significant acute stroke volume mismatch arises (Maclver et al., 2015). Moreover, Suen et al. (2019) found that pulmonary hypertension also results in RV dilation and systolic dysfunction and in male Fischer rats. Thus, future studies looking at whether Ang II-induced hypertension also affects RV structure and function in animal models of both sexes will contribute to our understanding of hypertension and HF in both sexes.

4.7 Ang II-induced hypertension promotes frailty in mice of both sexes

This work was the first to study the effects of Ang II-induced hypertension and HF on frailty as well as sex differences in older mice. Results showed that Ang II infusion worsened frailty, increased estimated biological age, and decreased estimated life expectancy in mice of both sexes. However, all of these effects were more severe in male mice. Previous preclinical studies found that frailty is closely related to age-associated

adverse remodeling in hearts from male mice (Feridooni et al., 2017; Moghtadaei et al., 2016; Jansen et al., 2017). In addition, adverse changes in myofilament proteins in the aging heart were graded by FI scores in male mice but not in female mice (Kane et al., 2020). Changes in EF, E/A ratios, fibrosis, and septal wall thickness were also graded by frailty in aging male mice, but this was not seen in females (Kane et al., 2021). Only septal wall thickness and LV mass are related to frailty in female mice, suggesting that females may be relatively more protected than males from adverse effects of frailty on the heart (Kane et al., 2021).

Studies on patients with HF, however, found that women with HF have a higher prevalence of frailty than men. Pandey et al. (2019) reported that older females with HF and other comorbidities are at a higher risk of frailty compared to older males with a similar profile. Other studies have also reported a higher prevalence of frailty among older female HF patients (Altimir et al., 2005; Murad and Kitzman, 2015; Lupon et al., 2008). Furthermore, a systemic review and analysis by Davis et al. (2021) found that women with HF have a 26% higher relative risk of frailty compared to men with HF. Other factors including other comorbidities may explain this sex difference in the prevalence of frailty in HF (Davis et al., 2021). Nonetheless, sex differences in the prevalence of frailty in HF remain poorly understood (Davis et al., 2021). Understanding gender differences in frailty among HF patients is critically needed to inform clinical management of HF.

Frailty involves impairments in multiple physiological systems including the endocrine system, respiratory system, cardiovascular system, and skeletal muscle system (Angulo et al., 2016). For instant the musculoskeletal system plays a role in frailty by accelerating sarcopenia or the decline of muscle strength and mass (Davies et al., 2018).

Sarcopenia is common in patients with chronic HF, and it contributes to frailty (Uchmanowicz et al., 2014). The manifestations of sarcopenia include slow gait speed, weakness, shortness of breath, and fatigue during exercise. In the present study, the proportions of mice with deficits in the musculoskeletal systems in both male and female treated mice were higher compared to same-sex controls. Ang II-infused females had higher proportions of deficits in body condition scores and kyphosis, whereas treated male mice had increased proportions of gait disorders and tail stiffening. Other frailty deficits including vision loss in treated females as well as breathing and hearing problems in treated mice of both sexes also suggest impairments in the ocular, respiratory, and auditory systems respectively. In humans, the prevalence of visual impairment is much higher in HF patients than in those without HF (Sterling et al., 2018a). Visual impairments in older adults are associated with worse frailty status (Swenor et al., 2019). Similarly, older patients with HF have a higher prevalence of hearing loss compared to those without HF (Sterling et al., 2018b). Hearing loss is also associated with increased risks of frailty and poor physical function in older adults with and without HF (Kamil et al., 2016; Cosciano et al., 2012). Moreover, respiratory muscle dysfunction contributes to breathing problems and reduces exercise tolerance in HF patients (Miyagi et al., 2018; Filusch et al., 2011). The decline in respiratory muscle strength is related to the severity of HF (Filusch et al., 2011). Pulmonary hypertension in HF patients also plays a role in respiratory muscle dysfunction by reducing ventilation efficiency (Filusch et al., 2011). There is a lack of studies on rodent models of HF that examine how individual deficits contribute to HF and poor health status. Overall, the results presented in this thesis suggest that deficits in multiple organs including adverse remodeling in the heart contribute to increased frailty in

Ang II-infused mice. It is important to highlight the fact that the FI tool is not composed of items that are direct measurements of cardiac function, but it can be used to measure poor overall health associated with HF.

4.8 Baseline frailty was not correlated to cardiac outcomes in Ang II-treated mice of both sexes

This study also aimed to determine whether high frailty levels at baseline led to worse cardiac outcomes after Ang II treatment. Results showed that high baseline FI scores were not associated with adverse cardiac outcomes in treated mice of both sexes. Kane et al. (2020) showed that cardiac remodeling associated with adverse changes in cardiomyocyte contractions is graded by FI scores in male mice and proposed that these changes during aging may lead to cardiovascular disease including HF (Kane et al., 2020). In the present study, none of the *in vivo* cardiac outcomes correlated with baseline frailty. This may be due the age and limited range of FI scores in the mice used in this study. The mice in this study were between 13 and 16 months of age with FI scores ranging from 0.05 to 0.32. On the other hand, Kane et al. (2020) used mice that were ~12 and ~24 months old within a range of FI scores of 0.15 to 0.5. A relationship between frailty and cardiac changes in Ang II-infused mice may become more apparent with the use of older, frailer animals.

4.9 Potential mechanisms in cardiac remodeling and enhanced frailty in Ang II-induced hypertension

Adverse cardiac remodeling including cardiac hypertrophy following Ang II infusion observed in the present study could be due to an increase in Ang II-induced oxidative stress. Studies found that Ang II upregulates ROS production in all types of vascular cells including smooth muscle cells, endothelial cells, and adventitial fibroblasts (Touyz et al., 2003). Ang II-induced ROS, such as superoxide (O_2^-), hydrogen peroxide (H_2O_2), cytokines, and adhesion molecules, cause damage to the vascular walls and alter ECM content (Pueyo et al., 2000; Yoon et al., 2002; Brasier et al., 2002). Specifically, O_2^- and H_2O_2 are implicated in the pathologic regulations of vascular structural remodelling (Griendling et al., 2000). Furthermore, Ang II-induced hypertension involves the upregulation of vascular NADPH oxidase, which contributes to increased vascular smooth muscle cell growth (Griendling et al., 2000; Touyz et al., 2002). Inhibition of NADPH oxidase activity supresses cardiovascular remodeling and vascular smooth muscle cell hypertrophy induced by Ang II (Touyz et al., 2002; Chen et al., 2001). Oudit et al. (2007) found adverse cardiac remodeling including LV hypertrophy, LV dilation and systolic dysfunction in mice is associated with enhanced Ang II-mediated oxidative stress pathways. In patients with chronic HF, oxidative stress is closely associated with the activation of Ang II (Reina-Couto et al., 2020). Thus, oxidative stress due to increased Ang II levels could be implicated in the development of adverse cardiac remodeling observed in the present study. It would be interesting to examine the levels of ROS after Ang II infusion and determine whether this is associated with Ang II-associated cardiovascular structural and functional changes in both male and female mice.

Increased oxidative stress levels may also play a role in enhanced frailty in Ang II-treated mice. Studies have found that oxidative stress plays an important role in the pathogenesis of frailty (Uchmanowicz, 2020). Excessive ROS can lead to frailty by inducing apoptosis, cell damage, protein degradation, and impaired repair mechanisms (Derbre et al., 2014). For example, high levels of ROS in the musculoskeletal system impair muscle function and reduce strength, which promotes frailty (Derbre et al., 2014). Indeed, studies have shown that frailty and markers of oxidative stress are closely associated (Serviddio et al., 2009; Wu et al., 2009). Markers of oxidative stress are present at high levels in frail patients (Serviddio et al., 2009). Moreover, Ingles et al. (2014) demonstrated that markers of oxidative damage including malondialdehyde and protein carbonyls in plasma of older adults were associated with frailty but not chronological age. Increased lipid peroxidation was also found to be associated with increased risks of frailty and slow gait speed in older patients (Liu et al., 2016). Moreover, increased O_2^- production via NADPH oxidase stimulation, which is upregulated in Ang II-induced hypertension, is associated with physical frailty in older adults (Baptista et al., 2012). When exercise was introduced as an intervention, oxidative stress was associated with frailty and not chronological age in both mice and humans (Gomez-Cabrera et al., 2017). Vina et al. (2018) also demonstrated that measures of oxidative stress were better associated with frailty than chronological age. Together, these findings suggest that oxidative stress induced by Ang II infusion exacerbates frailty as observed in the present study. Future research is needed to determine the oxidative stress levels in Ang II infused mice and whether this is associated with higher FI scores.

Besides oxidative stress, inflammation may also contribute to adverse cardiac changes and poor overall health in Ang II-infused mice. Studies have reported that chronic inflammation plays an important role in the development of cardiac hypertrophy and HF (Bellumkonda et al., 2017; Shimizu et al., 2016). For example, the pro-inflammatory cytokine IL-6 is implicated in the pathogenesis of hypertrophy and HF (Chaikijurajai amd Tang, 2020). It promotes cardiac hypertrophy in male rats via the interaction with IL-6 receptors on cardiomyocytes (Melendez et al., 2010). Furthermore, Kane et al. (2021) found that increased LV mass was positively correlated with serum IL-6 levels in older male mice but not in age-matched females. That study also found that serum IL-1β and TNF-α as well as chemokines eotaxin and MIP-1α are related to cardiac hypertrophy in older male mice only (Kane et al., 2021). The serum levels of chemokines eotaxin and MIP-1α were previously found to be correlated with right ventricular hypertrophy in mouse models of HF (Vistnes et al., 2010). The pro-inflammatory cytokines IL-1β and TNF-α bind to IL-1 or TNF receptors in cardiomyocytes and promote cardiac hypertrophy, similar to IL-6 (Sriramula et al., 2008; Bujak et al., 2009). Pro-inflammatory cytokines including IL-6, IL-1 and TNF-α stimulate the production of chemokines or secondary cytokines (Mantovani, 1997). Along with high inflammation levels, high frailty scores in older male mice are also associated with cardiac hypertrophy and dysfunction, but this is not seen in females (Kane et al., 2020). Interestingly, in females, the levels of the anti-inflammatory cytokine IL-10 are higher in older females than males (Kane et al., 2020). IL-10 plays a role in suppressing the production pro-inflammatory cytokines (Minciullo et al., 2016). IL-10 knockout mice exhibit premature aging characteristics and are used to model frailty (Sikka et al., 2013). Female mice may be protected from age-related cardiac dysfunction

due to the higher IL-10 levels (Kane et al., 2021). The results from Kane et al. (2021) suggest that adverse age-associated cardiac remodeling is linked to inflammation and poor frailty status in male mice. Thus, it is possible that pro-inflammatory cytokines may drive the increase in frailty scores and worse cardiac dysfunction in Ang II-infused male mice in the present study. On the other hand, higher levels of anti-inflammatory cytokines may protect females from functional decline in the cardiovascular system.

Previous studies have found that there are sex differences in immune responses following Ang II infusion. Zhang et al. (2009) found that Ang II infusion (1.5 μg/kg/min) for 7 days increased circulating plasma IL-6, TNF-α, and IL-1β in younger male C57BL/6 mice. Among plasma cytokines, IL-6 levels were the highest following Ang II infusion and a contributing factor in muscle wasting in treated mice (Zhang et al., 2009). However, IL-6 deficient mice treated with Ang II did not exhibit muscle loss, supporting the important role of this cytokine in promoting muscle degradation (Zhang et al., 2009). TNF-α has also been shown to contribute to Ang II-induced ventricular remodeling (Sriramula and Francis, 2015). In addition, younger male Sprague-Dawley rats infused with Ang II (200 ng/kg/min/) for 2 weeks developed greater increases in pro-inflammatory T cells, whereas younger females had greater increases in anti-inflammatory T cells (Zimmerman et al., 2015). Furthermore, studies have suggested that the AT_2 receptor is involved the activation of anti-inflammatory cytokines and cardiovascular protection in females (Gillis et al., 2016). Dhande et al., (2015) found that treatment with an AT_2 receptor agonist increases IL-10 levels and attenuates IL-6 and TNF-α release in human kidney cells. Treatment with an AT_2 receptor agonist also attenuates renal inflammation in diabetic male mice, while AT_2 receptor antagonists decrease circulating and renal IL-10 levels in male

obese rats (Koulis et al., 2015). Much is still not known about how Ang II-AT_2 interaction affects circulating inflammatory cytokine levels in females. Since the AT_2 receptor plays a more important role in maintaining renal and cardiovascular homeostasis in females than males, it is possible that AT_2 protective actions involve promoting anti-inflammatory cytokines (Gillis et al., 2016). Overall, it is likely that inflammation, along with oxidative stress, contribute to Ang II-induced cardiac remodeling and subsequently worsen frailty status in Ang II-infused mice in the present study. Females may be more protected during hypertension due to a greater anti-inflammatory immune profile compared to males who have a more pro-inflammatory profile (Gillis et al., 2016). Future studies are needed to confirm how inflammation is related to frailty and cardiac remodeling in the Ang II-induced model of HF as well as whether this helps explain sex differences in these outcomes.

In contrast to AT_2 receptors, angiotensin type 1 (AT_1) receptor mediates Ang II-induced vasoconstriction, sodium reabsorption, aldosterone production, cardiac hypertrophy, and cardiac fibrosis (Kumar et al., 2019). AT_1 receptor blockers are currently used in the treatment of HF (Januzzi and Ibrahim, 2017). In rats, AT_1 receptor expression increases while AT_2 receptor expression decreases in hearts of older animals (Monteonofrio et al., 2021). Furthermore, AT_1 receptor levels are higher in males, whereas females have higher AT_2 receptor levels in mice and rats (Monteonofrio et al., 2021). Together, these studies suggest that higher AT_1 receptor expression may modulate worse cardiac outcomes in Ang II-treated male mice, whereas higher AT_2 receptor levels in treated females have cardio-protective effects. More research is needed to examine this hypothesis.

The angiotensin converting enzyme 2 (ACE2) may also play a role in sex differences in HF and frailty in Ang II-treated mice. Ang ACE2 is expressed in various cardiac cells including fibroblasts, cardiomyocytes and endothelial cells (Gallagher et al., 2008). As a part of the RAAS system, ACE2 is a monocarboxypeptidase that generates Ang 1-7 from Ang II (Uri et al., 2014). Ang 1-7 stimulates vasodilation, which decreases total peripheral resistance and arterial blood pressure (Raffai and Lombard, 2016). It has been shown that Ang 1-7 has cardioprotective effects as it can reduce Ang II-induced adverse cardiac remodeling and hypertension-induced HF (Liang et al., 2015). Enhanced ACE2 or Ang 1-7 in preclinical models of HFpEF and HFrEF has been shown to reduce tissue inflammation and myocardial fibrosis, improve endothelial dysfunction, and reverse cardiac hypertrophy (Patel et al., 2017). Studies in ACE2-knockout mice of both sexes demonstrate that ACE2 protects females but not males from developing hypertension (Stanic et al., 2021). Furthermore, human studies examining ACE2 levels with aging found that older women (≥55 years) had significantly higher ACE2 activity than younger women (<55 years), whereas this was not seen in men (Fernandez-Atucha et al., 2017). However, higher serum ACE2 levels are typically found in men with hypertension and HF when compared to matched women (Salah and Mehta, 2021). These studies suggest that ACE2 may play a protective role in Ang II-treated female mice. Nonetheless, more studies are required to determine ACE2 levels in male and female animal models of both sexes and whether this is associated with adverse cardiac outcomes.

4.10 Limitations

The present study assessed frailty in response to Ang II infusion. This is the first study to assess frailty in an Ang II-induced HF mouse model of both sexes. The relationship between frailty and HF has not been previously explored in animal models. Thus, the results of the present study are novel but also need to be validated in future studies.

The study has some limitations. First, the study was not blinded which may have led to some bias. Another limitation was that Ang II infusion also caused the mice to lose weight rapidly. When a mouse reached its HEP weight, it was sacrificed. As a result, mice were sacrificed due to low HEP weight and did not reach the endpoint. The present study used a mixed effects model for analysis, which takes into account all animals including those that did not have all time points (Judd et al., 2012). This statistical model allows the results to be generalized to the population of treatment conditions, even when there are missing data (Barr et al., 2013). Although the mixed effects model allows for analysis of incomplete data, this method may mask potential differences that may have resulted from the missing values.

Echocardiography was used to assess the impact of Ang II infusion on *in vivo* cardiac structure and function in mice used in this study. Anesthetic is required when performing echocardiography in mice, which causes heart rate to decrease and may not reflect the natural state of the heart. In addition, echocardiography requires precision since the mouse heart is very small. Slight changes in the placement of the transducer could potentially affect the results and mask sex differences. Finally, echocardiography is a load-

dependent measure. Future studies could use a cardiac catheter to compare load-independent ventricular function via pressure-volume loops (Hassink et al., 2008).

Since Ang II-infused mice are subjected to higher blood pressure, the constant pressure model of Langendorff perfused hearts may not have been the best choice to use in this study. The constant volume Langendorff system may be a better choice to investigate the impact of Ang II-induced hypertension on *ex vivo* heart function.

4.11 Summary

The present study demonstrated pressure overload induced by Ang II treatment revealed sex differences in cardiac remodelling, and frailty increased in treated mice of both sexes. Concentric cardiac hypertrophy with dilated LV chambers was seen in treated females, while eccentric hypertrophy was more prominent in treated males. Male mice also had more severe systolic and diastolic LV dysfunction. Baseline frailty was not associated with *in vivo* adverse cardiac outcomes in any group. Ang II-infused mice also had higher biological age and reduced life expectancy compared to same-sex controls, and this was more severe in males. In Langendorff-perfused hearts, there were no changes in contractile parameters between control and treated female animals. By contrast, Langendorff-perfused hearts of Ang II-treated mice exhibited reduced normalized RPP when compared to hearts of control male animals. On the other hand, treated females had markedly larger hearts and exhibited pulmonary edema, which were not seen in treated males. These results demonstrate sex-differences in cardiac remodeling as hypertension transitions to HF in older mice. The study also demonstrates the importance of using both sexes in pre-clinical research.

4.12 Future directions

This is the first study of frailty in the Ang II-induced animal model of HF. Results from this study showed that baseline frailty did not predict adverse cardiac changes that preceded HF in Ang II-infused mice of both sexes. Since frailty increases with advancing age, it is possible that the mice in the present study were not frail enough. Future studies should re-examine the relationship between frailty and cardiac changes in Ang II infused mice using older, frailer male and female animals.

As mentioned in the previous sections, calcium handling and myocyte contractile function may be implicated in the development of hypertensive HF. It would be valuable to examine these mechanisms in the Ang II-induced model of HF, and whether they are associated with frailty in both sexes. Other parameters including inflammatory cytokines, levels of oxidative stress, and B-type natriuretic peptide, a predictor of HF, should also be examined in relation to frailty and sex in future research.

Nauta et al. (2020) demonstrated that MMP2 plays a role in post-myocardial infarction remodelling of the LV, which leads to eccentric hypertrophy. Furthermore, Dahl salt-sensitive rats with hypertensive HF have increased myocardial fibrosis that is associated with increased MMP2 activities (Iwanaga et al., 2002). It has also been shown that stimulation with Ang II promotes MMP2 expression and activity in cultured cardiovascular cells (Coker et al., 2001). Interestingly, MMPs and their interactions with TIMPs in the atria were found to be correlated with FI scores in aged male mice (Jansen et al., 2017). Thus, MMPs may be implicated in adverse cardiac changes in Ang II-treated mice. More studies are needed to investigate the role of MMPs in cardiac remodeling in male and female mice treated with Ang II. Furthermore, histological analysis of frozen

heart samples could be used to confirm concentric and eccentric hypertrophy phenotypes as well as differences in cardiac fibrosis.

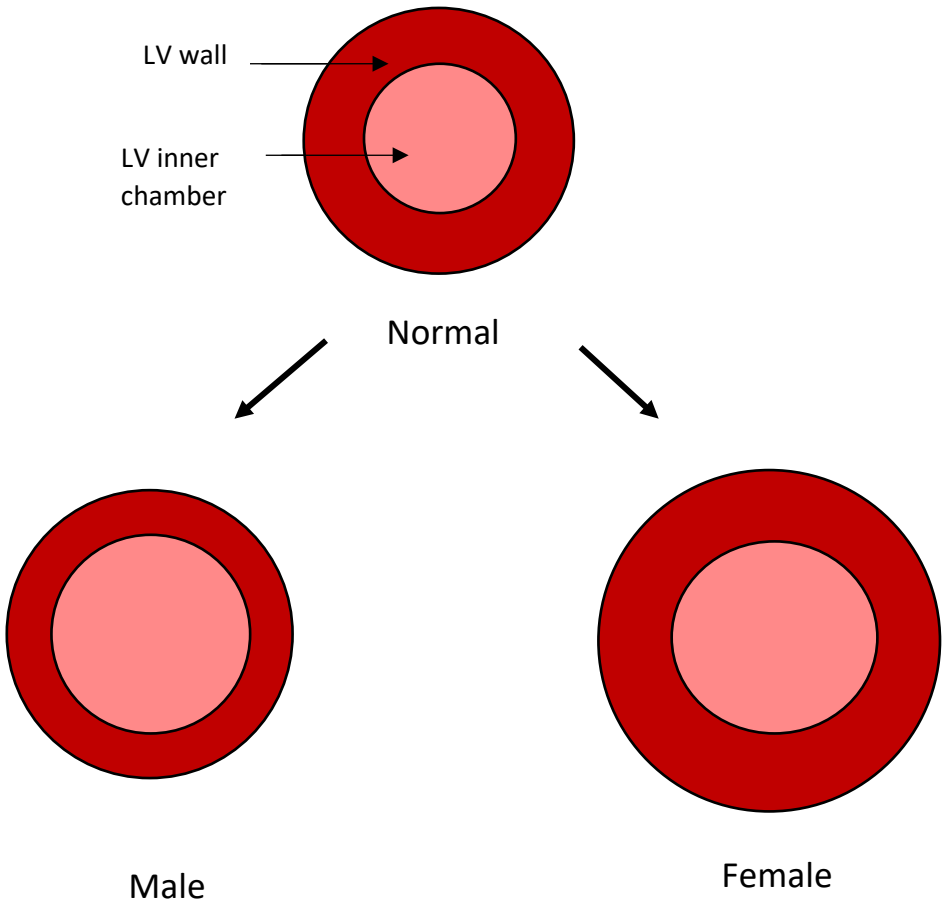

Figure 4.1. Ang II-induced hypertension promoted sex differences in cardiac remodeling in older mice. Treated female mice developed thicker LV walls and slightly dilated LV chambers, while treated male mice developed thinner LV walls and showed marked LV dilation. Both male and female treated mice had larger hearts compared to same-sex controls.

References

Abadir, P.M., 2011. The frail renin-angiotensin system. *Clinics in Geriatric Medicine*, *27*(1), pp.53-65.

Afilalo, J., Alexander, K.P., Mack, M.J., Maurer, M.S., Green, P., Allen, L.A., Popma, J.J., Ferrucci, L. and Forman, D.E., 2014. Frailty assessment in the cardiovascular care of older adults. *Journal of the American College of Cardiology*, *63*(8), pp.747-762.

Ahmad, F.S., Ning, H., Rich, J.D., Yancy, C.W., Lloyd-Jones, D.M. and Wilkins, J.T., 2016. Hypertension, obesity, diabetes, and heart failure–free survival: the Cardiovascular Disease Lifetime Risk Pooling Project. *JACC: Heart Failure*, *4*(12), pp.911-919.

Akasheva, D.U., Plokhova, E.V., Tkacheva, O.N., Strazhesko, I.D., Dudinskaya, E.N., Kruglikova, A.S., Pykhtina, V.S., Brailova, N.V., Pokshubina, I.A., Sharashkina, N.V. and Agaltsov, M.V., 2015. Age-related left ventricular changes and their association with leukocyte telomere length in healthy people. *PloS one*, *10*(8), p.e0135883.

Akintunde, A.A., Oladosu, Y. and Opadijo, O.G., 2013. Gender specific pattern of left ventricular cardiac adaptation to hypertension and obesity in a tertiary health facility in Nigeria. *African Health Sciences*, *13*(3), pp.595-600.

Aksentijević, D., Lewis, H.R. and Shattock, M.J., 2016. Is rate–pressure product of any use in the isolated rat heart? Assessing cardiac 'effort'and oxygen consumption in the Langendorff-perfused heart. *Experimental Physiology*, *101*(2), pp.282-294.

Alhakak, A.S., Møgelvang, R., Schnohr, P., Modin, D., Brainin, P., Gislason, G. and Biering-Sørensen, T., 2020. The cardiac isovolumetric contraction time is an independent predictor of incident heart failure in the general population. *International Journal of Cardiology*, *312*, pp.81-86.

Ali, S.S., Xiong, C., Lucero, J., Behrens, M.M., Dugan, L.L. and Quick, K.L., 2006. Gender differences in free radical homeostasis during aging: shorter-lived female C57BL6 mice have increased oxidative stress. *Aging Cell*, *5*(6), pp.565-574.

Altimir, S., Lupón, J., González, B., Prats, M., Parajín, T., Urrutia, A., Coll, R. and Valle, V., 2005. Sex and age differences in fragility in a heart failure population. *European Journal of Heart Failure*, *7*(5), pp.798-802.

Angulo, J., El Assar, M. and Rodriguez-Manas, L., 2016. Frailty and sarcopenia as the basis for the phenotypic manifestation of chronic diseases in older adults. *Molecular Aspects of Medicine*, *50*, pp.1-32.

Austad, S.N. and Fischer, K.E., 2016. Sex differences in lifespan. *Cell Metabolism*, *23*(6), pp.1022-1033.

Avendano, M. and Mackenbach, J., 2008. Changes in physical health among older Europeans. *Health and Health Care*, p.116.

Baidurin, S., Blyalova, D., Bekenova, F., Tkachev, V. and Akhmetzhanova, S., 2020. Indicators of Cardiohemodynamics of Rhythm Disturbances in Elderly People with Chronic Heart Failure. *Georgian Medical News*, *299*, pp.61-65.

Baptista, G., Dupuy, A.M., Jaussent, A., Durant, R., Ventura, E., Sauguet, P., Picot, M.C., Jeandel, C. and Cristol, J.P., 2012. Low-grade chronic inflammation and superoxide anion production by NADPH oxidase are the main determinants of physical frailty in older adults. *Free Radical Research*, *46*(9), pp.1108-1114.

Barr, D.J., Levy, R., Scheepers, C. and Tily, H.J., 2013. Random effects structure for confirmatory hypothesis testing: Keep it maximal. *Journal of Memory and Language*, *68*(3), pp.255-278.

Baumann, C.W., Kwak, D. and Thompson, L.V., 2019. Sex-specific components of frailty in C57BL/6 mice. *Aging (Albany NY)*, *11*(14), p.5206.

Beery, A.K., 2018. Inclusion of females does not increase variability in rodent research studies. *Current Opinion in Behavioral Sciences*, *23*, pp.143-149.

Bellumkonda, L., Tyrrell, D., Hummel, S.L. and Goldstein, D.R., 2017. Pathophysiology of heart failure and frailty: a common inflammatory origin? *Aging Cell*, *16*(3), pp.444-450.

Bergman, H., Ferrucci, L., Guralnik, J., Hogan, D.B., Hummel, S., Karunananthan, S. and Wolfson, C., 2007. Frailty: an emerging research and clinical paradigm—issues and controversies. *The Journals of Gerontology Series A: Biological Sciences and Medical Sciences*, *62*(7), pp.731-737.

Bers, D.M., 2014. Cardiac sarcoplasmic reticulum calcium leak: basis and roles in cardiac dysfunction. *Annual Review of Physiology*, *76*, pp.107-127.

Bertero, E. and Maack, C., 2018. Metabolic remodelling in heart failure. *Nature Reviews Cardiology*, *15*(8), pp.457-470.

Billet, S., Aguilar, F., Baudry, C. and Clauser, E., 2008. Role of angiotensin II AT1 receptor activation in cardiovascular diseases. *Kidney international*, *74*(11), pp.1379-1384.

Bing, O.H., Brooks, W.W., Robinson, K.G., Slawsky, M.T., Hayes, J.A., Litwin, S.E., Sens, S. and Conrad, C.H., 1995. The spontaneously hypertensive rat as a model of the transition from compensated left ventricular hypertrophy to failure. *Journal of Molecular and Cellular Cardiology*, *27*(1), pp.383-396.

Bing, O.H., Conrad, C.H., Boluyt, M.O., Robinson, K.G. and Brooks, W.W., 2002. Studies of prevention, treatment and mechanisms of heart failure in the aging spontaneously hypertensive rat. *Heart Failure Reviews*, *7*(1), pp.71-88.

Boluyt, M.O., Bing, O.H.L. and Lakatta, E.G., 1995. The ageing spontaneously hypertensive rat as a model of the transition from stable compensated hypertrophy to heart failure. *European Heart Journal*, *16*(suppl_N), pp.19-30.

Boxer, R.S., Shah, K.B. and Kenny, A.M., 2014. Frailty and prognosis in advanced heart failure. *Current Opinion in Supportive and Palliative Care*, *8*(1), pp.25-29.

Bozkurt, B. and Khalaf, S., 2017. Heart failure in women. *Methodist DeBakey Cardiovascular Journal*, *13*(4), p.216-223

Brasier, A.R., Recinos III, A. and Eledrisi, M.S., 2002. Vascular inflammation and the renin-angiotensin system. *Arteriosclerosis, Thrombosis, and Vascular Biology*, *22*(8), pp.1257-1266.

Brouwers, F.P., de Boer, R.A., van der Harst, P., Voors, A.A., Gansevoort, R.T., Bakker, S.J., Hillege, H.L., van Veldhuisen, D.J. and van Gilst, W.H., 2013. Incidence and epidemiology of new onset heart failure with preserved vs. reduced ejection fraction in a community-based cohort: 11-year follow-up of PREVEND. *European Heart Journal, 34*(19), pp.1424-1431.

Brown, R.D., Hilliard, L.M., Head, G.A., Jones, E.S., Widdop, R.E. and Denton, K.M., 2012. Sex differences in the pressor and tubuloglomerular feedback response to angiotensin II. *Hypertension*, *59*(1), pp.129-135.

Bruch, C., Schmermund, A., Marin, D., Katz, M., Bartel, T., Schaar, J. and Erbel, R., 2000. Tei-index in patients with mild-to-moderate congestive heart failure. *European heart journal*, *21*(22), pp.1888-1895.

Bujak, M. and Frangogiannis, N.G., 2009. The role of IL-1 in the pathogenesis of heart disease. *Archivum Immunologiae Et Therapiae Experimentalis*, *57*(3), pp.165-176.

Buta, B.J., Walston, J.D., Godino, J.G., Park, M., Kalyani, R.R., Xue, Q.L., Bandeen-Roche, K. and Varadhan, R., 2016. Frailty assessment instruments: systematic characterization of the uses and contexts of highly-cited instruments. *Ageing Research Reviews*, *26*, pp.53-61.

Butts, B., Gary, R.A., Dunbar, S.B. and Butler, J., 2015. The importance of NLRP3 inflammasome in heart failure. *Journal of Cardiac Failure*, *21*(7), pp.586-593.

Cacciatore, F., Abete, P., Mazzella, F., Viati, L., Della Morte, D., D'Ambrosio, D., Gargiulo, G., Testa, G., De Santis, D., Galizia, G. and Ferrara, N., 2005. Frailty predicts long-term mortality in elderly subjects with chronic heart failure. *European Journal of Clinical Investigation*, *35*(12), pp.723-730.

Chaanine, A.H., Kohlbrenner, E., Gamb, S.I., Guenzel, A.J., Klaus, K., Fayyaz, A.U., Nair, K.S., Hajjar, R.J. and Redfield, M.M., 2016. FOXO3a regulates BNIP3 and modulates mitochondrial calcium, dynamics, and function in cardiac stress. *American Journal of Physiology-Heart and Circulatory Physiology*, *311*(6), pp.H1540-H1559.

Chaikijurajai, T. and Tang, W.W., 2020. Reappraisal of inflammatory biomarkers in heart failure. *Current Heart Failure Reports*, *17*(1), pp.9-19.

Chen, X., Touyz, R.M., Park, J.B. and Schiffrin, E.L., 2001. Antioxidant effects of vitamins C and E are associated with altered activation of vascular NADPH oxidase and superoxide dismutase in stroke-prone SHR. *Hypertension*, *38*(3), pp.606-611.

Chen, Y., Guo, H., Xu, D., Xu, X., Wang, H., Hu, X., Lu, Z., Kwak, D., Xu, Y., Gunther, R. and Huo, Y., 2012. Left ventricular failure produces profound lung remodeling and pulmonary hypertension in mice: heart failure causes severe lung disease. *Hypertension*, *59*(6), pp.1170-1178.

Chinnakkannu, P., Reese, C., Gaspar, J.A., Panneerselvam, S., Pleasant-Jenkins, D., Mukherjee, R., Baicu, C., Tourkina, E., Hoffman, S. and Kuppuswamy, D., 2018. Suppression of angiotensin II-induced pathological changes in heart and kidney by the caveolin-1 scaffolding domain peptide. *PloS one*, *13*(12), p.e0207844.

Chugh, G., Pokkunuri, I. and Asghar, M., 2013. Renal dopamine and angiotensin II receptor signaling in age-related hypertension. *American Journal of Physiology-Renal Physiology*, *304*(1), pp.F1-F7.

Chung, C.J., Wu, C., Jones, M., Kato, T.S., Dam, T.T., Givens, R.C., Templeton, D.L., Maurer, M.S., Naka, Y., Takayama, H. and Mancini, D.M., 2014. Reduced handgrip strength as a marker of frailty predicts clinical outcomes in patients with heart failure undergoing ventricular assist device placement. *Journal of Cardiac Failure*, *20*(5), pp.310-315.

Clegg, A., Young, J., Iliffe, S., Rikkert, M.O. and Rockwood, K., 2013. Frailty in elderly people. *The Lancet*, *381*(9868), pp.752-762.

Coker, M.L., Jolly, J.R., Joffs, C., Etoh, T., Holder, J.R., Bond, B.R. and Spinale, F.G., 2001. Matrix metalloproteinase expression and activity in isolated myocytes after neurohormonal stimulation. *American Journal of Physiology-Heart and Circulatory Physiology*, *281*(2), pp.H543-H551.

Collard, R.M., Boter, H., Schoevers, R.A. and Oude Voshaar, R.C., 2012. Prevalence of frailty in community-dwelling older persons: a systematic review. *Journal of the American Geriatrics Society*, *60*(8), pp.1487-1492.

Conrad, C.H., Brooks, W.W., Robinson, K.G. and Bing, O.H., 1991. Impaired myocardial function in spontaneously hypertensive rats with heart failure. *American Journal of Physiology-Heart and Circulatory Physiology*, *260*(1), pp.H136-H145.

Cosiano, M.F., Jannat-Khah, D., Lin, F.R., Goyal, P., McKee, M. and Sterling, M.R., 2020. Hearing Loss and Physical Functioning Among Adults with Heart Failure: Data from NHANES. *Clinical Interventions in Aging*, *15*, p.635.

Cowling, R.T., Kupsky, D., Kahn, A.M., Daniels, L.B. and Greenberg, B.H., 2019. Mechanisms of cardiac collagen deposition in experimental models and human disease. *Translational Research*, *209*, pp.138-155.

Creemers, E.E. and Pinto, Y.M., 2011. Molecular mechanisms that control interstitial fibrosis in the pressure-overloaded heart. *Cardiovascular Research*, *89*(2), pp.265-272.

Crimmins, E.M., Kim, J.K. and Solé-Auró, A., 2011. Gender differences in health: results from SHARE, ELSA and HRS. *European Journal of Public Health*, *21*(1), pp.81-91.

Csige, I., Ujvárosy, D., Szabó, Z., Lőrincz, I., Paragh, G., Harangi, M. and Somodi, S., 2018. The impact of obesity on the cardiovascular system. *Journal of Diabetes Research*, *2018*.

Cutler, R.G., Kelly, J., Storie, K., Pedersen, W.A., Tammara, A., Hatanpaa, K., Troncoso, J.C. and Mattson, M.P., 2004. Involvement of oxidative stress-induced abnormalities in ceramide and cholesterol metabolism in brain aging and Alzheimer's disease. *Proceedings of the National Academy of Sciences*, *101*(7), pp.2070-2075.

Dassanayaka, S. and Jones, S.P., 2015. Recent developments in heart failure. *Circulation Research*, *117*(7), pp.e58-e63.

Davies, B., García, F., Ara, I., Artalejo, F.R., Rodriguez-Manas, L. and Walter, S., 2018. Relationship between sarcopenia and frailty in the toledo study of healthy aging: a population based cross-sectional study. *Journal of the American Medical Directors Association*, *19*(4), pp.282-286.

Davis, M.R., Lee, C.S., Corcoran, A., Gupta, N., Uchmanowicz, I. and Denfeld, Q.E., 2021. Gender differences in the prevalence of frailty in heart failure: A systematic review and meta-analysis. *International Journal of Cardiology*.

De Simone, G., Verdecchia, P., Pede, S., Gorini, M. and Maggioni, A.P., 2002. Prognosis of inappropriate left ventricular mass in hypertension: the MAVI Study. *Hypertension*, *40*(4), pp.470-476.

De Simone, Giovanni, 2014. Concentric or eccentric hypertrophy: how clinically relevant is the difference?. *American Heart Association, 43*(4), pp.714-715.

De Vries, N.M., Staal, J.B., Van Ravensberg, C.D., Hobbelen, J.S.M., Rikkert, M.O. and Nijhuis-Van der Sanden, M.W.G., 2011. Outcome instruments to measure frailty: a systematic review. *Ageing Research Reviews*, *10*(1), pp.104-114.

Denfeld, Q.E., Winters-Stone, K., Mudd, J.O., Gelow, J.M., Kurdi, S. and Lee, C.S., 2017. The prevalence of frailty in heart failure: a systematic review and meta-analysis. *International Journal of Cardiology*, *236*, pp.283-289.

Dent, E., Kowal, P. and Hoogendijk, E.O., 2016. Frailty measurement in research and clinical practice: a review. *European Journal of Internal Medicine*, *31*, pp.3-10.

Derbré, F., Gratas-Delamarche, A., Gómez-Cabrera, M.C. and Viña, J., 2014. Inactivity-induced oxidative stress: a central role in age-related sarcopenia?. *European Journal of Sport Science*, *14*(sup1), pp.S98-S108.

Dewan, P., Rørth, R., Jhund, P.S., Shen, L., Raparelli, V., Petrie, M.C., Abraham, W.T., Desai, A.S., Dickstein, K., Køber, L. and Mogensen, U.M., 2019. Differential impact of heart failure with reduced ejection fraction on men and women. *Journal of the American College of Cardiology*, *73*(1), pp.29-40.

Dhande, I., Ma, W. and Hussain, T., 2015. Angiotensin AT 2 receptor stimulation is anti-inflammatory in lipopolysaccharide-activated THP-1 macrophages via increased interleukin-10 production. *Hypertension Research*, *38*(1), pp.21-29.

Dodson, J.A. and Chaudhry, S.I., 2012. Geriatric conditions in heart failure. *Current Cardiovascular Risk Reports*, *6*(5), pp.404-410.

Doi, R., Masuyama, T., Yamamoto, K., Doi, Y., Mano, T., Sakata, Y., Ono, K., Kuzuya, T., Hirota, S., Koyama, T. and Miwa, T., 2000. Development of different phenotypes of hypertensive heart failure: systolic versus diastolic failure in Dahl salt-sensitive rats. *Journal of Hypertension*, *18*(1), pp.111-120.

Drake, R.E. and Doursout, M.F., 2002. Pulmonary edema and elevated left atrial pressure: four hours and beyond. *Physiology, 17*(6), pp.223-226.

Drazner, M.H., 2011. The progression of hypertensive heart disease. *Circulation*, *123*(3), pp.327-334.

Dudoignon, E., Dépret, F. and Legrand, M., 2019. Is the renin-angiotensin-aldosterone system good for the kidney in acute settings?. *Nephron*, *143*(3), pp.179-183.

El-Dosouky, Ibrahim, I. and Abumandour, H.G., 2019. Rate pressure product and severely impaired systolic function in heart failure patients. *European Journal of Heart Failure* 21, pp. 68-69.

Ergatoudes, C., Schaufelberger, M., Andersson, B., Pivodic, A., Dahlström, U. and Fu, M., 2019. Non-cardiac comorbidities and mortality in patients with heart failure with reduced vs. preserved ejection fraction: a study using the Swedish Heart Failure Registry. *Clinical Research in Cardiology, 108*(9), pp.1025-1033.

Estrada, A.C., Yoshida, K., Saucerman, J.J. and Holmes, J.W., 2021. A multiscale model of cardiac concentric hypertrophy incorporating both mechanical and hormonal drivers of growth. *Biomechanics and Modeling in Mechanobiology*, *20*(1), pp.293-307.

Fairweather, D., Cooper Jr, L.T. and Blauwet, L.A., 2013. Sex and gender differences in myocarditis and dilated cardiomyopathy. *Current Problems in Cardiology*, *38*(1), pp.7-46.

Fares, E. and Howlett, S.E., 2010. Effect of age on cardiac excitation–contraction coupling. *Clinical and Experimental Pharmacology and Physiology*, *37*(1), pp.1-7.

Feridooni, H.A., Dibb, K.M. and Howlett, S.E., 2015. How cardiomyocyte excitation, calcium release and contraction become altered with age. *Journal of Molecular and Cellular Cardiology*, *83*, pp.62-72.

Feridooni, H.A., Kane, A.E., Ayaz, O., Boroumandi, A., Polidovitch, N., Tsushima, R.G., Rose, R.A. and Howlett, S.E., 2017. The impact of age and frailty on ventricular structure and function in C57BL/6J mice. *The Journal of Physiology*, *595*(12), pp.3721-3742.

Feridooni, H.A., Sun, M.H., Rockwood, K. and Howlett, S.E., 2015. Reliability of a frailty index based on the clinical assessment of health deficits in male C57BL/6J mice. *Journals of Gerontology Series A: Biomedical Sciences and Medical Sciences*, *70*(6), pp.686-693.

Fernández-Atucha, A., Izagirre, A., Fraile-Bermúdez, A.B., Kortajarena, M., Larrinaga, G., Martinez-Lage, P., Echevarría, E. and Gil, J., 2017. Sex differences in the aging pattern of renin–angiotensin system serum peptidases. *Biology of Sex Differences*, *8*(1), pp.1-8.

Filusch, A., Ewert, R., Altesellmeier, M., Zugck, C., Hetzer, R., Borst, M.M., Katus, H.A. and Meyer, F.J., 2011. Respiratory muscle dysfunction in congestive heart failure—the role of pulmonary hypertension. *International Journal of Cardiology*, *150*(2), pp.182-185.

Flint, K.M., Matlock, D.D., Lindenfeld, J. and Allen, L.A., 2012. Frailty and the selection of patients for destination therapy left ventricular assist device. *Circulation: Heart Failure*, *5*(2), pp.286-293.

Frangogiannis, N.G., 2019. The extracellular matrix in ischemic and nonischemic heart failure. *Circulation Research*, *125*(1), pp.117-146.

Frick, K.M., 2009. Estrogens and age-related memory decline in rodents: what have we learned and where do we go from here? *Hormones and Behavior*, *55*(1), pp.2-23.

Fried, L.P., Tangen, C.M., Walston, J., Newman, A.B., Hirsch, C., Gottdiener, J., Seeman, T., Tracy, R., Kop, W.J., Burke, G. and McBurnie, M.A., 2001. Frailty in older adults: evidence for a phenotype. *The Journals of Gerontology Series A: Biological Sciences and Medical Sciences*, *56*(3), pp.M146-M157.

Gallagher, P.E., Ferrario, C.M. and Tallant, E.A., 2008. Regulation of ACE2 in cardiac myocytes and fibroblasts. *American Journal of Physiology-Heart and Circulatory Physiology*, *295*(6), pp.H2373-H2379.

Gandhi, S.K., Powers, J.C., Nomeir, A.M., Fowle, K., Kitzman, D.W., Rankin, K.M. and Little, W.C., 2001. The pathogenesis of acute pulmonary edema associated with hypertension. *New England Journal of Medicine*, *344*(1), pp.17-22.

García, E.H., Perna, E.R., Farías, E.F., Obregón, R.O., Macin, S.M., Parras, J.I., Agüero, M.A., Moratorio, D.A., Pitzus, A.E., Tassano, E.A. and Rodriguez, L., 2006. Reduced systolic performance by tissue Doppler in patients with preserved and abnormal ejection fraction: new insights in chronic heart failure. *International Journal of Cardiology*, *108*(2), pp.181-188.

García-González, J. J., García-Peña, C., Franco-Marina, F., and Gutiérrez-Robledo, L. M., 2009. A frailty index to predict the mortality risk in a population of senior Mexican adults. *BMC Geriatrics*, *9*(1), pp.1-8.

Gebhard, C., Stähli, B.E., Gebhard, C.E., Tasnady, H., Zihler, D., Wischnewsky, M.B., Jenni, R. and Tanner, F.C., 2013. Age-and gender-dependent left ventricular remodeling. *Echocardiography*, *30*(10), pp.1143-1150.

Gillis, E.E. and Sullivan, J.C., 2016. Sex differences in hypertension: recent advances. *Hypertension*, *68*(6), pp.1322-1327.

Go, A.S., Mozaffarian, D., Roger, V.L., Benjamin, E.J., Berry, J.D., Borden, W.B., Bravata, D.M., Dai, S., Ford, E.S., Fox, C.S. and Franco, S., 2013. Heart disease and stroke statistics—2013 update: a report from the American Heart Association. *Circulation*, *127*(1), pp.e6-e245.

Goldwater, D.S. and Pinney, S.P., 2015. Frailty in advanced heart failure: a consequence of aging or a separate entity?. *Clinical Medicine Insights: Cardiology*, *9*, pp.CMC-S19698.

Gomez-Cabrera, M.C., Garcia-Valles, R., Rodriguez-Mañas, L., Garcia-Garcia, F.J., Olaso-Gonzalez, G., Salvador-Pascual, A., Tarazona-Santabalbina, F.J. and Viña, J., 2017. A new frailty score for experimental animals based on the clinical phenotype: inactivity as a model of frailty. *The Journals of Gerontology: Series A*, *72*(7), pp.885-891.

González, A., Ravassa, S., Beaumont, J., López, B. and Díez, J., 2011. New targets to treat the structural remodeling of the myocardium. *Journal of the American College of Cardiology*, *58*(18), pp.1833-1843.

Gopal, A.S., Schnellbaecher, M.J., Shen, Z., Akinboboye, O.O., Sapin, P.M. and King, D.L., 1997. Freehand three-dimensional echocardiography for measurement of left ventricular mass: in vivo anatomic validation using explanted human hearts. *Journal of the American College of Cardiology*, *30*(3), pp.802-810.

Gordon, E.H., Peel, N.M., Samanta, M., Theou, O., Howlett, S.E. and Hubbard, R.E., 2017. Sex differences in frailty: a systematic review and meta-analysis. *Experimental Gerontology*, *89*, pp.30-40.

Gottdiener, J.S., Reda, D.J., Materson, B.J., Massie, B.M., Notargiacomo, A., Hamburger, R.J., Williams, D.W., Henderson, W.G. and Department of Veterans Affairs Cooperative Study Group on Antihypertensive Agenis, 1994. Importance of obesity, race and age to the cardiac structural and functional effects of hypertension. *Journal of the American College of Cardiology*, *24*(6), pp.1492-1498.

Gragasin, F.S., Xu, Y., Arenas, I.A., Kainth, N. and Davidge, S.T., 2003. Estrogen reduces angiotensin II–induced nitric oxide synthase and NAD (P) H oxidase expression in endothelial cells. *Arteriosclerosis, Thrombosis, and Vascular Biology*, *23*(1), pp.38-44.

Griendling, K.K., Sorescu, D., Lassègue, B. and Ushio-Fukai, M., 2000. Modulation of protein kinase activity and gene expression by reactive oxygen species and their role in vascular physiology and pathophysiology. *Arteriosclerosis, Thrombosis, and Vascular Biology*, *20*(10), pp.2175-2183.

Grobe, J.L., Mecca, A.P., Lingis, M., Shenoy, V., Bolton, T.A., Machado, J.M., Speth, R.C., Raizada, M.K. and Katovich, M.J., 2007. Prevention of angiotensin II-induced cardiac remodeling by angiotensin-(1–7). *American Journal of Physiology-Heart and Circulatory Physiology*, *292*(2), pp.H736-H742.

Gu, D., Dupre, M.E., Sautter, J., Zhu, H., Liu, Y. and Yi, Z., 2009. Frailty and mortality among Chinese at advanced ages. *Journals of Gerontology: Series B*, *64*(2), pp.279-289.

Guo, K.K. and Ren, J., 2006. Cardiac overexpression of alcohol dehydrogenase (ADH) alleviates aging-associated cardiomyocyte contractile dysfunction: role of intracellular Ca2+ cycling proteins. *Aging Cell*, *5*(3), pp.259-265.

Hagdorn, Q.A., Bossers, G.P., Koop, A.M.C., Piek, A., Eijgenraam, T.R., van der Feen, D.E., Silljé, H.H., de Boer, R.A. and Berger, R.M., 2019. A novel method optimizing the normalization of cardiac parameters in small animal models: the importance of dimensional indexing. *American Journal of Physiology-Heart and Circulatory Physiology*, *316*(6), pp.H1552-H1557.

Hamblin, M., Friedman, D.B., Hill, S., Caprioli, R.M., Smith, H.M. and Hill, M.F., 2007. Alterations in the diabetic myocardial proteome coupled with increased myocardial oxidative stress underlies diabetic cardiomyopathy. *Journal of Molecular and Cellular Cardiology*, *42*(4), pp.884-895.

Hamilton, S. and Terentyev, D., 2019. Altered intracellular calcium homeostasis and arrhythmogenesis in the aged heart. *International Journal of Molecular Sciences*, *20*(10), p.2386.

Harada, E., Mizuno, Y., Kugimiya, F., Shono, M., Maeda, H., Yano, N. and Yasue, H., 2018. Sex differences in heart failure with preserved ejection fraction reflected by B-type natriuretic peptide level. *The American Journal of the Medical Sciences*, *356*(4), pp.335-343.

Harding, P., Yang, X.P., He, Q. and LaPointe, M.C., 2011. Lack of microsomal prostaglandin E synthase-1 reduces cardiac function following angiotensin II infusion. *American Journal of Physiology-Heart and Circulatory Physiology*, *300*(3), pp.H1053-H1061.

Hartupee, J. and Mann, D.L., 2017. Neurohormonal activation in heart failure with reduced ejection fraction. *Nature Reviews Cardiology*, *14*(1), pp.30-38.

Hashimoto, A., Fujiki, S., Nakamura, W. and Nakamura, T.J., 2019. Effects of testosterone on circadian rhythmicity in old mice. *The Journal of Physiological Sciences*, *69*(5), pp.791-798.

Hassink, R.J., Pasumarthi, K.B., Nakajima, H., Rubart, M., Soonpaa, M.H., De La Rivière, A.B., Doevendans, P.A. and Field, L.J., 2008. Cardiomyocyte cell cycle activation improves cardiac function after myocardial infarction. *Cardiovascular Research*, *78*(1), pp.18-25.

Haudek, S.B., Cheng, J., Du, J., Wang, Y., Hermosillo-Rodriguez, J., Trial, J., Taffet, G.E. and Entman, M.L., 2010. Monocytic fibroblast precursors mediate fibrosis in angiotensin-II-induced cardiac hypertrophy. *Journal of Molecular and Cellular Cardiology*, *49*(3), pp.499-507.

Heidenreich, P.A., Albert, N.M., Allen, L.A., Bluemke, D.A., Butler, J., Fonarow, G.C., Ikonomidis, J.S., Khavjou, O., Konstam, M.A., Maddox, T.M. and Nichol, G., 2013. Forecasting the impact of heart failure in the United States: a policy statement from the American Heart Association. *Circulation: Heart Failure*, *6*(3), pp.606-619.

Héliès-Toussaint, C., Moinard, C., Rasmusen, C., Tabbi-Anneni, I., Cynober, L. and Grynberg, A., 2005. Aortic banding in rat as a model to investigate malnutrition associated with heart failure. *American Journal of Physiology-Regulatory, Integrative and Comparative Physiology*, *288*(5), pp.R1325-R1331.

Hilliard, L.M., Chow, C.L., Mirabito, K.M., Steckelings, U.M., Unger, T., Widdop, R.E. and Denton, K.M., 2014. Angiotensin type 2 receptor stimulation increases renal function in female, but not male, spontaneously hypertensive rats. *Hypertension*, *64*(2), pp.378-383.

Ho, J.E., Enserro, D., Brouwers, F.P., Kizer, J.R., Shah, S.J., Psaty, B.M., Bartz, T.M., Santhanakrishnan, R., Lee, D.S., Chan, C. and Liu, K., 2016. Predicting heart failure with preserved and reduced ejection fraction: the international collaboration on heart failure subtypes. *Circulation: Heart Failure*, *9*(6), p.e003116.

Horn, M.A. and Trafford, A.W., 2016. Aging and the cardiac collagen matrix: Novel mediators of fibrotic remodelling. *Journal of Molecular and Cellular Cardiology*, *93*, pp.175-185.

Howlett, S.E. and Rockwood, K., 2013. New horizons in frailty: ageing and the deficit-scaling problem. *Age and Ageing*, *42*(4), pp.416-423.

Hubbard, R.E. and Rockwood, K., 2011. Frailty in older women. *Maturitas*, *69*(3), pp.203-207.

Hubbard, R.E., Peel, N.M., Samanta, M., Gray, L.C., Mitnitski, A. and Rockwood, K., 2017. Frailty status at admission to hospital predicts multiple adverse outcomes. *Age and Ageing*, *46*(5), pp.801-806.

Huentelman, M.J., Grobe, J.L., Vazquez, J., Stewart, J.M., Mecca, A.P., Katovich, M.J., Ferrario, C.M. and Raizada, M.K., 2005. Protection from angiotensin II-induced cardiac hypertrophy and fibrosis by systemic lentiviral delivery of ACE2 in rats. *Experimental Physiology*, *90*(5), pp.783-790.

Inglés, M., Gambini, J., Carnicero, J.A., García-García, F.J., Rodríguez-Mañas, L., Olaso-González, G., Dromant, M., Borrás, C. and Viña, J., 2014. Oxidative stress is related to frailty, not to age or sex, in a geriatric population: lipid and protein oxidation as biomarkers of frailty. *Journal of the American Geriatrics Society*, *62*(7), pp.1324-1328.

Iwanaga, Y., Aoyama, T., Kihara, Y., Onozawa, Y., Yoneda, T. and Sasayama, S., 2002. Excessive activation of matrix metalloproteinases coincides with left ventricular remodeling during transition from hypertrophy to heart failure in hypertensive rats. *Journal of the American College of Cardiology*, *39*(8), pp.1384-1391.

Izumiya, Y., Araki, S., Usuku, H., Rokutanda, T., Hanatani, S. and Ogawa, H., 2012. Chronic C-Type Natriuretic Peptide Infusion Attenuates Angiotensin II-Induced Myocardial Superoxide Production and Cardiac Remodeling. *International Journal of Vascular Medicine*, *2012*, pp.68-76.

Jacoby, J.J., Kalinowski, A., Liu, M.G., Zhang, S.S.M., Gao, Q., Chai, G.X., Ji, L., Iwamoto, Y., Li, E., Schneider, M. and Russell, K.S., 2003. Cardiomyocyte-restricted knockout of STAT3 results in higher sensitivity to inflammation, cardiac fibrosis, and heart failure with advanced age. *Proceedings of the National Academy of Sciences*, *100*(22), pp.12929-12934.

Jakovljevic, D.G., 2018. Physical activity and cardiovascular aging: Physiological and molecular insights. *Experimental Gerontology*, *109*, pp.67-74.

Jansen, H.J., Moghtadaei, M., Mackasey, M., Rafferty, S.A., Bogachev, O., Sapp, J.L., Howlett, S.E. and Rose, R.A., 2017. Atrial structure, function and arrhythmogenesis in aged and frail mice. *Scientific Reports*, *7*(1), pp.1-17.

Januzzi, J.L. and Ibrahim, N.E., 2017. Renin-Angiotensin System Blockade in Heart Failure. *Journal of the American College of Cardiology*, *7*(69), pp.820-822.

Jarnert, C., Mejhert, M., Ring, M., Persson, H. and Edner, M., 2000. Doppler tissue imaging in congestive heart failure patients due to diastolic or systolic dysfunction: a comparison with Doppler echocardiography and the atrio-ventricular plane displacement technique. *European Journal of Heart Failure 2*(2), pp.151-160.

Jha, S.R., Ha, H.S., Hickman, L.D., Hannu, M., Davidson, P.M., Macdonald, P.S. and Newton, P.J., 2015. Frailty in advanced heart failure: a systematic review. *Heart Failure Reviews*, *20*(5), pp.553-560.

Jia, N., Dong, P., Ye, Y., Qian, C. and Dai, Q., 2012. Allopurinol Attenuates Oxidative Stress and Cardiac Fibrosis in Angiotensin II-Induced Cardiac Diastolic Dysfunction. *Cardiovascular Therapeutics, 30*(2), pp.117-123.

Joseph, S.M. and Rich, M.W., 2017. Targeting frailty in heart failure. *Current Treatment Options in Cardiovascular Medicine*, *19*(4), pp.31.

Joyce, E., 2016. Frailty in advanced heart failure. *Heart Failure Clinics*, *12*(3), pp.363-374.

Judd, C.M., Westfall, J. and Kenny, D.A., 2012. Treating stimuli as a random factor in social psychology: A new and comprehensive solution to a pervasive but largely ignored problem. *Journal of Personality and Social Psychology*, *103*(1), P.54.

Kalogeropoulos, A., Georgiopoulou, V., Psaty, B.M., Rodondi, N., Smith, A.L., Harrison, D.G., Liu, Y., Hoffmann, U., Bauer, D.C., Newman, A.B. and Kritchevsky, S.B., 2010. Inflammatory markers and incident heart failure risk in older adults: the Health ABC (Health, Aging, and Body Composition) study. *Journal of the American College of Cardiology*, *55*(19), pp.2129-2137.

Kamil, R.J., Betz, J., Powers, B.B., Pratt, S., Kritchevsky, S., Ayonayon, H.N., Harris, T.B., Helzner, E., Deal, J.A., Martin, K. and Peterson, M., 2016. Association of hearing impairment with incident frailty and falls in older adults. *Journal of Aging and Health*, *28*(4), pp.644-660.

Kane, A.E., Bisset, E.S., Heinze-Milne, S., Keller, K.M., Grandy, S.A. and Howlett, S.E., 2021. Maladaptive changes associated with cardiac aging are sex-specific and graded by frailty and inflammation in C57BL/6 mice. *The Journals of Gerontology: Series A*, *76*(2), pp.233-243.

Kane, A.E., Bisset, E.S., Heinze-Milne, S., Keller, K.M., Grandy, S.A. and Howlett, S.E., 2021. Maladaptive changes associated with cardiac aging are sex-specific and graded by frailty and inflammation in C57BL/6 mice. *The Journals of Gerontology: Series A*, *76*(2), pp.233-243.

Kane, A.E., Bisset, E.S., Keller, K.M., Ghimire, A., Pyle, W.G. and Howlett, S.E., 2020. Age, sex and overall health, measured as frailty, modify myofilament proteins in hearts from naturally aging mice. *Scientific Reports*, *10*(1), pp.1-15.

Kane, A.E., Keller, K.M., Heinze-Milne, S., Grandy, S.A. and Howlett, S.E., 2019. A murine frailty index based on clinical and laboratory measurements: links between frailty and pro-inflammatory cytokines differ in a sex-specific manner. *The Journals of Gerontology: Series A*, *74*(3), pp.275-282.

Kassiri, Z. and Khokha, R., 2005. Myocardial extra-cellular matrix and its regulation by metalloproteinases and their inhibitors. *Thrombosis and Haemostasis*, *93*(02), pp.212-219.

Kawaguchi, M., Hay, I., Fetics, B. and Kass, D.A., 2003. Combined ventricular systolic and arterial stiffening in patients with heart failure and preserved ejection fraction: implications for systolic and diastolic reserve limitations. *Circulation*, *107*(5), pp.714-720.

Kawano, H., Do, Y.S., Kawano, Y., Starnes, V., Barr, M., Law, R.E. and Hsueh, W.A., 2000. Angiotensin II has multiple profibrotic effects in human cardiac fibroblasts. *Circulation, 101*(10), pp.1130-1137.

Keller, K.M. and Howlett, S.E., 2016. Sex differences in the biology and pathology of the aging heart. *Canadian Journal of Cardiology*, *32*(9), pp.1065-1073.

Kemp, C.D. and Conte, J.V., 2012. The pathophysiology of heart failure. *Cardiovascular Pathology, 21(5)*, pp.365-371.

Khan, M.S., Fonarow, G.C., Khan, H., Greene, S.J., Anker, S.D., Gheorghiade, M. and Butler, J., 2017. Renin–angiotensin blockade in heart failure with preserved ejection fraction: a systematic review and meta-analysis. *ESC Heart Failure*, *4*(4), pp.402-408.

Kim, C.H., Wheatley, C.M., Behnia, M. and Johnson, B.D., 2016. The effect of aging on relationships between lean body mass and VO2max in rowers. *PLoS One*, *11*(8), p.e0160275.

Kim, S. and Iwao, H., 2000. Molecular and cellular mechanisms of angiotensin II-mediated cardiovascular and renal diseases. *Pharmacological Reviews*, *52*(1), pp.11-34.

Kim, S., Ohta, K., Hamaguchi, A., Yukimura, T., Miura, K. and Iwao, H., 1995. Angiotensin II induces cardiac phenotypic modulation and remodeling in vivo in rats. *Hypertension*, *25*(6), pp.1252-1259.

King, M., Kingery, J.E. and Casey, B., 2012. Diagnosis and evaluation of heart failure. *American Family Physician*, *85*(12), pp.1161-1168.

Kitzman, D.W., Nicklas, B., Kraus, W.E., Lyles, M.F., Eggebeen, J., Morgan, T.M. and Haykowsky, M., 2014. Skeletal muscle abnormalities and exercise intolerance in older patients with heart failure and preserved ejection fraction. *American Journal of Physiology-Heart and Circulatory Physiology*, *306*(9), pp.H1364-H1370.

Klotz, S., Hay, I., Zhang, G., Maurer, M., Wang, J. and Burkhoff, D., 2006. Development of heart failure in chronic hypertensive Dahl rats: focus on heart failure with preserved ejection fraction. *Hypertension*, *47*(5), pp.901-911.

Kong, P., Christia, P. and Frangogiannis, N.G., 2014. The pathogenesis of cardiac fibrosis. *Cellular and Molecular Life Sciences*, *71*(4), pp.549-574.

Kono, M., Kisanuki, A., Ueya, N., Kubota, K., Kuwahara, E., Takasaki, K., Yuasa, T., Mizukami, N., Miyata, M. and Tei, C., 2010. Left ventricular global systolic dysfunction has a significant role in the development of diastolic heart failure in patients with systemic hypertension. *Hypertension Research*, *33*(11), pp.1167-1173.

Kono, M., Kisanuki, A., Ueya, N., Kubota, K., Kuwahara, E., Takasaki, K., Yuasa, T., Mizukami, N., Miyata, M. and Tei, C., 2010. Left ventricular global systolic dysfunction has a significant role in the development of diastolic heart failure in patients with systemic hypertension. *Hypertension Research*, *33*(11), pp.1167-1173.

Koulis, C., Chow, B.S., McKelvey, M., Steckelings, U.M., Unger, T., Thallas-Bonke, V., Thomas, M.C., Cooper, M.E., Jandeleit-Dahm, K.A. and Allen, T.J., 2015. AT2R agonist, compound 21, is reno-protective against type 1 diabetic nephropathy. *Hypertension*, *65*(5), pp.1073-1081.

Krishnamoorthy, A., Brown, T., Ayers, C.R., Gupta, S., Rame, J.E., Patel, P.C., Markham, D.W. and Drazner, M.H., 2011. Progression from normal to reduced left ventricular ejection fraction in patients with concentric left ventricular hypertrophy after long-term follow-up. *The American Journal of Cardiology*, *108*(7), pp.997-1001.

Kühl, H.P., Hanrath, P. and Franke, A., 2003. M-mode echocardiography overestimates left ventricular mass in patients with normal left ventricular shape: a comparative study using three-dimensional echocardiography. *European Journal of Echocardiography*, *4*(4), pp.313-319.

Kumar, U., Wettersten, N. and Garimella, P.S., 2019. Cardiorenal syndrome: pathophysiology. *Cardiology Clinics*, *37*(3), pp.251-265.

Lam, C.S., Arnott, C., Beale, A.L., Chandramouli, C., Hilfiker-Kleiner, D., Kaye, D.M., Ky, B., Santema, B.T., Sliwa, K. and Voors, A.A., 2019. Sex differences in heart failure. *European Heart Journal*, *40*(47), pp.3859-3868c.

Lam, C.S., Roger, V.L., Rodeheffer, R.J., Bursi, F., Borlaug, B.A., Ommen, S.R., Kass, D.A. and Redfield, M.M., 2007. Clinical Perspective. *Circulation*, *115*(15), pp.1982-1990.

Le Couteur, D.G., Anderson, R.M. and de Cabo, R., 2018. Sex and aging. *The Journals of Gerontology: Series A*, *73*(2), pp.139-140.

Leete, J., Gurley, S. and Layton, A.T., 2018. Modeling sex differences in the renin angiotensin system and the efficacy of antihypertensive therapies. *Computers & Chemical Engineering*, *112*, pp.253-264.

Lembo, M., Santoro, C., Sorrentino, R., Trimarco, B., Galderisi, M. and Esposito, R., 2019. Impact of left ventricular mass/end-diastolic volume ratio by three-dimensional echocardiography on two-dimensional global longitudinal strain and diastolic function in native hypertensive patients. *Journal of Hypertension*, *37*(10), pp.2041-2047.

Li, H.L., She, Z.G., Li, T.B., Wang, A.B., Yang, Q., Wei, Y.S., Wang, Y.G. and Liu, D.P., 2007. Overexpression of myofibrillogenesis regulator-1 aggravates cardiac hypertrophy induced by angiotensin II in mice. *Hypertension*, *49*(6), pp.1399-1408.

Li, Y.Q., Li, X.B., Guo, S.J., Chu, S.L., Gao, P.J., Zhu, D.L., Niu, W.Q. and Jia, N., 2013. Apocynin attenuates oxidative stress and cardiac fibrosis in angiotensin II-induced cardiac diastolic dysfunction in mice. *Acta Pharmacologica Sinica, 34*(3), pp.352-359.

Liang, B., Wang, X., Zhang, N., Yang, H., Bai, R., Liu, M., Bian, Y., Xiao, C. and Yang, Z., 2015. Angiotensin-(1-7) attenuates angiotensin II-induced ICAM-1, VCAM-1, and MCP-1 expression via the MAS receptor through suppression of P38 and NF-κB pathways in HUVECs. *Cellular Physiology and Biochemistry*, *35*(6), pp.2472-2482.

Lin, C.H., Liao, C.C., Huang, C.H., Tung, Y.T., Chang, H.C., Hsu, M.C. and Huang, C.C., 2017. Proteomics analysis to identify and characterize the biomarkers and physical activities of non-frail and frail older adults. *International Journal of Medical Sciences*, *14*(3), p.231.

Litwin, S.E., Katz, S.E., Weinberg, E.O., Lorell, B.H., Aurigemma, G.P. and Douglas, P.S., 1995. Serial echocardiographic-Doppler assessment of left ventricular geometry and function in rats with pressure-overload hypertrophy: chronic angiotensin-converting enzyme inhibition attenuates the transition to heart failure. *Circulation*, *91*(10), pp.2642-2654.

Liu, C.K., Lyass, A., Larson, M.G., Massaro, J.M., Wang, N., D'Agostino, R.B., Benjamin, E.J. and Murabito, J.M., 2016. Biomarkers of oxidative stress are associated with frailty: the Framingham Offspring Study. *Age*, *38*(1), p.1.

Liu, J., Yang, F., Yang, X.P., Jankowski, M. and Pagano, P.J., 2003. NAD (P) H oxidase mediates angiotensin II–induced vascular macrophage infiltration and medial hypertrophy. *Arteriosclerosis, Thrombosis, and Vascular Biology*, *23*(5), pp.776-782.

Liu, L., Yin, X., Chen, M., Jia, H., Eisen, H.J. and Hofman, A., 2018. Geographic variation in heart failure mortality and its association with hypertension, diabetes, and behavioral-related risk factors in 1,723 counties of the United States. *Frontiers in Public Health*, *6*, p.132.

Loong, C.K., Badr, M.A. and Chase, P.B., 2012. Tropomyosin flexural rigidity and single Ca2+ regulatory unit dynamics: implications for cooperative regulation of cardiac muscle contraction and cardiomyocyte hypertrophy. *Frontiers in Physiology*, *3*, p.80.

Lu, X., Heeley, D.H., Smillie, L.B. and Kawai, M., 2010. The role of tropomyosin isoforms and phosphorylation in force generation in thin-filament reconstituted bovine cardiac muscle fibres. *Journal of Muscle Research and Cell Motility*, *31*(2), pp.93-109.

Lundorff, I.J., Sengeløv, M., Jørgensen, P.G., Pedersen, S., Modin, D., Eske Bruun, N., Fritz-Hansen, T., Skov Jensen, J. and Biering-Sørensen, T., 2018. Echocardiographic predictors of mortality in women with heart failure with reduced ejection fraction. *Circulation: Cardiovascular Imaging*, *11*(11), p.e008031.

Lupón, J., González, B., Santaeugenia, S., Altimir, S., Urrutia, A., Más, D., Díez, C., Pascual, T., Cano, L. and Valle, V., 2008. Prognostic implication of frailty and depressive symptoms in an outpatient population with heart failure. *Revista Española de Cardiología (English Edition)*, *61*(8), pp.835-842.

Ma, C., Luo, H., Fan, L., Liu, X. and Gao, C., 2020. Heart failure with preserved ejection fraction: an update on pathophysiology, diagnosis, treatment, and prognosis. *Brazilian Journal of Medical and Biological Research*, *53*(7), pp.1-16.

MacIver, D.H. and Clark, A.L., 2015. The vital role of the right ventricle in the pathogenesis of acute pulmonary edema. *The American Journal of Cardiology*, *115*(7), pp.992-1000.

Mann, D.L., 2015. Innate immunity and the failing heart: the cytokine hypothesis revisited. *Circulation Research*, *116*(7), pp.1254-1268.

Mantovani, A., 1997. The interplay between primary and secondary cytokines. *Drugs*, *54*(1), pp.15-23.

Maurer, M.S., Horn, E., Reyentovich, A., Dickson, V.V., Pinney, S., Goldwater, D., Goldstein, N.E., Jimenez, O., Teruya, S., Goldsmith, J. and Helmke, S., 2017. Can a left ventricular assist device in individuals with advanced systolic heart failure improve or reverse frailty?. *Journal of the American Geriatrics Society*, *65*(11), pp.2383-2390.

Meléndez, G.C., McLarty, J.L., Levick, S.P., Du, Y., Janicki, J.S. and Brower, G.L., 2010. Interleukin 6 mediates myocardial fibrosis, concentric hypertrophy, and diastolic dysfunction in rats. *Hypertension*, *56*(2), pp.225-231.

Mellor, K.M., Curl, C.L., Chandramouli, C., Pedrazzini, T., Wendt, I.R. and Delbridge, L.M., 2014. Ageing-related cardiomyocyte functional decline is sex and angiotensin II dependent. *Age*, *36*(3), pp.1155-1167.

Meric, M., Yesildag, O., Yuksel, S., Soylu, K., Arslandag, M., Dursun, I., Zengin, H., Koprulu, D. and Yilmaz, O., 2014. Tissue doppler myocardial performance index in patients with heart failure and its relationship with haemodynamic parameters. *The International Journal of Cardiovascular Imaging*, *30*(6), pp.1057-1064.

Meschiari, C.A., Ero, O.K., Pan, H., Finkel, T. and Lindsey, M.L., 2017. The impact of aging on cardiac extracellular matrix. *Geroscience*, *39*(1), pp.7-18.

Meyer, S., Brouwers, F.P., Voors, A.A., Hillege, H.L., de Boer, R.A., Gansevoort, R.T., van der Harst, P., Rienstra, M., van Gelder, I.C., van Veldhuisen, D.J. and van Gilst, W.H., 2015. Sex differences in new-onset heart failure. *Clinical Research in Cardiology*, *104*(4), pp.342-350.

Miglioranza, M.H., Picano, E., Badano, L.P., Sant'Anna, R., Rover, M., Zaffaroni, F., Sicari, R., Kalil, R.K., Leiria, T.L. and Gargani, L., 2017. Pulmonary congestion evaluated by lung ultrasound predicts decompensation in heart failure outpatients. *International Journal of Cardiology*, *240*, pp.271-278.

Mihl, C., Dassen, W.R.M. and Kuipers, H., 2008. Cardiac remodelling: concentric versus eccentric hypertrophy in strength and endurance athletes. *Netherlands Heart Journal*, *16*(4), pp.129-133.

Miličić Stanić, B., Maddox, S., de Souza, A.M., Wu, X., Mehranfard, D., Ji, H., Speth, R.C. and Sandberg, K., 2021. Male bias in ACE2 basic science research: Missed opportunity for discovery in the time of COVID-19. *American Journal of Physiology-Regulatory, Integrative and Comparative Physiology*, *320*(6), pp.R925-R937.

Miller, M.A. and Zachary, J.F., 2017. Mechanisms and morphology of cellular injury, adaptation, and death. *Pathologic Basis of Veterinary Disease*, pp.2-43.

Miller, R.A., Harper, J.M., Dysko, R.C., Durkee, S.J. and Austad, S.N., 2002. Longer life spans and delayed maturation in wild-derived mice. *Experimental Biology and Medicine*, *227*(7), pp.500-508.

Minciullo, P.L., Catalano, A., Mandraffino, G., Casciaro, M., Crucitti, A., Maltese, G., Morabito, N., Lasco, A., Gangemi, S. and Basile, G., 2016. Inflammaging and anti-inflammaging: the role of cytokines in extreme longevity. *Archivum Immunologiae Et Therapiae Experimentalis*, *64*(2), pp.111-126.

Mirza, M., Strunets, A., Shen, W.K. and Jahangir, A., 2012. Mechanisms of arrhythmias and conduction disorders in older adults. *Clinics in Geriatric Medicine*, *28*(4), pp.555-573.

Mishra, J.S., More, A.S., Gopalakrishnan, K. and Kumar, S., 2019. Testosterone plays a permissive role in angiotensin II-induced hypertension and cardiac hypertrophy in male rats. *Biology of reproduction*, *100*(1), pp.139-148.

Mitnitski, A., Howlett, S.E. and Rockwood, K., 2017. Heterogeneity of human aging and its assessment. *Journals of Gerontology Series A: Biomedical Sciences and Medical Sciences*, *72*(7), pp.877-884.

Mitnitski, A.B., Mogilner, A.J. and Rockwood, K., 2001. Accumulation of deficits as a proxy measure of aging. *The Scientific World Journal*, *1*, pp.323-336.

Miyagi, M., Kinugasa, Y., Sota, T., Yamada, K., Ishisugi, T., Hirai, M., Yanagihara, K., Haruki, N., Matsubara, K., Kato, M. and Yamamoto, K., 2018. Diaphragm muscle dysfunction in patients with heart failure. *Journal of Cardiac Failure*, *24*(4), pp.209-216.

Moghtadaei, M., Jansen, H.J., Mackasey, M., Rafferty, S.A., Bogachev, O., Sapp, J.L., Howlett, S.E. and Rose, R.A., 2016. The impacts of age and frailty on heart rate and sinoatrial node function. *The Journal of Physiology*, *594*(23), pp.7105-7126.

Monteonofrio, L., Florio, M.C., AlGhatrif, M., Lakatta, E.G. and Capogrossi, M.C., 2021. Aging-and gender-related modulation of RAAS: potential implications in COVID-19 disease. *Vascular Biology*, *3*(1), pp.R1-R14.

Mori, J., Basu, R., McLean, B.A., Das, S.K., Zhang, L., Patel, V.B., Wagg, C.S., Kassiri, Z., Lopaschuk, G.D. and Oudit, G.Y., 2012. Agonist-induced hypertrophy and diastolic dysfunction are associated with selective reduction in glucose oxidation: a metabolic contribution to heart failure with normal ejection fraction. *Circulation: Heart Failure, 5(*4*),* pp.493-503.

Mousa, T.M., Liu, D., Cornish, K.G. and Zucker, I.H., 2008. Exercise training enhances baroreflex sensitivity by an angiotensin II-dependent mechanism in chronic heart failure. *Journal of Applied Physiology*, *104*(3), pp.616-624.

Murad, K. and Kitzman, D.W., 2015. Reply: Heart Failure and Comorbidities. *JACC: Heart Failure*, *3*(12), pp.1003-1004.

Nadruz Jr, W., Kitzman, D., Windham, B.G., Kucharska-Newton, A., Butler, K., Palta, P., Griswold, M.E., Wagenknecht, L.E., Heiss, G., Solomon, S.D. and Skali, H., 2017. Cardiovascular dysfunction and frailty among older adults in the community: the ARIC study. *Journals of Gerontology Series A: Biomedical Sciences and Medical Sciences*, *72*(7), pp.958-964.

Nagase, H., Visse, R. and Murphy, G., 2006. Structure and function of matrix metalloproteinases and TIMPs. *Cardiovascular Research*, *69*(3), pp.562-573.

Nauta, J.F., Hummel, Y.M., Tromp, J., Ouwerkerk, W., van der Meer, P., Jin, X., Lam, C.S., Bax, J.J., Metra, M., Samani, N.J. and Ponikowski, P., 2020. Concentric vs. eccentric remodelling in heart failure with reduced ejection fraction: clinical characteristics, pathophysiology and response to treatment. *European Journal of Heart Failure*, *22*(7), pp.1147-1155.

Newman, A.B., Gottdiener, J.S., McBurnie, M.A., Hirsch, C.H., Kop, W.J., Tracy, R., Walston, J.D. and Fried, L.P., 2001. Associations of subclinical cardiovascular disease with frailty. *The Journals of Gerontology Series A: Biological Sciences and Medical Sciences*, *56*(3), pp.M158-M166.

Nickenig, G., Strehlow, K., Wassmann, S., Bäumer, A.T., Albory, K., Sauer, H. and Böhm, M., 2000. Differential effects of estrogen and progesterone on AT1 receptor gene expression in vascular smooth muscle cells. *Circulation*, *102*(15), pp.1828-1833.

Ogihara, T., Asano, T., Ando, K., Sakoda, H., Anai, M., Shojima, N., Ono, H., Onishi, Y., Fujishiro, M., Abe, M. and Fukushima, Y., 2002. High-salt diet enhances insulin signaling and induces insulin resistance in Dahl salt-sensitive rats. *Hypertension*, *40*(1), pp.83-89.

Okamoto, K., and Aoki, K., 1963. Development of a strain of spontaneously hypertensive rat. *Japanese Circulation Journal*, *27*, pp.282-293.

Oksuzyan, A., Juel, K., Vaupel, J.W. and Christensen, K., 2008. Men: good health and high mortality. Sex differences in health and aging. *Aging Clinical and Experimental Research*, *20*(2), pp.91-102.

Oktay, A.A. and Shah, S.J., 2014. Current perspectives on systemic hypertension in heart failure with preserved ejection fraction. *Current Cardiology Reports*, *16*(12), p.545.

Oudit, G.Y., Kassiri, Z., Patel, M.P., Chappell, M., Butany, J., Backx, P.H., Tsushima, R.G., Scholey, J.W., Khokha, R. and Penninger, J.M., 2007. Angiotensin II-mediated oxidative stress and inflammation mediate the age-dependent cardiomyopathy in ACE2 null mice. *Cardiovascular research*, *75*(1), pp.29-39.

Pagan, L.U., Damatto, R.L., Cezar, M.D., Lima, A.R., Bonomo, C., Campos, D.H., Gomes, M.J., Martinez, P.F., Oliveira Jr, S.A., Gimenes, R. and Rosa, C.M., 2015. Long-term low intensity physical exercise attenuates heart failure development in aging spontaneously hypertensive rats. *Cellular Physiology and Biochemistry*, *36*(1), pp.61-74.

Pal, G.K., Ganesh, V., Karthik, S., Nanda, N. and Pal, P., 2014. The effects of short-term relaxation therapy on indices of heart rate variability and blood pressure in young adults. *American Journal of Health Promotion*, *29*(1), pp.23-28.

Pandey, A., Kitzman, D. and Reeves, G., 2019. Frailty is intertwined with heart failure: mechanisms, prevalence, prognosis, assessment, and management. *JACC: Heart Failure*, *7*(12), pp.1001-1011.

Panesar, D.K. and Burch, M., 2017. Assessment of diastolic function in congenital heart disease. *Frontiers in Cardiovascular Medicine*, *4*, pp.5.

Parikh, K.S., Sharma, K., Fiuzat, M., Surks, H.K., George, J.T., Honarpour, N., Depre, C., Desvigne-Nickens, P., Nkulikiyinka, R., Lewis, G.D. and Gomberg-Maitland, M., 2018. Heart failure with preserved ejection fraction expert panel report: current controversies and implications for clinical trials. *JACC: Heart Failure*, *6*(8), pp.619-632.

Parks, R.J., Fares, E., MacDonald, J.K., Ernst, M.C., Sinal, C.J., Rockwood, K. and Howlett, S.E., 2012. A procedure for creating a frailty index based on deficit accumulation in aging mice. *Journals of Gerontology Series A: Biomedical Sciences and Medical Sciences*, *67*(3), pp.217-227.

Patel, A. and Patel, D., 2021. Congestive heart failure model representing aortic banding induced hypertrophy: A study to analyse extent of pressure overload and alteration in myocardial structure and function. *IJC Heart & Vasculature*, *34*, p.100755.

Patel, V.B., Lezutekong, J.N., Chen, X. and Oudit, G.Y., 2017. Recombinant human ACE2 and the angiotensin 1-7 axis as potential new therapies for heart failure. *Canadian Journal of Cardiology*, *33*(7), pp.943-946.

Paulus, W.J. and Tschöpe, C., 2013. A novel paradigm for heart failure with preserved ejection fraction: comorbidities drive myocardial dysfunction and remodeling through coronary microvascular endothelial inflammation. *Journal of the American College of Cardiology*, *62*(4), pp.263-271.

Pedram, A., Razandi, M., Korach, K.S., Narayanan, R., Dalton, J.T. and Levin, E.R., 2013. ERβ selective agonist inhibits angiotensin-induced cardiovascular pathology in female mice. *Endocrinology*, *154*(11), pp.4352-4364.

Peng, H., Yang, X.P., Carretero, O.A., Nakagawa, P., D'Ambrosio, M., Leung, P., Xu, J., Peterson, E.L., González, G.E., Harding, P. and Rhaleb, N.E., 2011. Angiotensin II-induced dilated cardiomyopathy in Balb/c but not C57BL/6J mice. *Experimental Physiology*, *96*(8), pp.756-764.

Perlini, S., Palladini, G., Ferrero, I., Tozzi, R., Fallarini, S., Facoetti, A., Nano, R., Clari, F., Busca, G., Fogari, R. and Ferrari, A.U., 2005. Sympathectomy or doxazosin, but not propranolol, blunt myocardial interstitial fibrosis in pressure-overload hypertrophy. *Hypertension*, *46*(5), pp.1213-1218.

Pessôa, B.S., Slump, D.E., Ibrahimi, K., Grefhorst, A., van Veghel, R., Garrelds, I.M., Roks, A.J., Kushner, S.A., Danser, A.J. and van Esch, J.H., 2015. Angiotensin II type 2 receptor–and acetylcholine-mediated relaxation: essential contribution of female sex hormones and chromosomes. *Hypertension*, *66*(2), pp.396-402.

Piek, A., De Boer, R.A. and Silljé, H.H.W., 2016. The fibrosis-cell death axis in heart failure. *Heart Failure Reviews*, *21*(2), pp.199-211.

Plitt, G.D., Spring, J.T., Moulton, M.J. and Agrawal, D.K., 2018. Mechanisms, diagnosis, and treatment of heart failure with preserved ejection fraction and diastolic dysfunction. *Expert Review of Cardiovascular Therapy*, *16*(8), pp.579-589.

Pomatto, L.C., Tower, J. and Davies, K.J., 2018. Sexual dimorphism and aging differentially regulate adaptive homeostasis. *The Journals of Gerontology: Series A*, *73*(2), pp.141-149.

Ponikowski, P., Voors, A.A., Anker, S.D., Bueno, H., Cleland, J.G., Coats, A.J., Falk, V., González-Juanatey, J.R., Harjola, V.P., Jankowska, E.A. and Jessup, M., 2016. 2016 ESC Guidelines for the diagnosis and treatment of acute and chronic heart failure: The Task Force for the diagnosis and treatment of acute and chronic heart failure of the European Society of Cardiology (ESC) Developed with the special contribution of the Heart Failure Association (HFA) of the ESC. *European Heart Journal*, *37*(27), pp.2129-2200.

Pueyo, M.E., Gonzalez, W., Nicoletti, A., Savoie, F., Arnal, J.F. and Michel, J.B., 2000. Angiotensin II stimulates endothelial vascular cell adhesion molecule-1 via nuclear factor-κB activation induced by intracellular oxidative stress. *Arteriosclerosis, Thrombosis, and Vascular Biology*, *20*(3), pp.645-651.

Puthucheary, Z.A., Rawal, J., McPhail, M., Connolly, B., Ratnayake, G., Chan, P., Hopkinson, N.S., Phadke, R., Dew, T., Sidhu, P.S. and Velloso, C., 2013. Acute skeletal muscle wasting in critical illness. *Jama*, *310*(15), pp.1591-1600.

Puts, M.T., Lips, P. and Deeg, D.J., 2005. Sex differences in the risk of frailty for mortality independent of disability and chronic diseases. *Journal of the American Geriatrics Society*, *53*(1), pp.40-47.

Qiu, B., Wei, F., Sun, X., Wang, X., Duan, B., Shi, C., Zhang, J., Zhang, J., Qiu, W. and Mu, W., 2014. Measurement of hydroxyproline in collagen with three different methods. *Molecular Medicine Reports*, *10*(2), pp.1157-1163.

Raffai, G. and Lombard, J.H., 2016. Angiotensin-(1-7) selectively induces relaxation and modulates endothelium-dependent dilation in mesenteric arteries of salt-fed rats. *Journal of Vascular Research*, *53*(1-2), pp.105-118.

Reckelhoff, J.F. and Romero, J.C., 2003. Role of oxidative stress in angiotensin-induced hypertension. *American Journal of Physiology-Regulatory, Integrative and Comparative Physiology*, *284*(4), pp.R893-R912.

Regan, J.A., Mauro, A.G., Carbone, S., Marchetti, C., Gill, R., Mezzaroma, E., Valle Raleigh, J., Salloum, F.N., Van Tassell, B.W., Abbate, A. and Toldo, S., 2015. A mouse model of heart failure with preserved ejection fraction due to chronic infusion of a low subpressor dose of angiotensin II. *American Journal of Physiology-Heart and Circulatory Physiology*, *309*(5), pp.H771-H778.

Reina-Couto, M., Afonso, J., Carvalho, J., Morgado, L., Ronchi, F.A., de Oliveira Leite, A.P., Dias, C.C., Casarini, D.E., Bettencourt, P., Albino-Teixeira, A. and Morato, M., 2021. Interrelationship between renin-angiotensin-aldosterone system and oxidative stress in chronic heart failure patients with or without renal impairment. *Biomedicine & Pharmacotherapy*, *133*, p.110938.

Ren, J., Li, Q., Wu, S., Li, S.Y. and Babcock, S.A., 2007. Cardiac overexpression of antioxidant catalase attenuates aging-induced cardiomyocyte relaxation dysfunction. *Mechanisms of Ageing and Development*, *128*(3), pp.276-285.

Restini, C.B.A., Garcia, A.F.E., Natalin, H.M., Natalin, G.M. and Rizzi, E., 2017. Signaling Pathways of Cardiac Remodeling Related to Angiotensin II. *Renin-Angiotensin System: Past, Present and Future*, pp.51-66.

Reynolds, T.H., Dalton, A., Calzini, L., Tuluca, A., Hoyte, D. and Ives, S.J., 2019. The impact of age and sex on body composition and glucose sensitivity in C57BL/6J mice. *Physiological Reports*, *7*(3), pp.e13995

Roberts, B.M., Lavin, K.M., Many, G.M., Thalacker-Mercer, A., Merritt, E.K., Bickel, C.S., Mayhew, D.L., Tuggle, S.C., Cross, J.M., Kosek, D.J. and Petrella, J.K., 2018. Human neuromuscular aging: Sex differences revealed at the myocellular level. *Experimental Gerontology*, *106*, pp.116-124.

Rockwood, K. and Mitnitski, A., 2007. Frailty in relation to the accumulation of deficits. *The Journals of Gerontology Series A: Biological Sciences and Medical Sciences*, *62*(7), pp.722-727.

Rockwood, K. and Mitnitski, A., 2011. Frailty defined by deficit accumulation and geriatric medicine defined by frailty. *Clinics in Geriatric Medicine*, *27*(1), pp.17-26.

Rockwood, K., Andrew, M. and Mitnitski, A., 2007. A comparison of two approaches to measuring frailty in elderly people. *The Journals of Gerontology Series A: Biological Sciences and Medical Sciences*, *62*(7), pp.738-743.

Rockwood, K., Blodgett, J.M., Theou, O., Sun, M.H., Feridooni, H.A., Mitnitski, A., Rose, R.A., Godin, J., Gregson, E. and Howlett, S.E., 2017. A frailty index based on deficit accumulation quantifies mortality risk in humans and in mice. *Scientific Reports*, *7*(1), pp.1-10.

Rockwood, K., Fox, R.A., Stolee, P., Robertson, D. and Beattie, B.L., 1994. Frailty in elderly people: an evolving concept. *CMAJ: Canadian Medical Association Journal*, *150*(4), p.489.

Rockwood, K., Song, X., MacKnight, C., Bergman, H., Hogan, D.B., McDowell, I. and Mitnitski, A., 2005. A global clinical measure of fitness and frailty in elderly people. *Cmaj*, *173*(5), pp.489-495.

Rockwood, K., Theou, O. and Mitnitski, A., 2015. What are frailty instruments for? *Age and Ageing*, *44*(4), pp.545-547.

Røe, Å.T., Aronsen, J.M., Skårdal, K., Hamdani, N., Linke, W.A., Danielsen, H.E., Sejersted, O.M., Sjaastad, I. and Louch, W.E., 2017. Increased passive stiffness promotes diastolic dysfunction despite improved Ca2+ handling during left ventricular concentric hypertrophy. *Cardiovascular Research*, *113*(10), pp.1161-1172.

Roger, V.L., 2013. Epidemiology of heart failure. *Circulation research*, *113*(6), pp.646-659.

Roger, V.L., Go, A.S., Lloyd-Jones, D.M., Benjamin, E.J., Berry, J.D., Borden, W.B., Bravata, D.M., Dai, S., Ford, E.S. and Fox, C.S., 2012. Heart disease and stroke statistics—2012 update: a report from the American Heart Association. *Circulation*, *125*(1), pp.e2-e220.

Romero-Ortuno, R., and Kenny, R. A., 2012. The frailty index in Europeans: association with age and mortality. *Age and Ageing*, *41*(5), pp.684-689.

Rosenfeld, C.S., 2017. Sex-dependent differences in voluntary physical activity. *Journal of Neuroscience Research*, *95*(1-2), pp.279-290.

Rossi, F., Mascolo, A. and Mollace, V., 2017. The pathophysiological role of natriuretic peptide-RAAS cross talk in heart failure. *International Journal of Cardiology, 226,* pp.121-125.

Rysä, J., Leskinen, H., Ilves, M. and Ruskoaho, H., 2005. Distinct upregulation of extracellular matrix genes in transition from hypertrophy to hypertensive heart failure. *Hypertension*, *45*(5), pp.927-933.

Salah, H.M. and Mehta, J.L., 2021. Hypothesis: sex-related differences in ACE2 activity may contribute to higher mortality in men versus women with COVID-19. *Journal of Cardiovascular Pharmacology and Therapeutics*, *26*(2), pp.114-118.

Sama, I.E., Ravera, A., Santema, B.T., Van Goor, H., Ter Maaten, J.M., Cleland, J.G., Rienstra, M., Friedrich, A.W., Samani, N.J., Ng, L.L. and Dickstein, K., 2020. Circulating plasma concentrations of angiotensin-converting enzyme 2 in men and women with heart failure and effects of renin–angiotensin–aldosterone inhibitors. *European Heart Journal*, *41*(19), pp.1810-1817.

Savarese, G. and Lund, L.H., 2017. Global public health burden of heart failure. *Cardiac Failure Review*, *3*(1), pp.7-11.

Schiattarella, G.G. and Hill, J.A., 2015. Inhibition of hypertrophy is a good therapeutic strategy in ventricular pressure overload. *Circulation*, *131*(16), pp.1435-1447.

Schultz, M.B., Kane, A.E., Mitchell, S.J., MacArthur, M.R., Warner, E., Vogel, D.S., Mitchell, J.R., Howlett, S.E., Bonkowski, M.S. and Sinclair, D.A., 2020. Age and life expectancy clocks based on machine learning analysis of mouse frailty. *Nature Communications*, *11*(1), pp.1-12.

Searle, S.D., Mitnitski, A., Gahbauer, E.A., Gill, T.M. and Rockwood, K., 2008. A standard procedure for creating a frailty index. *BMC Geriatrics*, *8*(1), pp.1-10.

Sequeira-Lopez, M.L.S. and Gomez, R.A., 2021. Renin cells, the kidney, and hypertension. *Circulation Research*, *128*(7), pp.887-907. Unger, T. and Li, J., 2004. The role of the rennin-angiotensin-aldosterone system in heart failure. *Journal of the Renin Angiotensin Aldosterone System*, *5*, pp.S7-S10.

Serviddio, G., Romano, A.D., Greco, A., Rollo, T., Bellanti, F., Altomare, E. and Vendemiale, G., 2009. Frailty syndrome is associated with altered circulating redox balance and increased markers of oxidative stress. *International Journal of Immunopathology and Pharmacology*, *22*(3), pp.819-827.

Shi, J., Yang, Z., Song, X., Yu, P., Fang, X., Tang, Z., Peng, D., Mitnitski, A. and Rockwood, K., 2014. Sex differences in the limit to deficit accumulation in late middle-aged and older Chinese people: results from the Beijing Longitudinal Study of Aging. *Journals of Gerontology Series A: Biomedical Sciences and Medical Sciences*, *69*(6), pp.702-709.

Shimizu, I. and Minamino, T., 2016. Physiological and pathological cardiac hypertrophy. *Journal of Molecular and Cellular Cardiology*, *97*, pp.245-262.

Shinmura, K., 2016. Cardiac senescence, heart failure, and frailty: a triangle in elderly people. *The Keio Journal of Medicine*, pp.2015-0015.

Sikka, G., Miller, K.L., Steppan, J., Pandey, D., Jung, S.M., Fraser III, C.D., Ellis, C., Ross, D., Vandegaer, K., Bedja, D. and Gabrielson, K., 2013. Interleukin 10 knockout frail mice develop cardiac and vascular dysfunction with increased age. *Experimental gerontology*, *48*(2), pp.128-135.

Simmonds, S.J., Cuijpers, I., Heymans, S. and Jones, E.A., 2020. Cellular and molecular differences between HFpEF and HFrEF: a step ahead in an improved pathological understanding. *Cells*, *9*(1), pp.242.

Singh, M., Stewart, R. and White, H., 2014. Importance of frailty in patients with cardiovascular disease. *European Heart Journal*, *35*(26), pp.1726-1731.

Šmalcelj, A., Puljević, D., Buljević, B. and Brida, V., 2000. Left ventricular hypertrophy in obese hypertensives: is it really eccentric?(An echocardiographic study). *Collegium Antropologicum*, *24*(1), pp.167-183.

Sopel, M.J., Rosin, N.L., Lee, T.D. and Légaré, J.F., 2011. Myocardial fibrosis in response to Angiotensin II is preceded by the recruitment of mesenchymal progenitor cells. *Laboratory investigation*, *91*(4), pp.565-578.

Spier, A.W. and Meurs, K.M., 2004. Use of signal-averaged electrocardiography in the evaluation of arrhythmogenic right ventricular cardiomyopathy in Boxers. *Journal of the American Veterinary Medical Association, 225*(7), pp.1050-1055.

Sriramula, S. and Francis, J., 2015. Tumor necrosis factor-alpha is essential for angiotensin II-induced ventricular remodeling: role for oxidative stress. *PLoS One*, *10*(9), p.e0138372.

Sriramula, S., Haque, M., Majid, D.S. and Francis, J., 2008. Involvement of tumor necrosis factor-α in angiotensin II–mediated effects on salt appetite, hypertension, and cardiac hypertrophy. *Hypertension*, *51*(5), pp.1345-1351.

Statistics Canada. The ten leading causes of death, 2012. CANSIM (death database) [Internet]. Ottawa (ON): Statistics Canada; 2015 Dec 10 [cited 2021 July 14]. Available from: www.statcan.gc.ca/pub/82-625-x/2015001/article/14296-eng.htm

Sterling, M.R., Jannat-Khah, D., Vitale, S. and Safford, M.M., 2018a. Can your patients with heart failure see? The prevalence of visual impairment among adults with heart failure. *Journal of General Internal Medicine*, *33*(5), pp.605-607.

Sterling, M.R., Silva, A.F. and Charlson, M.E., 2018b. Sensory Impairments in Heart Failure—Are We Missing the Basics?: A Teachable Moment. *JAMA Internal Medicine*, *178*(6), pp.843-844.

Stewart, G.A., Foster, J., Cowan, M., Rooney, E., Mcdonagh, T., Dargie, H.J., Rodger, R.S.C. and Jardine, A.G., 1999. Echocardiography overestimates left ventricular mass in hemodialysis patients relative to magnetic resonance imaging. *Kidney International*, *56*(6), pp.2248-2253.

Strehlow, K., Rotter, S., Wassmann, S., Adam, O., Grohé, C., Laufs, K., Böhm, M. and Nickenig, G., 2003. Modulation of antioxidant enzyme expression and function by estrogen. *Circulation Research*, *93*(2), pp.170-177.

Suen, C.M., Chaudhary, K.R., Deng, Y., Jiang, B. and Stewart, D.J., 2019. Fischer rats exhibit maladaptive structural and molecular right ventricular remodelling in severe pulmonary hypertension: a genetically prone model for right heart failure. *Cardiovascular Research*, *115*(4), pp.788-799.

Swenor, B.K., Lee, M.J., Tian, J., Varadaraj, V. and Bandeen-Roche, K., 2020. Visual impairment and frailty: examining an understudied relationship. *The Journals of Gerontology: Series A*, *75*(3), pp.596-602.

Takeda, Y., Sakata, Y., Higashimori, M., Mano, T., Nishio, M., Ohtani, T., Hori, M., Masuyama, T., Kaneko, M. and Yamamoto, K., 2009. Noninvasive assessment of wall distensibility with the evaluation of diastolic epicardial movement. *Journal of Cardiac Failure*, *15*(1), pp.68-77.

Touyz, R.M., Chen, X., Tabet, F., Yao, G., He, G., Quinn, M.T., Pagano, P.J. and Schiffrin, E.L., 2002. Expression of a functionally active gp91phox-containing neutrophil-type NAD (P) H oxidase in smooth muscle cells from human resistance arteries: regulation by angiotensin II. *Circulation Research*, *90*(11), pp.1205-1213.

Touyz, R.M., Yao, G. and Schiffrin, E.L., 2003. c-Src induces phosphorylation and translocation of p47phox: role in superoxide generation by angiotensin II in human vascular smooth muscle cells. *Arteriosclerosis, Thrombosis, and Vascular Biology*, *23*(6), pp.981-987.

Triposkiadis, F., Giamouzis, G., Boudoulas, K.D., Karagiannis, G., Skoularigis, J., Boudoulas, H. and Parissis, J., 2018. Left ventricular geometry as a major determinant of left ventricular ejection fraction: physiological considerations and clinical implications. *European Journal of Heart Failure*, *20*(3), pp.436-444.

Triposkiadis, F., Xanthopoulos, A. and Butler, J., 2019. Cardiovascular aging and heart failure: JACC review topic of the week. *Journal of the American College of Cardiology*, *74*(6), pp.804-813.

Tsukamoto, Y., Mano, T., Sakata, Y., Ohtani, T., Takeda, Y., Tamaki, S., Omori, Y., Ikeya, Y., Saito, Y., Ishii, R. and Higashimori, M., 2013. A novel heart failure mice model of hypertensive heart disease by angiotensin II infusion, nephrectomy, and salt loading. *American Journal of Physiology-Heart and Circulatory Physiology*, *305*(11), pp.H1658-H1667.

Uchmanowicz, I., 2020. Oxidative stress, frailty and cardiovascular diseases: current evidence. *Frailty and Cardiovascular Diseases*, pp.65-77.

Uchmanowicz, I., Łoboz-Rudnicka, M., Szeląg, P., Jankowska-Polańska, B. and Łoboz-Grudzień, K., 2014. Frailty in heart failure. *Current Heart Failure Reports*, *11*(3), pp.266-273.

Uchmanowicz, I., Nessler, J., Gobbens, R., Gackowski, A., Kurpas, D., Straburzynska-Migaj, E., Kałuzna-Oleksy, M. and Jankowska, E.A., 2019. Coexisting frailty with heart failure. *Frontiers in physiology*, *10*, pp.791.

Uri, K., Fagyas, M., Mányiné Siket, I., Kertesz, A., Csanadi, Z., Sandorfi, G., Clemens, M., Fedor, R., Papp, Z., Edes, I. and Toth, A., 2014. New perspectives in the renin-angiotensin-aldosterone system (RAAS) IV: circulating ACE2 as a biomarker of systolic dysfunction in human hypertension and heart failure. *PLoS One*, *9*(4), p.e87845.

Valentova, M., von Haehling, S., Bauditz, J., Doehner, W., Ebner, N., Bekfani, T., Elsner, S., Sliziuk, V., Scherbakov, N., Murín, J. and Anker, S.D., 2016. Intestinal congestion and right ventricular dysfunction: a link with appetite loss, inflammation, and cachexia in chronic heart failure. *European Heart Journal*, *37*(21), pp.1684-1691.

Van der Velden, J., van der Wall, E.E. and Paulus, W.J., 2016. Heart failure with preserved ejection fraction: current status and challenges for the future. *Netherlands Heart Journal*, *24*(4), pp.225-226.

Vina, J., Borras, C. and Gomez-Cabrera, M.C., 2018. A free radical theory of frailty. *Free Radical Biology and Medicine*, *124*, pp.358-363.

Vistnes, M., Wæhre, A., Nygård, S., Sjaastad, I., Andersson, K.B., Husberg, C. and Christensen, G., 2010. Circulating cytokine levels in mice with heart failure are etiology dependent. *Journal of Applied Physiology*, *108*(5), pp.1357-1364.

Wehner, G.J., Jing, L., Haggerty, C.M., Suever, J.D., Leader, J.B., Hartzel, D.N., Kirchner, H.L., Manus, J.N., James, N., Ayar, Z. and Gladding, P., 2020. Routinely reported ejection fraction and mortality in clinical practice: where does the nadir of risk lie? *European Heart Journal*, *41*(12), pp.1249-1257.

Westermann, D., Becher, P.M., Lindner, D., Savvatis, K., Xia, Y., Fröhlich, M., Hoffmann, S., Schultheiss, H.P. and Tschöpe, C., 2012. Selective PDE5A inhibition with sildenafil rescues left ventricular dysfunction, inflammatory immune response and cardiac remodeling in angiotensin II-induced heart failure in vivo. *Basic Research in Cardiology*, *107*(6), p.308.

Whitehead, J.C., Hildebrand, B.A., Sun, M., Rockwood, M.R., Rose, R.A., Rockwood, K. and Howlett, S.E., 2014. A clinical frailty index in aging mice: comparisons with frailty index data in humans. *Journals of Gerontology Series A: Biomedical Sciences and Medical Sciences*, *69*(6), pp.621-632.

Wu, I.C., Shiesh, S.C., Kuo, P.H. and Lin, X.Z., 2009. High oxidative stress is correlated with frailty in elderly chinese. *Journal of the American Geriatrics Society*, *57*(9), pp.1666-1671.

Xu, D., Guo, H., Xu, X., Lu, Z., Fassett, J., Hu, X., Xu, Y., Tang, Q., Hu, D., Somani, A. and Geurts, A.M., 2011. Exacerbated pulmonary arterial hypertension and right ventricular hypertrophy in animals with loss of function of extracellular superoxide dismutase. *Hypertension*, *58*(2), pp.303-309.

Xu, R.Y., Zhu, X.F., Yang, Y. and Ye, P., 2013. High-sensitive cardiac troponin T. *Journal of Geriatric Cardiology: JGC*, *10*(1), p.102.

Xu, Z., Okamoto, H., Akino, M., Onozuka, H., Matsui, Y. and Tsutsui, H., 2008. Pravastatin attenuates left ventricular remodeling and diastolic dysfunction in angiotensin II-induced hypertensive mice. *Journal of Cardiovascular Pharmacology*, *51*(1), pp.62-70.

Xue, B., Pamidimukkala, J. and Hay, M., 2005. Sex differences in the development of angiotensin II-induced hypertension in conscious mice. *American Journal of Physiology-Heart and Circulatory Physiology*, *288*(5), pp.H2177-H2184.

Yancy, C.W., Jessup, M., Bozkurt, B., Butler, J., Casey, D.E., Drazner, M.H., Fonarow, G.C., Geraci, S.A., Horwich, T., Januzzi, J.L. and Johnson, M.R., 2013. 2013 ACCF/AHA guideline for the management of heart failure: a report of the American College of Cardiology Foundation/American Heart Association Task Force on Practice Guidelines. *Journal of the American College of Cardiology*, *62*(16), pp.e147-e239.

Yang, Y. and Lee, L.C., 2010. Dynamics and heterogeneity in the process of human frailty and aging: evidence from the US older adult population. *Journals of Gerontology Series B: Psychological Sciences and Social Sciences*, *65*(2), pp.246-255.

Yoon, S.O., Park, S.J., Yoon, S.Y., Yun, C.H. and Chung, A.S., 2002. Sustained Production of H2O2Activates Pro-matrix Metalloproteinase-2 through Receptor Tyrosine Kinases/Phosphatidylinositol 3-Kinase/NF-κB Pathway. *Journal of Biological Chemistry*, *277*(33), pp.30271-30282.

Yorke, A., Kane, A.E., Hancock Friesen, C.L., Howlett, S.E. and O'Blenes, S., 2017. Development of a rat clinical frailty index. *The Journals of Gerontology: Series A*, *72*(7), pp.897-903.

Youm, Y.H., Grant, R.W., McCabe, L.R., Albarado, D.C., Nguyen, K.Y., Ravussin, A., Pistell, P., Newman, S., Carter, R., Laque, A. and Münzberg, H., 2013. Canonical Nlrp3 inflammasome links systemic low-grade inflammation to functional decline in aging. *Cell Metabolism*, *18*(4), pp.519-532.

Yuan, L., Wang, T., Liu, F., Cohen, E.D. and Patel, V.V., 2010. An evaluation of transmitral and pulmonary venous Doppler indices for assessing murine left ventricular diastolic function. *Journal of the American Society of Echocardiography*, *23*(8), pp.887-897.

Zabalgoitia, M., Berning, J., Koren, M.J., Støylen, A., Nieminen, M.S., Dahlöf, B., Devereux, R.B. and LIFE Study Investigators, 2001. Impact of coronary artery disease on left ventricular systolic function and geometry in hypertensive patients with left ventricular hypertrophy (the LIFE study). *The American Journal of Cardiology*, *88*(6), pp.646-650.

Zhang, L., Du, J., Hu, Z., Han, G., Delafontaine, P., Garcia, G. and Mitch, W.E., 2009. IL-6 and serum amyloid A synergy mediates angiotensin II–induced muscle wasting. *Journal of the American Society of Nephrology*, *20*(3), pp.604-612.

Zhang, Y., Yuan, M., Gong, M., Tse, G., Li, G. and Liu, T., 2018. Frailty and clinical outcomes in heart failure: a systematic review and meta-analysis. *Journal of the American Medical Directors Association*, *19*(11), pp.1003-1008.

Zhao, Q., Ishibashi, M., Hiasa, K.I., Tan, C., Takeshita, A. and Egashira, K., 2004. Essential role of vascular endothelial growth factor in angiotensin II–induced vascular inflammation and remodeling. *Hypertension*, *44*(3), pp.264-270.

Zhou, L., Ma, B. and Han, X., 2016. The role of autophagy in angiotensin II-induced pathological cardiac hypertrophy. *Journal of Molecular Endocrinology*, *57*(4), pp.R143-R152.

Zimmerman, M.A., Baban, B., Tipton, A.J., O'Connor, P.M. and Sullivan, J.C., 2015. Chronic ANG II infusion induces sex-specific increases in renal T cells in Sprague-Dawley rats. *American Journal of Physiology-Renal Physiology*, *308*(7), pp.F706-F712.